Calculation of three point asymmetric cumulant in high multiplicity Proton-Proton collitions at LHC

Ran Segev

Calculation of three point asymmetric cumulant in high multiplicity Proton-Proton collitions at LHC

Research Thesis

Ran Segev

Research Thesis In Partial Fulfillment of the Requirements
for the Degree of Master of Science in Physics

Submitted to the Senate of the Technion - Israel Institute of Technology
Haifa
Adar Aleph, 5782, February, 2022

Instruction

The Research Thesis Was Done Under the Supervision of Prof. Blok Boris, in the Physics Department.

The generous financial help of the Technion - Israel Institute of Technology is gratefully acknowledged.

List of Publications

- B. Blok, R. Segev, The three point asymmetric cumulants in high multiplicity pp collisions, Eur. Phys. J. C **81** (2021) 1091, https://doi.org/10.1140/epjc/s10052-021-09886-z [arXiv:2107.11885 [hep-ph]].
- R. Segev, The three point asymmetric cumulants in high multiplicity pp collisions, 12th International workshop on Multiple Partonic Interactions at the LHC, https://indico.lip.pt/event/688/

Contents

List of Figures

List of Tables

Abstract

The recent observation of non-trivial azimuthal correlation in high-multiplicity Proton-Proton (pp) collisions at the Large Hadron Collider (the so called **ridge** phenomena) aroused a considerable interest. The reason that similar correlation were observed previasly in heavy ion collisions in LHC and Relativistic Heavy-Ion Collier (RHIC), where they were considered as a vital sign of the creation of Quark Gluon Plasma (QGP). These correlation appear natural in the QGP frame work, duo to the large interactions between the particles emitted in the collisions (final state interaction), these interactions however absent in pp collisions. This lead to the study of new possible mechanisms for the ridge phenomena, in particular a new approach based on quantum interference and Multi-pParton Interaction (MPI) was developed. This formalism was recently secssesfully aplide to symmetric correlators.

In this thesis we study the influence of quantum interference and colour flow on three point correlations described by asymmetric cumulants in high multiplicity events in pp collisions. We use the model previously developed for the study of the collectivity in symmetric cumulants. We show that the resulting three point asymmetric cumulant is in qualitative agreement with the experimental data for the same parameters of the model as it was with the symmetric cumulants. Our results show that the initial state correlations must play a major role and may be even dominant in the explanation of the correlations in high multiplicity pp events.

We formulate the goals for our research in the introduction. in part two we review the basic ideas of the approach for high multiplicity pp collisions based on quantum interference and multi-parton interactions. In chapter three we carry the actual computation of the three-point cumulant and study the dependence of the momenta and number of emitted particles and compare it to experimental data.

List of symbols and abbreviations

pp	:	Proton-Proton
LHC	:	Large hadron collider
QGP	:	Quark gluon plasma
QCD	:	Quantum chromo dynamic
MPI	:	Multi parton interaction
AA	:	heavy-ions collisions
GeV	:	Giga electron Volt
ZYAM	:	Zero yield at minimum
sc	:	Symmetric cumulant
ac	:	Asymmetric cumulant
PDF	:	Parton Distribution Function
DGLAP	:	Dokshitzer–Gribov–Lipatov–Altarelli–Parisi
GPD	:	General partonic distribution
LT	:	Leading twist
pQCD	:	Perturbative QCD
DPS	:	Double parton scattering
NP	:	Non-perturbative
PT	:	Perturbative Theory
LPHD	:	local parton-hadron duality
CGC	:	Colour glass condensate

Chapter 1

Introduction

Recent studies of high-multiplicity proton-proton (pp) collisions at the Large Hadron Collidor (LHC) [1, 2, 3, 4, 5], have observed a collective behavior that was considered to be a sign for the creation of Quark-Gluon Plasma (QGP) when it was observed in heavy-ion collisions (AA) before [5, 6, 7, 8, 9], the so called **Ridge** phenomena.

The ridge phenomena is natural in heavy-ion collision where it can be explained by strong final state interactions of the emitted particles, however in pp collisions we expect much smaller transverse size and density in the collision, more over, these collisions are generally well described by Monte Carlo generators that assume independent emitted particles. consequently we need a new approach to ridge not based on strong final state interactions.

A new approach, based on quantum interference and Multi-Parton Interaction (MPI) was proposed in references [10, 11] to explain such collective behavior. Using this model we can calculate the azimuthal correlations in pp collisions and explain the emergence of the ridge phenomena.

The studies in papers [10, 11] was devoted to symmetric cumulants, recently ATLAS measured a new type of correlations in high-multiplicity pp collisions, the 3-point asymmetric cumulant [12].

In this thesis we use the approach of papers [10, 11] to calculate the 3-point asymmetric cumulant. We study the dependence on the momenta and multiplicity of emitted particles, we find our results are in good agreement with the experimental data.

The thesis is organised in the following way:

In chapter 2 we review the basic formalism developed in papers [10, 11] to study the collective behavior in high-multiplicity pp collisions. In particular, in section 2.1 we explain the geometry of high-multiplicity pp collisions and explain the basic experimental and mathematical tools used to describe this correlations (the so called

Flow analysis), in section 2.2 we review the basic ideas of multi-parton interaction, in section 2.3 the model of [10, 11] for the study of the correlations in pp collisions.

In chapter 3 we carry the actual calculations of the 3-point asymmetric cumulant. In particular, in section 3.1 we reestablish the physical problem we want to solve, in section 3.2 we go summaries the formalism we will use next, in section 3.3 we find the 3-point asymmetric cumulant for the case of 3 partonic interactions and 3 emitted particles and find the momenta dependence, in section 3.4 we extand the result to the case of general numbers of partonic interactions and emitted particles, and compare the multiplicity dependence to the experimental results.

The conclusions are presented in chapter 4.

Chapter 2

Review of Quantum Interference Approach

2.1 Ridge and Cumulants

2.1.1 Heavy-Ion Collisions

Experimentalists have been using heavy-ion (AA) collisions to create and study Quark-Gluon Plasma (QGP) since it was discovered in the beginning of the millennium [13]. One of the ways to study the emergence of QGP in AA collisions is to look at multi-particle production event, and quantify the distribution of the emitted particles rapidity and azimuthal directions related to reaction plane angle (The reaction plain is the plains that contains the centers of the colliding particles and is parallel to the beam axis).

In Fig. 2.1 we depict a simplified diagram taken from ref. [14], of the geometry of a collision, projected onto the plane transverse to the beam axis. To be able to compare measurements of the azimuthal distribution for single particles from different events we need to know the reaction plane angle for each event and shift the measurements accordingly. One way to get around that is by looking at the correlations between particles instead of the distribution of a single particle relative to reaction plain.

Looking at measurements like the ones shown in Fig. 2.2 (taken from ref. [6] and ref. [7]). We can see here several clear trends [6, 7], in particular we see that regardless of the the azimuthal difference between the particles, the correlation is almost independent of the the pseudorapidity difference, where the pseudorapidity (η) and rapidity (y) are defined as:

$$\eta = -\ln\left(\tan\left(\frac{\theta}{2}\right)\right), \tag{2.1}$$

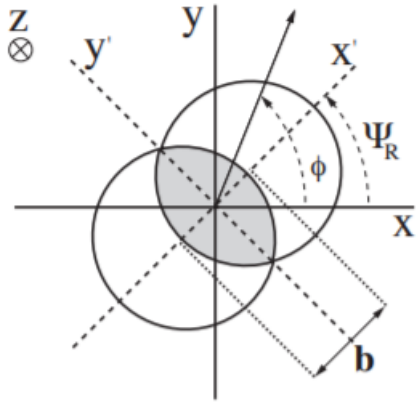

Figure 2.1: A diagram of a coordinates system used in flow analysis. The Z-axis is the beam axis coming out of the page, the XY plane the the transverse plane, where the X axis, or the azimuthal 0, is chosen arbitrarily. The $X'Y'$ plane is the XY plane rotated by the reaction plane angle $\mathbf{\Psi}_R$, where the reaction plane is the plane containing the beam axis and the two centers of the nuclei, making it that both centers are on the X' axis, b is the impact parameter given by the projection of the distance between the centers of the nuclei, and ϕ is the azimuthal angle of an emitted particle. diagram taken from [14].

$$y = \frac{1}{2} \ln \left(\frac{E + p_z}{E - p_z} \right). \tag{2.2}$$

Here θ is the angle between the particle momentum and the beam axis, E is the particle energy and p_z is it's momentum along the beam axis. Recall that for massless or ultra-relativistic particles this is the same as the pseudorapidity that is used in the measurements, $y \approx \eta$.

The phenomena where the azimuthal correlations are almost independent of the pseudorapidity difference, is called **ridge**. This correlation between very distant in rapidity particles is a sign of collective behavior that points to a the existence of a medium, that way information can be shared between the emitted particles. The existence of such a medium is somewhat expected in AA collisions where we axpact the creation of QGP. As was stated at the beginning of the chapter, one of the many research topics that we study via AA collisions is the existence and properties of QGP. The collective behavior in PbPb collisions have also been observed in ref. [5, 8, 9, 15, 16].

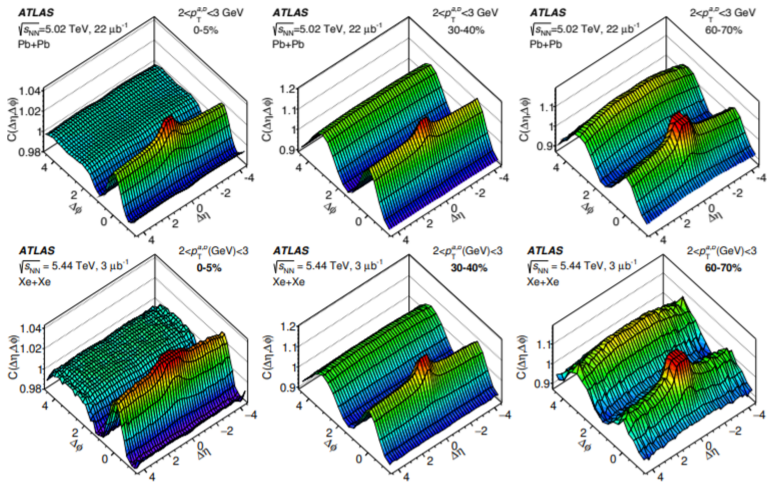

Figure 2.2: 3D Plots of two particles correlations, $C(\Delta\eta, \Delta\phi)$, from AA collisions as a function of the $\Delta\phi$, the azimuthal difference between the particles, and $\Delta\eta$, the pseudorapidity difference between the particles, Pb+Pb on top [6], and Xe+Xe on the bottom [7], for different centrality intervals, $0-5\%$ (left), $30\%-40\%$ (center) and $60\%-70\%$ (right). Both experiments looked at particles with transverse momentum in the range of $2\text{GeV} < p_t < 3\text{GeV}$ and pseudorapidity in the range $|\eta| < 2.5$, $\sqrt{s_{NN}}$ is the center of mass energy of the collisions in each experiment. We can see few clear trends from those measurements, the most important one for us is the apparent independence of the correlation on the pseudorapidity difference, this phenomena is called **ridge**. The correlations peak around $\Delta\phi = \Delta\eta = 0$, this is partly a non-flow contribution that comes from looking at particles that are originating from the same jet.

2.1.2 High Multiplicity Proton-Proton Collisions

In High Multiplicity Proton-Proton (pp) collisions transverse size of the collision is very small in comparison to AA collisions, for example, in ultra-relatevistic Pb+Pb collitions the ratio of gluon density is much higher compared to pp collisions. So it is not expected for QGP to be created in those systems (sometimes called small systems, relative to large systems created in AA collisions). Therefore we cannot explain the correlations between high rapidity difference particles by the emergence of new medium. The particles emitted from a pp collision should act almost as free particles with no sign for a collective behavior, in other words, we do not expect ridge in pp collisions.

the first observation of ridge in pp collisions was made by the CMS collaboration in 2010 [1]. Those measurements and more that came out since, such as the ones in [2, 3, 4, 5] as depicted in Fig. 2.3 and Fig. 2.4, lead us to ask the question how do the particles that are almost completely free embody this collective behavior? We need to find a different origin for correlations in pp collisions other then final state interactions. [htbp]

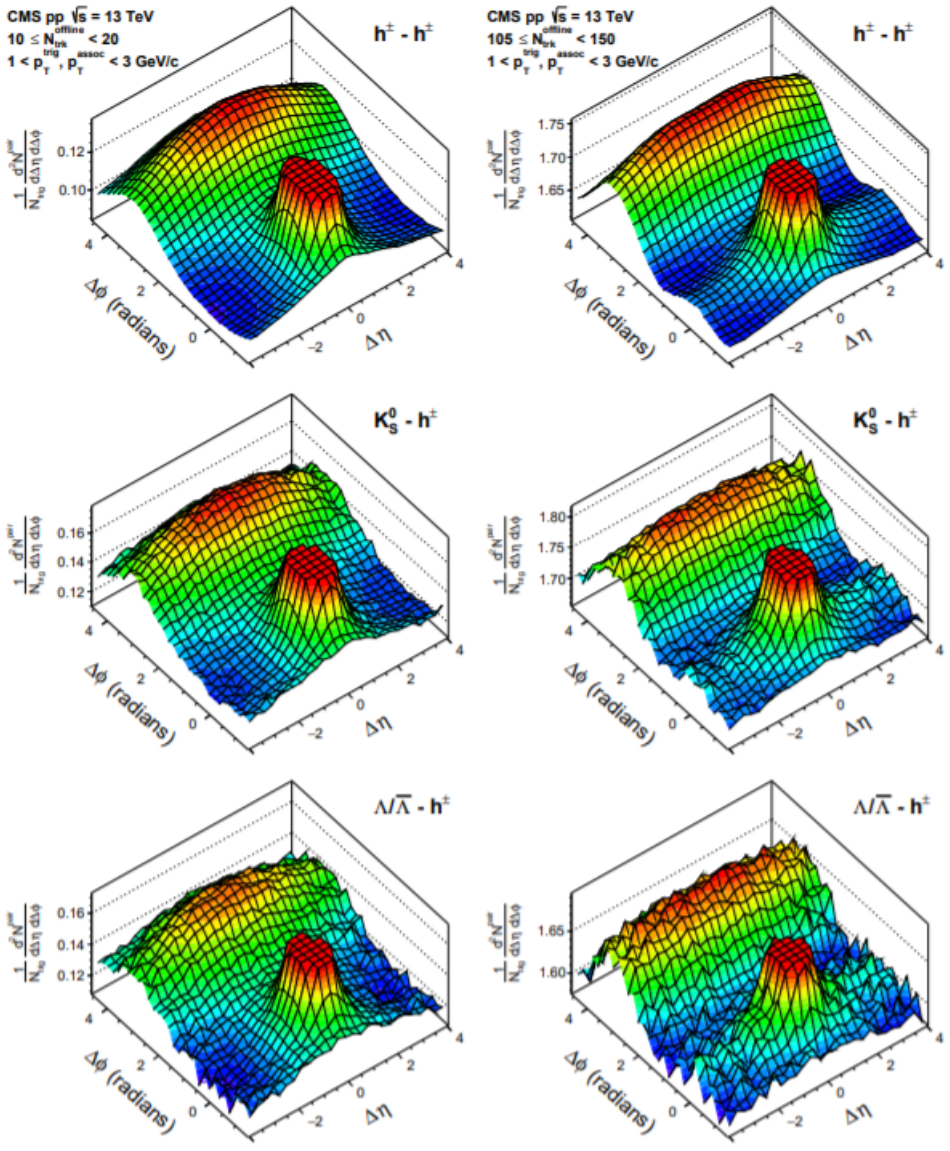

Figure 2.3: Correlations for 2 particles in a proton-proton collision as a function of the $\Delta\phi$, the azimuthal difference, and $\Delta\eta$, the pseudorapidity difference, from [2]. The different plots show different selection parameters. From top to bottom: only charged particles (top), events with kion particles (middle), and and events with lambda (or anti-lambda) particles (bottom). Low Multiplicity events (left) and high multiplicity events (right). As we saw in the correlations in AA collisions, the correlations peak at two regions. The correlations peak around $\Delta\phi = \Delta\eta = 0$, is mostly a non-flow contribution that comes from from looking at particles that are originating from the same jet, like it was in Fig. 2.2. The peak around $\Delta\phi$ π is very similar to the same peak as in the AA collisions, including the very weak dependence on the pseudorapidity difference.

[htbp]

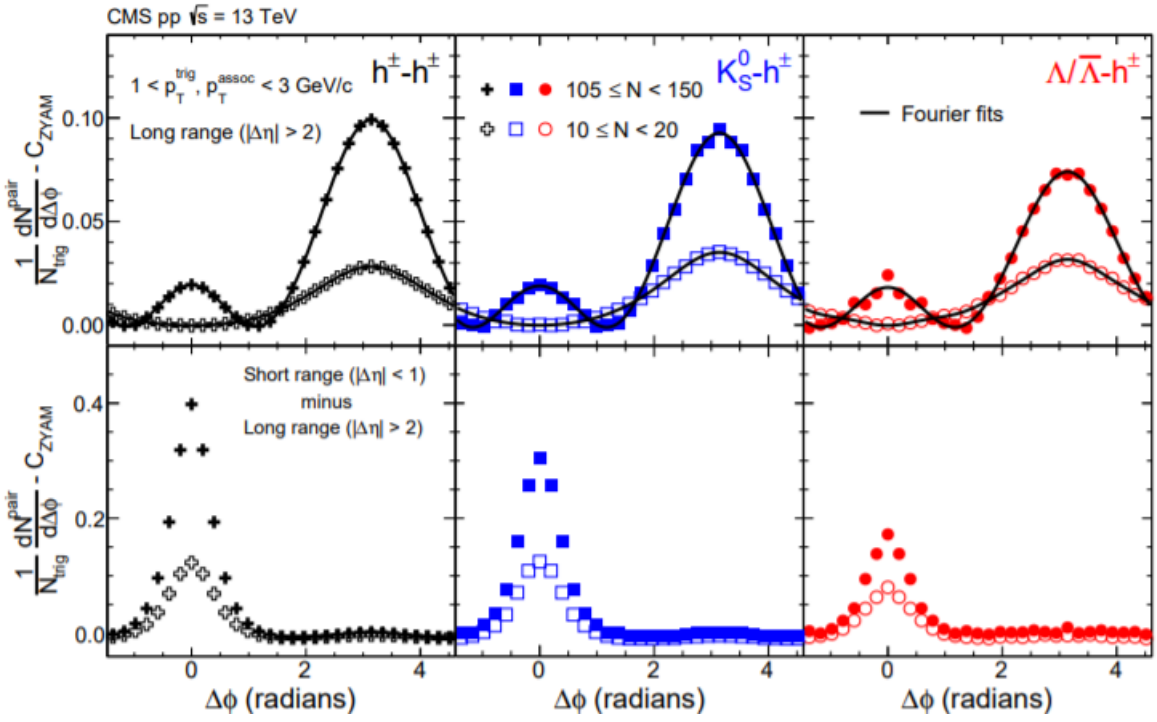

Figure 2.4: Correlations for 2 particles in a proton-proton collision after applying ZYAM procedure, the ZYAM procedure is a shift to the measurements be 0 at minimum, as a function of the $\Delta\phi$, the azimuthal difference, from [2]. On the top there are long-range correlations, for particles pairs with high $\Delta\eta$, and on the bottom are short range correlations, particles pairs with low $\Delta\eta$. Filled symbols show multiplicity between 105 and 150, empty symbols show multiplicity between 10 and 20. The Different colors show different types of events: only charged particles (black), events with kion particles (blue), and and events with lambda (or anti-lambda) particles (red). The black line is a Fourier fit.

2.1.3 Cumulants

When we study correlations between s particles we want to be sure that what we calculate comes from the correlations of **all** particles. To do this we need to define the cumulants. Let us assume that the 1-particle momentum distribution function as defined in [17]:

$$f(\mathbf{p}) \equiv \frac{dN}{d^3p}. \tag{2.3}$$

Here dN is the differential multiplicity, or the number of particles within a small momentum space $d^3\boldsymbol{p}$. To calculate the properties of the emitted particles we can think of taking the average with respect to the momentum distribution function, for example we can take the average of a function $F(\mathbf{p})$ over the azimuthal component of the particle momentum, leaving us with a function of the transverse momentum

and rapidity:

$$\langle F(\mathbf{p})\rangle(p_t,y)=\frac{\int F(\mathbf{p})\,f(\boldsymbol{p})\,d\phi}{\int f(\boldsymbol{p})\,d^3p}, \tag{2.4}$$

here $\langle\ \rangle$ marks an average. The correlation between two different particles is then defined by the 2-particles distribution function:

$$f(\mathbf{p}_1,\mathbf{p}_2)\equiv\frac{d^2N}{d^3p_1d^3p_2}, \tag{2.5}$$

here $\mathbf{p}_1$ and $\mathbf{p}_2$ are the 3-momentum of the 2 different particles. If the two particles are not correlated the distribution function will factorize $f(\mathbf{p}_1,\mathbf{p}_2)=f(\mathbf{p}_1)\,f(\mathbf{p}_2)$, however in general case we have:

$$f(\mathbf{p}_1,\mathbf{p}_2)\equiv f(\mathbf{p}_1)\,f(\mathbf{p}_2)+f_c(\mathbf{p}_1,\mathbf{p}_2), \tag{2.6}$$

here $f_c(\mathbf{p}_1,\mathbf{p}_2)$ denotes the correlated part of the distribution. An important note here is that for a single particle $f_c(\mathbf{p})\equiv f(\mathbf{p})$ since we can't break it down to smaller pieces.

This approach can be generalized to any number of particles correlations, for example, the 3-particles distribution is given by: ******

$$f(\boldsymbol{p}_1,\boldsymbol{p}_2,\boldsymbol{p}_3)\equiv\frac{d^3N}{d^3p_1d^3p_2d^3p_3}=f_c(\boldsymbol{p}_1)\,f_c(\boldsymbol{p}_2)\,f_c(\boldsymbol{p}_3)+\sum_{j=1}^{3}f_c(\boldsymbol{p}_j)\,f_c\left(\{\boldsymbol{p}_k\}_{k\neq j}\right)+f_c(\boldsymbol{p}_1,\boldsymbol{p}_2,\boldsymbol{p}_3), \tag{2.7}$$

where the first term on the right-hand side is the product of the 1-particles distributions, the second term comes from the pair correlations within the three particles, and the last term is the 3-particles true correlation. In general to decompose the s-particles distribution function we first take all possible partitions of $\{\boldsymbol{p}_1,\boldsymbol{p}_2,\ldots,\boldsymbol{p}_s\}$. For each subset $\{\boldsymbol{p}_{j_1},\boldsymbol{p}_{j_2},\ldots,\boldsymbol{p}_{j_m}\}$ We find the corresponding correlated function, $f_c(\boldsymbol{p}_{j_1},\boldsymbol{p}_{j_2},\ldots,\boldsymbol{p}_{j_m})$. The contribution of a given partition is the product of the contributions of each subset. Finally, $f(\boldsymbol{p}_1,\boldsymbol{p}_2,\ldots,\boldsymbol{p}_s)$ is the sum of the contributions of all partitions.

Using those relations we can express the true correlated distributions in terms of the full correlation functions, for example, for 1, 2 and 3 particles:

$$\begin{aligned}
f_c(\boldsymbol{p}) &= f(\boldsymbol{p})\\
f_c(\boldsymbol{p}_1,\boldsymbol{p}_2) &= f(\boldsymbol{p}_1,\boldsymbol{p}_2)-f(\boldsymbol{p}_1)\,f(\boldsymbol{p}_2)\\
f_c(\boldsymbol{p}_1,\boldsymbol{p}_2,\boldsymbol{p}_3) &= f(\boldsymbol{p}_1,\boldsymbol{p}_2,\boldsymbol{p}_3)-f(\boldsymbol{p}_1,\boldsymbol{p}_2)\,f(\boldsymbol{p}_3)-f(\boldsymbol{p}_1,\boldsymbol{p}_3)\,f(\boldsymbol{p}_2)-f(\boldsymbol{p}_2,\boldsymbol{p}_3)\,f(\boldsymbol{p}_1)\\
&+ 2f(\boldsymbol{p}_1)\,f(\boldsymbol{p}_2)\,f(\boldsymbol{p}_3).
\end{aligned} \tag{2.8}$$

This true correlations f_c are called cumulants.

2.1.4 Flow Analysis

Studying the azimuthal distributions and correlations of particles gave rise to the subject of "flow analysis". Flow analysis studies the anisotropic behavior in the azimuthal direction by breaking down the distribution of the emitted particles into a Fourier expansion [14], for example:

$$f(\boldsymbol{p}) = \frac{1}{2\pi E}\frac{dN}{p_t dp_t dy}\left(1 + 2\sum_{n=1}^{\infty} v_n(p_t, y)\cos\left(n\left(\phi - \boldsymbol{\Psi}_R\right)\right)\right), \tag{2.9}$$

here $f(\boldsymbol{p})$ is the 1-particle momentum distribution function as defined in eq. (2.3), y is the rapidity of the particle, E is the energy of the particle, p_t is the transverse momentum of the particle, ϕ is its azimuthal coordinate of the particles momentum, $\boldsymbol{\Psi}_R$ is the azimuthal angle between the X-axis, that was chosen arbitrarily, and the projection of the vector connecting the two centers of the nuclei onto the XY plane, also known as the reaction plane angle, and v_n are the Fourier coefficients, also known as flow harmonics.

It is important to note that in general v_n are functions of the transverse momentum and pseudorapidity of the emitted particles, but since we are looking at the case of ridge we can neglect the pseudorapidity. The coefficients v_n can be defined by the following average over the azimuthal angle ϕ:

$$v_n(p_t) \equiv \left\langle e^{in(\phi - \boldsymbol{\Psi}_R)}\right\rangle = \left\langle cos\left(n\left(\phi - \boldsymbol{\Psi}_R\right)\right)\right\rangle = \frac{\int e^{in(\phi - \boldsymbol{\Psi}_R)} f(\boldsymbol{p})\, d\phi}{\int f(\boldsymbol{p})\, d^3p}. \tag{2.10}$$

In a similar way we can decompose the correlations into Fourier expansion, for example, the two particle correlation can be found using the 2-particles distribution function by taking the average over both azimuthal components:

$$\left\langle e^{in(\phi_1 - \boldsymbol{\Psi}_R)} e^{-in(\phi_2 - \boldsymbol{\Psi}_R)}\right\rangle = \left\langle e^{in(\phi_1 - \phi_2)}\right\rangle = \frac{\int e^{in(\phi_1 - \phi_2)} f(\boldsymbol{p}_1, \boldsymbol{p}_2)\, d\phi_1 d\phi_2}{\int f(\boldsymbol{p}_1, \boldsymbol{p}_2)\, d^3p_1 d^3p_2}. \tag{2.11}$$

In such a way we get read of the explicit dependence on the position of the reaction plane.

Flow analysis is the study of the flow harmonics, v_1 and v_2 are commonly known as direct and elliptic flow respectively, v_1 corresponds to a preference to a single direction, v_2 represents a symmetry by a half way rotation around the Z-axis, this symmetry is expected in a system of AA collision. In general v_n are sensitive to the geometry of the collision, that is why higher order flow harmonics, $n > 2$, are also important in studying the collision structure.

Using the approach of the of the previous section correlations between many particles can be reduced to sums of correlations between smaller numbers of particles,

similar to the s-particles distribution functions, i.e. the two particles correlation can be reduced to:

$$\left\langle e^{in(\phi_1-\phi_2)}\right\rangle = \left\langle e^{in\phi_1}\right\rangle \left\langle e^{-in\phi_2}\right\rangle + \left\langle e^{in(\phi_1-\phi_2)}\right\rangle_c . \tag{2.12}$$

Here $\left\langle e^{in(\phi_1-\phi_2)}\right\rangle_c$ is just the two particles cumulant defined in the previous section.

If we assume a perfect detector it is easy to see that $\left\langle e^{in\phi_j}\right\rangle$ vanish due to axial symmetry of the system for any $n \neq 0$, since it implies also an average over the reaction plane angle, there for it is not the same as v_n. In the same way, all the correlations of the form $\left\langle e^{i\sum_{j=1}^{s} n_j\phi_j}\right\rangle$ where $\sum_{j=1}^{s} n_j \neq 0$ also vanish.

2.1.5 Calculating Cumulants From Data

Determination the s-particles cumulant out of measurements is done with few steps. First, we calculate the single-event multi-particle correlations, for example the 2- and 4-particles single event correlations are given by:

$$\begin{aligned} \langle 2\rangle_n &\equiv \left\langle e^{in(\phi_1-\phi_2)}\right\rangle = \frac{1}{P_{m,2}}{\sum_{i,j}}' e^{in(\phi_i-\phi_j)}, \\ \langle 4\rangle_n &\equiv \left\langle e^{in(\phi_1+\phi_2-\phi_3-\phi_4)}\right\rangle = \frac{1}{P_{m,4}}{\sum_{i,j,k,l}}' e^{in(\phi_i+\phi_j-\phi_k-\phi_l)}. \end{aligned} \tag{2.13}$$

Where $\langle s\rangle_n$ is the single event n'th s-particle correlation, m is the multiplicity, or number of emitted particles in the event, $P_{m,s} \equiv m!/(m-s)!$ and the sum $\sum'$ means all the indices are different. We then average over all events:

$$\langle\langle s\rangle\rangle_n \equiv \frac{\sum_{events}\left(W_{\langle s\rangle}\right)_i \langle s\rangle_n}{\sum_{events}\left(W_{\langle s\rangle}\right)_i}. \tag{2.14}$$

Where $\langle\langle s\rangle\rangle_n$ denote the averaged n'th s-particles correlation, first over all particles and then over all events. $\left(W_{\langle s\rangle}\right)_i$ is the weight of the i'th event, which are used to account for the multiplicity variations in different events, we can take them to be $\left(W_{\langle s\rangle}\right)_i = \delta_{m_i,M}$ to look only at events with a fixed multiplicity M, or $\left(W_{\langle s\rangle}\right)_i = P_{m_i,s}$ for general multiplicity, picking this option will result in $\langle\langle s\rangle\rangle_n$ independent of multiplicity, or many other functions.

The connection between the double bracketed correlations and the cumulants is discussed in detail in [18], we write here the cumulants for $s = 2, 4, 6$, marked as $c_n\{s\}$, functions of the transverse momenta and pseudorapidity of all s particles being correlated, to provide examples that are helpful to see the patterns:

$$c_n\{2\} = \langle\langle 2\rangle\rangle_n$$

$$
\begin{aligned}
c_n\{4\} &= \langle\langle 4\rangle\rangle_n - 2\left(\langle\langle 2\rangle\rangle_n\right)^2 \\
c_n\{6\} &= \langle\langle 6\rangle\rangle_n - 9\langle\langle 4\rangle\rangle_n\langle\langle 2\rangle\rangle_n + 12\left(\langle\langle 2\rangle\rangle_n\right)^3
\end{aligned} \tag{2.15}
$$

Those examples assume both large average multiplicity and a detector with uniform acceptance, more general definitions can be found in [14, 18]. The cumulants are defined in such a away that for all $c_n\{2k\}$ for $k > 1$ they vanish unless there is a sizable $s = 2k$ correlation. For example, if we assumed that there are no 4-particle correlations we could expand $\langle\langle 4\rangle\rangle_n$ into a product of a pair 2-particle correlations, like so:

$$
\langle\langle 4\rangle\rangle_n = \left\langle\left\langle e^{in(\phi_1+\phi_2-\phi_3-\phi_4)}\right\rangle\right\rangle \approx 2\left\langle\left\langle e^{in(\phi_1-\phi_3)}\right\rangle\right\rangle\left\langle\left\langle e^{in(\phi_2-\phi_4)}\right\rangle\right\rangle = 2\left(\langle\langle 2\rangle\rangle_n\right)^2 \tag{2.16}
$$

Plugging this result back to $c_n\{4\}$ in eq. (2.15) we see it vanish identically, this will be the same for $c_n\{6\}$ and any other $c_n\{s\}$ for $s > 2$.

Using the cumulants we can approximate the flow harmonics, with $c_n\{s\}$ giving us better approximation for higher values of s, using the results from [18] we can write the approximations:

$$
\begin{aligned}
\left(v_n\{2\}\right)^2 &= c_n\{2\} \\
\left(v_n\{4\}\right)^4 &= -c_n\{4\} \\
\left(v_n\{6\}\right)^6 &= c_n\{6\}/4
\end{aligned} \tag{2.17}
$$

The fact that $v_n\{2k\} \propto (-1)^{k+1} c_n\{2k\}$ is called collectivity.

2.1.6 Three-Particles Cumulant

So far we have only talked about symmetric cumulants, all the particles have the same flow harmonic index, but this limit us to only look at even number of particles, that way the reaction plane angle dependent cancels out. We can extend the notion of the cumulant to odd numbers of particles by allowing correlations between flow harmonics with different indices. For the case of 3-particle correlations it is common to define them in a similar way to the 4-particle correlations where the two particles with a negative weight are chosen to be the same one:

$$
\left\langle e^{in(\phi_1+\phi_2-2\phi_3)}\right\rangle \equiv \frac{\int e^{in(\phi_1+\phi_2-2\phi_3)}\frac{d^3N}{d^3\boldsymbol{p}_1 d^3\boldsymbol{p}_2 d^3\boldsymbol{p}_3}d\phi_1 d\phi_2 d\phi_3}{\int \frac{d^3N}{d^3\boldsymbol{p}_1 d^3\boldsymbol{p}_2 d^3\boldsymbol{p}_3}d^3p_1 d^3p_2 d^3p_3}. \tag{2.18}
$$

To calculate it from data we can define the single event average is then given by:

$$
\langle 3\rangle_{n,n|2n} \equiv \left\langle e^{in(\phi_1+\phi_2-2\phi_3)}\right\rangle = \frac{1}{P_{m,3}}{\sum_{i,j,k}}' e^{in(\phi_i+\phi_j-2\phi_k)}. \tag{2.19}
$$

We can also considered taking the harmonic indices with the opposite sign, but if we assume a perfect detector we find that correlation is just the complex conjugate of the one we defined, $\langle 3\rangle_{n,n|2n} = \left(\langle 3\rangle_{-n,-n|-2n}\right)^* = \left(\langle 3\rangle_{2n|n,n}\right)^*$, and since the correlations are real, from the symmetry between the particles, they are the same. Taking this correlation and averaging over many events gives us the average correlation, $\langle\langle 3\rangle\rangle_{n,n|2n}$, from which we get the 3-particles cumulant also known as the 3-particles asymmetric cumulant:

$$ac_{n,n|2n}\{3\} = \langle\langle 3\rangle\rangle_{n,n|2n}\,. \tag{2.20}$$

Note that like the 2-particles cumulant, the asymmetric 3-particles cumulant is the same as the 3-particles average correlation, that is because it is impossible to break the correlations down into pairs without separating the angle with the greater weight from itself. The 3-particles cumulant is called asymmetric cumulant as it breaks the symmetry between the flow harmonics indices, but this property is not limited to 3 particles correlations, we can define cumulant with different flow indices for any number of particles, see ref. [12] for example, where 4-particles correlation defined as $\langle\langle 4\rangle\rangle_{n,m|n,m}$ was studied. As long as the sums of the positive and negative indices are equal the correlation and associated cumulants are well defined. But even then, in general it is common to call the even number particles cumulants the symmetric cumulants and the asymmetric cumulants stand for the odd number cumulants. For the sake of brevity and to follow naming conventions it is common to write $ac_{n,n|2n}\{3\}$ as $ac_n\{3\}$.

In Fig. 2.5 we depict the results of the measurements of $ac_2\{3\}$ there were published by the ATLAS collaboration in 2019 [12] for both pp collisions and AA collisions. We see the correlations in pp collisions are the same order of magnitude as in AA collisions. We expected to see such collective behavior in the presence of QGP, that can be the medium for the information between the particles, but it's appearance in pp collisions as well is the reason we need to develop a model that can explain this behavior for free particles. In Fig. 2.6, taken from [19], we see the same measurements with the non-flow contributions reduced, leaving a sizable flow contribution that need to be accounted for.

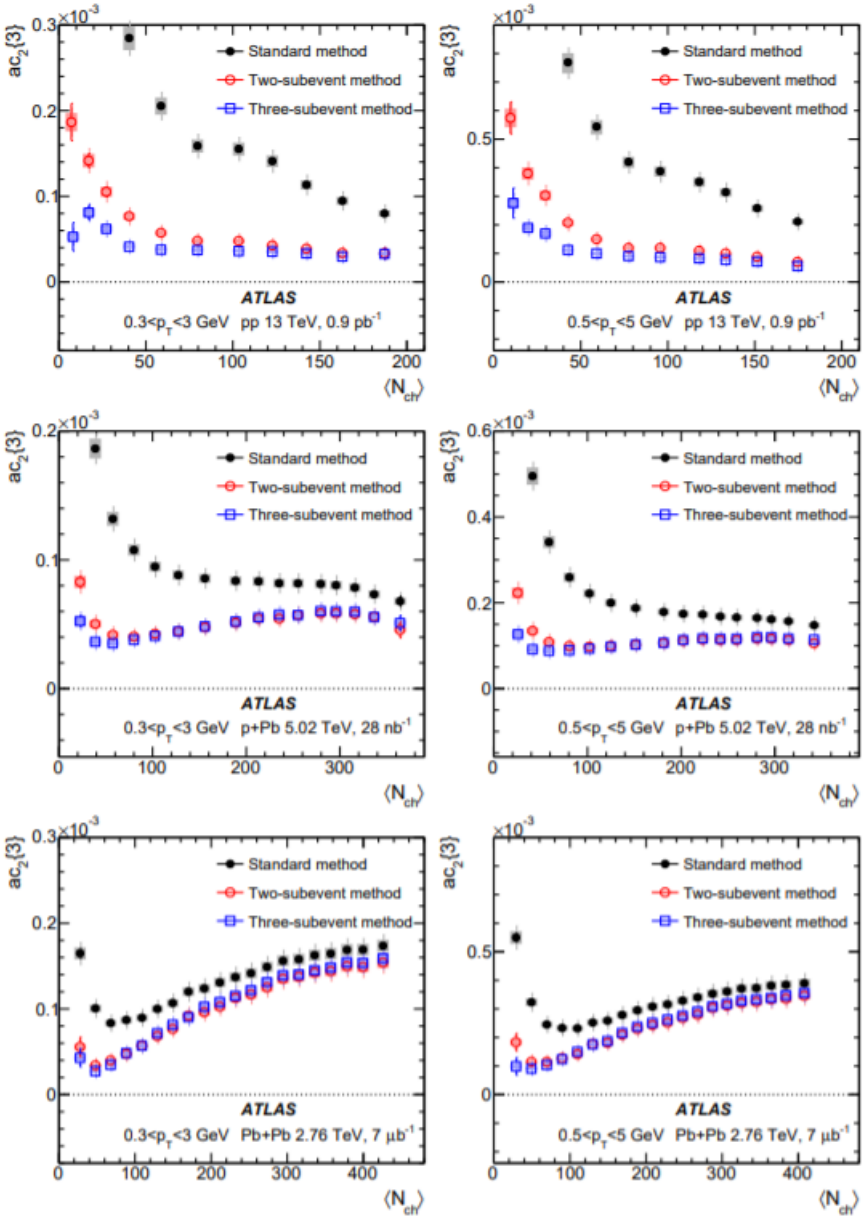

Figure 2.5: The second asymmetric cumulant for 3 particles $ac_2\{3\}$, or the azimuthal correlations $\left\langle e^{i2(\phi_1+\phi_2-2\phi_3)}\right\rangle$ as a function of $\langle N_{ch}\rangle$, the number of charged particles detected, in pp (top), p+Pb (middle) and Pb+Pb (bottom) collisions for different ranges of the emitted particles transverse momentum, $0.3\text{GeV} < p_T < 3\text{GeV}$ (left) and $0.5\text{GeV} < p_T < 5\text{GeV}$ (right), as measured by [12]. The 2(3)-sub event methods refer to dividing the detector into 2(3) equal parts respectively in the range $|\eta| < \eta_{max} = 2.5$ and taking the particles from the different parts, this gives us more confidence that the correlations come from the existence of ridge, and don't just arise from taking particles out of the same jet, see Fig. 2.2 and Fig. 2.3.

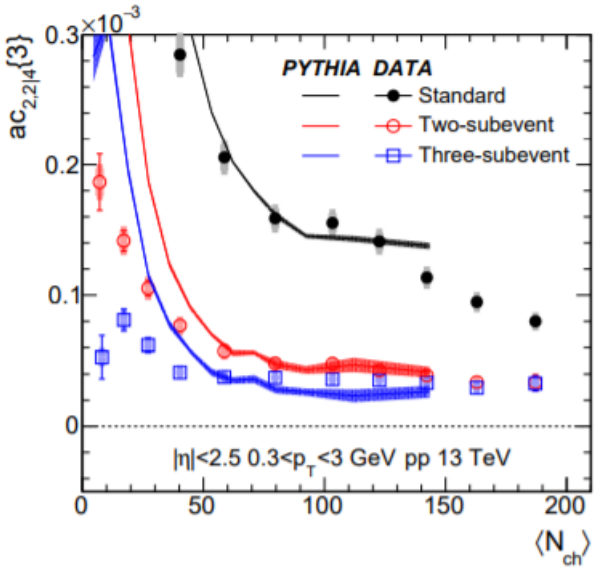

Figure 2.6: The second asymmetric cumulant for 3 particles $ac_2\{3\}$, or the azimuthal correlations $\left\langle e^{i2(\phi_1+\phi_2-2\phi_3)}\right\rangle$ as a function of $\langle N_{ch}\rangle$, the number of charged particles detected, in pp collisions for emitted particles with transverse momentum in the range $0.3\text{GeV} < p_T < 3\text{GeV}$ with the non-flow contributions reduced. The reduction of the non-flow contribution is done by [19]

2.2 Multi-Parton Interactions

The processes in which several partons from one nuclion collide from several partons from another nuclion are called Multi-Parton Interaction (MPI). A diagram of an MPI process with an arbitrary amount of partonic interactions is depicted in Fig. 2.7 (right). Each partonic interaction involves one parton from hadron h_a and one parton from haron h_b and results in a hard event, producing 2 or more hard out-going partons. In each collision there can be any number of MPIs. In Fig. 2.7 (left) we see an example of a collision with only two hard processes, this case is usualy called Double Parton Scattering (DPS) and will be discussed in detail later this chapter.

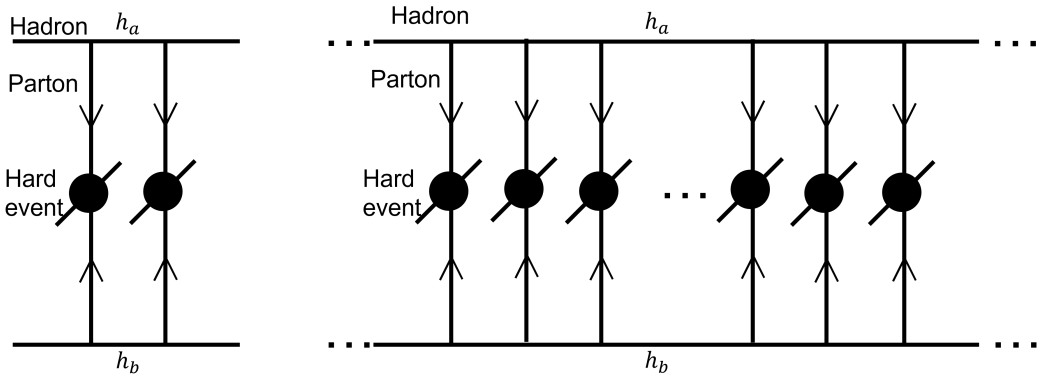

Figure 2.7: Two diagrams of amplitudes for two hadrons collision, the horizontal lines represent the hadrons h_a and h_b, the vertical arrows represent the hard partons, the circles represent different hard events, and the diagonal lines represent out-going particles. The cross section of the process is the square of those diagrams. On the left we see an event with only two partonic interactions, on the right we see an event with an arbitrary amount of partonic interactions, where the points indicate the possibility for many more partoninc interactions not shown on the diagram.

2.2.1 Hard Process in QCD

In this section we will discuss the example of a collision with a single partonic interaction and define tools that will help us work with partonic interactions.

An important parameter in a hadronic interaction is the hard scale Q^2, which characterises the transverse scale of the hard event.

The behavior of a parton inside a hadron is only defined in a quasi-probabilistic manner. For each parton we define the parameter x, called the longitudinal fraction,

or the light-cone hadron's momentum fraction of the parton. Given a hadron with 4-momentum P^μ and a parton with initial 4-momentum as p^μ, we define:

$$x \equiv \frac{p_0 + p_z}{P_0 + P_z}. \tag{2.21}$$

This parameter was first defined by Bjorken and is often depicted as x_B, here the index z indicates the momentum component along the beam axis, and we see that x goes from 0 to 1. Assuming the partons are massless, the parton's momentum is therefore defined by x and it's transverse momentum.

As seen in Fig. 2.8, the two hadrons are a bundle of many partons, in this example, a parton from h_a with momentum $x, \vec{k}$ and a parton from h_b with momentum of $x', \vec{k}'$ interact and two new particles with momentum q_i and q_j are emitted. Here we need to separate two types of cross sections, the first is the hadronic cross section, that is the cross section of the two hadrons to produce the particles q_i and q_j, or any other products, this is the cross section of the entire diagram, this cross section can be measured. In the grey dashed rectangle there is a diagram of just two parton interacting with no connection to the hadrons, this is the partonic cross section that can be calculated via QCD with fundamental particles, but never measured directly.

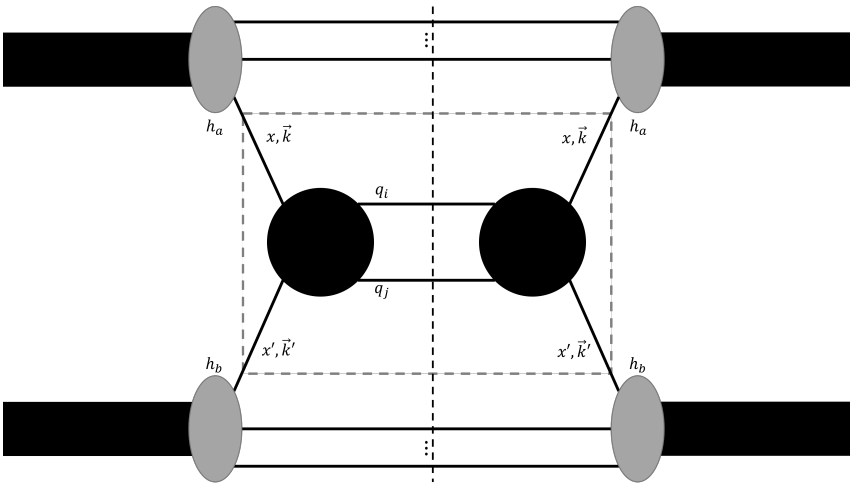

Figure 2.8: A diagram of hadronic cross section, of two hadrons colliding via a single partonic interaction. Each parton is contributes a parton that then interact with the other parton, the black circles represent the QCD processes that can originate from the two partons and emit two new particles. The grey dashed rectangle represent the diagram of a partonic cross section.

To find the hadronic cross section of this process we need to know the probability to find a parton with momentum fraction x inside a hadron, and use it to reduce the

problem to the partonic cross section diagram. Those probabilities are dependant on the hard scale Q^2 of the process and on QCD processes inside the hadron. We say that when we look at an event with hard scale of Q^2, the quasi-probability to find a parton of type j with momentum fraction of x inside a hadron is given by $f_j\left(x,Q^2\right)$, where f is known as the standard Parton Distribution Function (PDF).

The PDFs satisfy a number of the following sum rules. The first is the valence rule, for every hadron the integral over x for the valence partons need to be the number of those partons in that hadron. For example, in a proton there are 2 valence up quarks and 1 valence down quark so we write:

$$\int_0^1 dx\left[f_u\left(x,Q^2\right)-f_{\overline{u}}\left(x,Q^2\right)\right]=2 \qquad \int_0^1 dx\left[f_d\left(x,Q^2\right)-f_{\overline{d}}\left(x,Q^2\right)\right]=1. \tag{2.22}$$

For all other flavors of quarks, i.e. $f\neq u,d$, we write $f_j\left(x,Q^2\right)=f_{\overline{j}}\left(x,Q^2\right)$. This implies that for every hadron we will need a different set of PDFs, but we only work with protons so we don't need to keep indices for the hadron type.

The other sum rule is the condition that the total momentum fraction is 1:

$$\int_0^1 dx\, x\left[f_g\left(x,Q^2\right)+\sum_f\left(f_f\left(x,Q^2\right)+f_{\overline{f}}\left(x,Q^2\right)\right)\right]=1. \tag{2.23}$$

To define the way the PDF change for different hard scales we need to define the splitting functions. The splitting function $P_{j\leftarrow i}\left(z\right)$ is proportional to the quasi-probability of a parton of type i with momentum fraction x/z to split into two partons that one of them is real particle of type j with momentum fraction z. In QCD there are 3 diagrams that contribute to finding the splitting functions: $q\rightarrow q+g$, $g\rightarrow q+\bar{q}$ and $g\rightarrow g+g$.

When calculating the splitting functions we need to avoid a pole at $z=1$, for this we define the function:

$$\frac{1}{\left(1-z\right)_+}=\lim_{\varepsilon\rightarrow 0}\left[\frac{1}{1-z}\Theta\left(1-\varepsilon-z\right)-\delta\left(1-z\right)\int_0^{1-\varepsilon}\frac{dz'}{1-z'}\right]. \tag{2.24}$$

Where Θ is the step function, it is 1 for a positive argument and 0 for a negative argument.

Using this function we can define the splitting functions:

$$\begin{aligned}
P_{q\leftarrow q}\left(z\right) &= \frac{4}{3}\left[\frac{1+z^2}{\left(1-z\right)_+}+\frac{3}{2}\delta\left(1-z\right)\right],\\
P_{g\leftarrow q}\left(z\right) &= \frac{4}{3}\left[\frac{1+\left(1-z\right)^2}{z}\right],\\
P_{q\leftarrow g}\left(z\right) &= \frac{1}{2}\left[z^2+\left(1-z\right)^2\right],
\end{aligned}$$

$$P_{g\leftarrow g}(z) = 6\left[\frac{1-z}{z} + \frac{z}{(1-z)_+} + z(1-z) + \left(\frac{11}{12} - \frac{n_f}{18}\right)\delta(1-z)\right]. \quad (2.25)$$

Where n_f is the number of light quarks with masses lower than hard scale Q.

The diagrams that define the splitting functions also include a factor $\alpha_s(Q^2)/\pi$, where $\alpha_s(Q^2)$ is the QCD running coupling, in the one loop approximation is expressed us:

$$\alpha_s\left(Q^2\right) = \frac{4\pi}{\left(\frac{11}{3}N_c - \frac{2}{3}n_f\right)\ln\left(Q^2/\Lambda_{QCD}\right)}. \quad (2.26)$$

Here N_c is the number of colors (for QCD $N_c = 3$), n_f is the number of light quarks, and $\Lambda_{QCD} \approx 0.3$GeV is the QCD scale parameter.

Using the splitting functions we can write the Dokshitzer–Gribov–Lipatov–Altarelli–Parisi (DGLAP) equations that describe perturbative QCD (PQCD) in the leading logaritmic approximation (LLA):

$$\begin{aligned}
\frac{d}{d\log Q}f_g\left(x,Q^2\right) &= \frac{\alpha_s(Q^2)}{\pi}\int_x^1\frac{dz}{z}\left\{P_{g\leftarrow q}(z)\sum_f\left[f_f\left(\frac{x}{z},Q^2\right) + f_{\overline{f}}\left(\frac{x}{z},Q^2\right)\right]\right. \\
&+ \left. P_{g\leftarrow g}(z)\, f_g\left(\frac{x}{z},Q^2\right)\right\}, \\
\frac{d}{d\log Q}f_f\left(x,Q^2\right) &= \frac{\alpha_s(Q^2)}{\pi}\int_x^1\frac{dz}{z}\left\{P_{q\leftarrow q}(z)\, f_f\left(\frac{x}{z},Q^2\right) + P_{q\leftarrow g}(z)\, f_g\left(\frac{x}{z},Q^2\right)\right\}, \\
\frac{d}{d\log Q}f_{\overline{f}}\left(x,Q^2\right) &= \frac{\alpha_s(Q^2)}{\pi}\int_x^1\frac{dz}{z}\left\{P_{q\leftarrow q}(z)\, f_{\overline{f}}\left(\frac{x}{z},Q^2\right) + P_{q\leftarrow g}(z)\, f_g\left(\frac{x}{z},Q^2\right)\right\}.
\end{aligned} \quad (2.27)$$

Since the derivation of the DGLAP equations respects the conservation laws of QCD, namely conservation of flavor and longitudinal momentum, they obey the summation rules in Fig. 2.22 and Fig. 2.23.

We now want to write the connection between the hadronic and partonic cross sections. The inclusive hadronic cross section, σ_h, for colliding hadrons h_a with momentum P and h_b with momentum P', to the production of two particles i and j with momenta q_i and q_j is given by:

$$\begin{aligned}
\sigma_h\left(h_a(P) + h_b(P') \to i + j + X\right) &= \int_0^1 dx\int_0^1 dx'\sum_{\alpha,\beta} f_\alpha\left(x,Q^2\right) f_\beta\left(x',Q^2\right) \\
&\times \sigma_p\left(\alpha(x) + \beta(x') \to i + j\right).
\end{aligned} \quad (2.28)$$

Where σ_p is the hard partonic cross section of the process $\alpha(x) + \beta(x') \to i + j$, the indices α and β go over all types of partons, (quarks, anti-quarks for each flavor, or gluons).

From here on out we will not write the type index for the PDF, since at high hard scales, such as in the LHC, the gluons dominate the proton structure [20], meaning we will assume that all partons are gluons.

It is important to remember that the PDF are not real probabilities, the real probabilities are defined via the wave functions of the partons, and we can define many other quasi-distributions that can be useful.

A natural framework for visualization of the MPI is the impact parameter representation of the collision, as seen in Fig. 2.1, in the high energy limit the angular momentum conservation implies that the impact parameter b becomes a constant for the collision. In addition hard collisions have the hard scale that localise them in an transverse area $1/Q^2$.

To describe the transverse geometry of the pp collisions it is convenient to consider quasi-probability to find a parton with given x and transverse distance $\vec{r}$ from the hadron transverse center of mass, in hard scale Q^2: $\rho\left(x,\vec{r}|Q^2\right)$. This quantity is referred to as the diagonal Generalized Parton Distribution (GPD), and is related to the PDF by:

$$f\left(x,Q^2\right)=\int d^2r\rho\left(x,\vec{r}|Q^2\right), \tag{2.29}$$

The inclusive cross section does not depend on the transverse structure of the colliding hadrons in the Leading Twist (LT) pQCD regime. The cross section is expressed through the convolution of parton densities. Indeed, we can write the connection between the hadronic and partonic cross sections as:

$$\begin{aligned}\sigma_h\left(h_a+h_b\to Y+X\right) &\propto \int d^2bd^2rd^2r'\delta^{(2)}\left(\vec{r}-\vec{r}'-\vec{b}\right)\rho\left(x,\vec{r}|Q^2\right)\rho\left(x',\vec{r}'|Q^2\right)\\ &\times \sigma_p\left(\alpha\left(x\right)+\beta\left(x'\right)\to Y\right)\\ &= f\left(x,Q^2\right)f\left(x',Q^2\right)\sigma_p\left(\alpha\left(x\right)+\beta\left(x'\right)\to Y\right),\end{aligned} \tag{2.30}$$

Which is equivalent to eq. (2.28).

2.2.2 Double Parton Scattering

In this section we want to look at the example of Double Parton Scattering (DPS), and use it to define the tools we will use for the general MPI.

The case of DPS, in which each of the two colliding hadrons contribute two partons that collide and create two independent hard processes. DPS are normally parameterized as:

$$\sigma^{(DPS)}=\frac{\sigma_1\sigma_2}{\sigma_{eff}}. \tag{2.31}$$

Here $\sigma^{(DPS)}$ is the total hadronic cross section of the process of two partons from each hadron coming in and making two hard processes, the quantities σ_1 and σ_2 are the hadronic cross sections of a process with only one partonic interaction, and σ_{eff} characterizes the geometry of the DPS process.

Note that $\sigma^{(DPS)}$ and σ_{eff} are functions of the hard scale, Q_i^2, and $x_i,\ x'_i$, the light-cone hadron's momentum fractions for both hard processes ($i = 1, 2$), while σ_i are functions of only the the variables with the same index, meaning they are assumed to be independent.

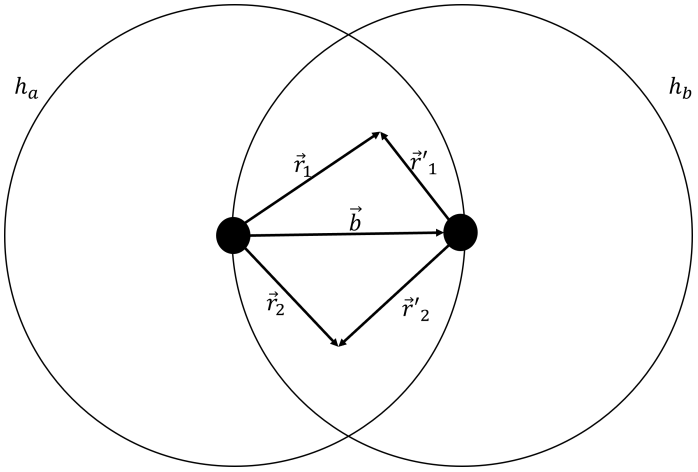

Figure 2.9: The geometry of a DPS process in the transverse plain. The two big circles represent the hadrons h_a and h_b, the two small circles are their centers and $\vec{b}$ is the impact parameter vector. The vectors $\vec{r}_1,\ \vec{r}'_1,\ \vec{r}_2$ and $\vec{r}'_2$ are the transverse positions of the four partons that perform the interactions.

In Fig. 2.9 we depict the geometry of this process in the transverse plain. We see that in the transverse plain the two hadrons are almost circles, the vector connecting their centers is the impact parameter $\vec{b}$, as seen in Fig. 2.1. To simplify our calculations, we can use the single parton transverse position distribution functions to treat the partons as a point like particle, that can only interact with partons from the other hadron if they are in the same transverse position.

If we note the transverse position of a parton from h_a as $\vec{r}$ with respect to the center of h_a, and a parton the transverse position of a parton from h_b as $\vec{r}'$ with respect to the center of h_b, then for both of them to be in the same travnsverse position the vectors need to satisfy the connection $\vec{b} = \vec{r} - \vec{r}'$.

Using the diagonal GPD we can write σ_{eff} by averaging over all possible hard

processes positions for all possible values of impact parameters:

$$(\sigma_{eff})^{-1} = \int d^2b \left(\prod_{i=1}^{2} d^2r_i d^2r'_i \rho\left(x_i, \vec{r}_i | Q_i^2\right) \rho\left(x'_i, \vec{r}'_i | Q_i^2\right) \delta^{(2)}\left(\vec{r}_i - \vec{r}'_i - \vec{b}\right) \right). \quad (2.32)$$

2.2.3 Generalized Partons Distribution.

In order to find the cross section of a hard processes with N partons interactions we need to intrudes a new physical quantety, the N-particle Generalized Partons Distribution, normally denoted as ${}_N$GPD.

The ${}_N$GPD can be defined using the light cone wave function of the hadron:

$$\begin{aligned} D_h\left(\left\{x_i, Q_i^2, \vec{\Delta}_i\right\}_{i=1}^{N}\right) \equiv & \sum_{p=N+1}^{\infty} \int \left(\prod_{l=1}^{N} \frac{d^2k_l}{(2\pi)^2} \Theta\left(Q_l^2 - k_l^2\right) \right) \left(\prod_{l=N+1}^{p} \frac{d^2k_l}{(2\pi)^2} dx_l \right) \\ & \times (2\pi)^3 \delta\left(\left(\sum_{m=1}^{p} x_m \right) - 1 \right) \delta^{(2)}\left(\sum_{m=1}^{p} \vec{k}_m \right) \delta^{(2)}\left(\sum_{m=1}^{p} \vec{\Delta}_m \right) \\ & \times \psi_p\left(\left\{x_l, \vec{k}_l\right\}_{l=1}^{p}\right) \psi_p^{\dagger}\left(\left\{x_l, \vec{k}_l + \vec{\Delta}_l\right\}_{l=1}^{N}, \left\{x_l, \vec{k}_l\right\}_{l=N+1}^{p}\right). \end{aligned} \quad (2.33)$$

Where h is an index for the hadron, x_i is the light-cone hadron momentum fraction of i'th parton, the integral over x_l for $l > N$ goes from 0 to 1, Q_i^2 is the hard scale of the i'th partonic interaction, $\vec{\Delta}_i$ is the Fourier conjugate to the transverse positions of the i'th parton, p is the number of partons in the hadron, $\vec{k}_l$ is the transverse momentum of the l'th parton, $\Theta\left(Q_l^2 - k_l^2\right)$ is the step function, 1 for $Q_l^2 > k_l^2$ and 0 for $Q_l^2 < k_l^2$, in the second line the first delta function forces the condition that the sum over the light-cone fraction of all the partons is 1, the second delta function forces the condition that the sum over the transverse momentum is 0, and ψ_p is the p-parton wave function normalized to 1.

Note that unlike the diagonal GPD we defined in section 2.1, that were defined in the coordinate space, we define the ${}_N$GPD here in the transverse momentum space, those definitions are equivalent via Fourier transformation. This connection will be shown in section 2.4.

For an MPI with N partonic interactions we can generalize the parameterization of the cross section from eq. (2.31) to:

$$\sigma_N^{(MPI)} = \frac{\prod_{i=1}^{N} \sigma_i\left(x_i, x'_i, Q_i^2\right)}{K_N\left(\{x_i, x'_i, Q_i^2\}_{i=1}^{N}\right)}. \quad (2.34)$$

Where $\sigma_N^{(MPI)}$ is the total hadronic MPI cross section, i is an index going over all the N partonic interactions in the process, σ_i is the hadronic cross section of a single

independent hard process, and K_N is a dimensionful function, $K_N \propto (area)^{N-1}$, of the following parameters: $x_i,\ x'_i$ that are the light-cone hadron momentum fractions of the partons, the unprimed index comes from hadron h_a and the primed ones comes from hadron h_b, and Q_i^2 is the hard scale of the i'th hard process. Note that for $N = 2$ we get $K_2 = \sigma_{eff}$.

Using the ${}_N$GPD we can see that the total cross section for N partonic interactions is proportional to:

$$\sigma_N^{(MPI)} \propto \int D_a\left(\left\{x_i, Q_i^2, \vec{\Delta}_i\right\}_{i=1}^N\right) D_b\left(\left\{x'_i, Q_i^2, -\vec{\Delta}_i\right\}_{i=1}^N\right) \delta^{(2)}\left(\sum_{i=1}^N \vec{\Delta}_i\right) \prod_{i=1}^N \frac{d^2\Delta_i}{(2\pi)^2}. \tag{2.35}$$

To compare this to our example of DPS we take $N = 2$, we can use the delta function $\delta^{(2)}\left(\sum_{i=1}^2 \vec{\Delta}_i\right)$ to write:

$$\begin{aligned} D_h\left(x_1, x_2, Q_1^2, Q_2^2, \vec{\Delta}\right) \equiv & \sum_{p=3}^{\infty} \int \left(\prod_{l=1}^p \frac{d^2k_l}{(2\pi)^2}\right)\left(\prod_{l=3}^p dx_l\right) \Theta\left(Q_1^2 - k_1^2\right) \Theta\left(Q_2^2 - k_2^2\right) \\ & \times (2\pi)^3 \delta\left(\left(\sum_{m=1}^p x_m\right) - 1\right) \delta^{(2)}\left(\sum_{m=1}^p \vec{k}_m\right) \\ & \times \psi\left(\left\{x_l, \vec{k}_l\right\}_{l=1}^p\right) \psi^{\dagger}\left(x_1, \vec{k}_1 + \vec{\Delta}, x_2, \vec{k}_2 - \vec{\Delta}, \left\{x_l, \vec{k}_l\right\}_{l=3}^p\right). \end{aligned} \tag{2.36}$$

The DPS cross section is then given by:

$$\begin{aligned} \sigma_2^{(MPI)} = & \int \frac{d^2\Delta}{(2\pi)^2} d\Omega_1 d\Omega_2 D_a\left(x_1, x_2, Q_1^2, Q_2^2, \vec{\Delta}\right) D_b\left(x'_1, x'_2, Q_1^2, Q_2^2, -\vec{\Delta}\right) \\ & \times \frac{d\sigma\left(x_1, x'_1, Q_1^2\right)}{d\Omega_1} \frac{d\sigma\left(x_2, x'_2, Q_2^2\right)}{d\Omega_2}. \end{aligned} \tag{2.37}$$

From this we can find that σ_{eff} is given by:

$$\left(\sigma_{eff}\right)^{-1} = \int \frac{d^2\Delta}{(2\pi)^2} \frac{D_a\left(x_1, x_2, Q_1^2, Q_2^2, \vec{\Delta}\right) D_b\left(x'_1, x'_2, Q_1^2, Q_2^2, -\vec{\Delta}\right)}{f\left(x_1, Q_1^2\right) f\left(x_2, Q_2^2\right) f\left(x'_1, Q_1^2\right) f\left(x'_2, Q_2^2\right)}, \tag{2.38}$$

where $f\left(x, Q^2\right)$ is the standard PDF. For general N we can write:

$$\frac{1}{K_N} = \int \left(\prod_{j=1}^N \frac{d^2\Delta_j}{(2\pi)^2}\right) \frac{D_a\left(\left\{x_j, Q_j^2, \vec{\Delta}_j\right\}_{j=1}^N\right) D_b\left(\left\{x'_j, Q_j^2, -\vec{\Delta}_j\right\}_{j=1}^N\right) \delta^{(2)}\left(\sum_{j=1}^N \vec{\Delta}_j\right)}{\prod_{j=1}^N \left(f\left(x_j, Q_j^2\right) f\left(x'_j, Q_j^2\right)\right)} \tag{2.39}$$

It is important to note here that a hard parton can split perturbatively and the resulting partons interact with the partons from the other hadrons, resulting in

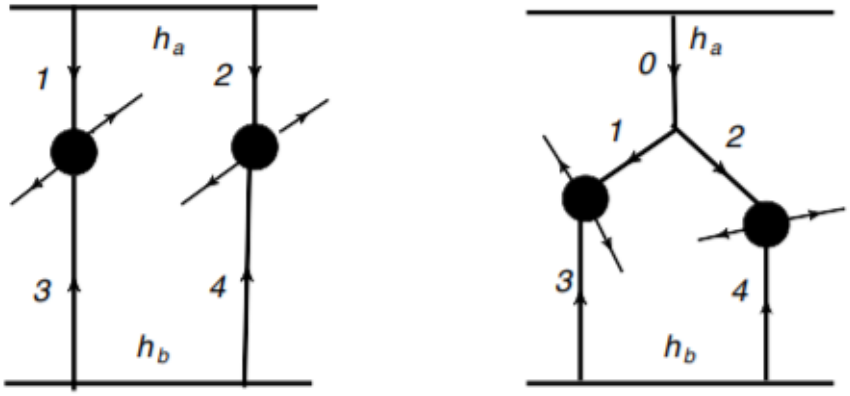

Figure 2.10: Two diagrams of collisions between two hadrons h_a and h_b with two partonic interactions. On the left each of interacting partons is originating in the hadron's wave funtion. On the right is an example for a $1 \otimes 2$ process, where the parton from h_a split into two partons that each perform its own partonic interaction with a parton from h_b. The diagrams are taken from [21].

different dependence on the transverse momentum, a process like this is represented in Fig. 2.10 on the right and is called $1 \otimes 2$ process.

When we calculate the GPD we need to take into account the possibility of the splitting process, this is done by summing over all possible splitting combinations. For example, for the two parton GPD we can write:

$$\begin{aligned} D_h\left(x_1, x_2, Q_1^2, Q_2^2, \vec{\Delta}_1, \vec{\Delta}_2\right) &= {}_{[2]}D_h\left(x_1, x_2, Q_1^2, Q_2^2, \vec{\Delta}_1, \vec{\Delta}_2\right) \\ &+ {}_{[1]}D_h\left(x_1, x_2, Q_1^2, Q_2^2, \vec{\Delta}_1, \vec{\Delta}_2\right) \end{aligned} \tag{2.40}$$

Where the index $_{[2]}$ represents the Non-Perturbative (NP) part of the production of two hard partons from the wave function, as in the diagram on the left in Fig. 2.10, and $_{[1]}$ represents the Perturbative Theory (PT) part of the production of one hard parton from the wave function that then split into two, as in the diagram on the right in Fig. 2.10.

2.2.4 Single Parton Distribution

We will now define the generalized single-parton distribution and the two gluon form factor, and use them to find a parameterization of the diagonal GPD in coordinate space, $\rho\left(x, \vec{r}|Q^2\right)$.

The generalized single-parton distribution, marked as G_1, is the non-forward

parton correlator, and is defined using the light cone wave function of the hadron:

$$\begin{aligned} G_1\left(x,Q^2,\vec{\Delta}\right) &\equiv \sum_{p=2}^{\infty}\int\left(\prod_{l=1}^{p}\frac{d^2k_l}{(2\pi)^2}\right)\left(\prod_{l=2}^{p}dx_l\right)\Theta\left(Q_1^2-k_1^2\right) \\ &\times (2\pi)^3\,\delta\left(\left(\sum_{m=1}^{p}x_m\right)-1\right)\delta^{(2)}\left(\sum_{m=1}^{p}\vec{k}_m\right) \\ &\times \psi\left(\left\{x_l,\vec{k}_l\right\}_{l=1}^{p}\right)\psi^{\dagger}\left(x_1,\vec{k}_1+\vec{\Delta},\left\{x_l,\vec{k}_l\right\}_{l=2}^{p}\right). \end{aligned} \tag{2.41}$$

This function can be parametrise, using the processes like the ones shown in Fig. 2.11, where a parton with momentum $x_1, \vec{k}_1$ inside a proton interacts with a virtual photon γ^*, emitting a vector meson V^0 and a new parton with momentum $x_1, \vec{k}_1+\vec{\Delta}$ is absorbed into the proton.

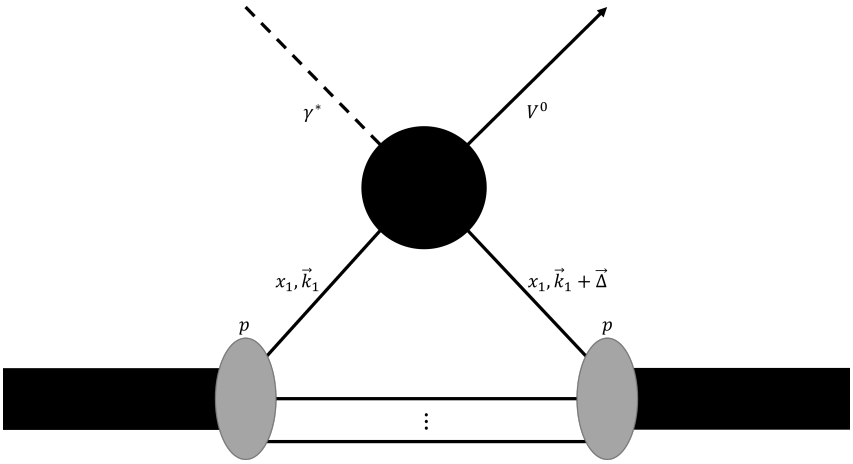

Figure 2.11: A diagram of the process measured in HERA [22], of a proton interacting with a virtual photon, γ^*, and a emitting a vector meson, V^0. The particles connected to the protons are partons, and we see one parton with parameters $x_1, \vec{k}_1$, participate in the interaction, and a parton with $x_1, \vec{k}_1+\vec{\Delta}$ gets back in the proton.

It is related to the diagonal GPD in coordinate space via Fourier transformation over the transverse position:

$$G_1\left(x,Q^2,\vec{\Delta}\right)=\int d^2r e^{-i\vec{\Delta}\cdot\vec{r}}\rho\left(x,\vec{r}|Q^2\right). \tag{2.42}$$

We see from here that for $\vec{\Delta}=\vec{0}$, using eq. (2.29) we get:

$$G_1\left(x,Q^2,\vec{0}\right)=\int d^2r\rho\left(x,\vec{r}|Q^2\right)=f\left(x,Q^2\right). \tag{2.43}$$

It is common to parametrise G_1 as a product of two functions:

$$G_1\left(x,Q^2,\vec{\Delta}\right)=f\left(x,Q^2\right)\cdot F_{2g}\left(x,Q^2,\vec{\Delta}\right). \tag{2.44}$$

Here $f\left(x,Q^2\right)$ is the standard PDF and $F_{2g}\left(x,Q^2,\vec{\Delta}\right)$ is called the two-gluons form factor.

There are two common parameterizations for the two-gluons form factor referred to as exponential and dipole parameterizations. We can write them as:

$$F_{2g}\left(x,\Delta|Q^2\right)=\begin{cases} e^{\frac{-B\left(x,Q^2\right)\Delta^2}{2}} \\ \left(1+\Delta^2/m_g^2\left(x,Q^2\right)\right)^{-2} \end{cases}. \tag{2.45}$$

Here the first one is the exponential parameterization and the second is the dipole parameterization. B and m_g are functions of x and Q^2. The two parametrizations give very similar results for the right choices of B and m_g and both can be fitted to the data as seen in [23] where the relation $B=3.24/m_g^2$ is used.

For our calculations it is much easier to work with the exponential parameterization, so we will only consider it.

We can now also find the diagonal GPD in coordinate space $\rho\left(x,\vec{r}|Q^2\right)$:

$$\rho\left(x,r|Q^2\right)=\int\frac{d^2\Delta}{\left(2\pi\right)^2}e^{i(\Delta\cdot r)}G_1\left(x,Q^2,\vec{\Delta}\right)=f\left(x,Q^2\right)\int\frac{d^2\Delta}{\left(2\pi\right)^2}e^{i(\Delta\cdot r)}F_{2g}\left(x,Q^2,\vec{\Delta}\right). \tag{2.46}$$

Taking the exponential parameterization, $F_{2g}\left(x,Q^2,\vec{\Delta}\right)=e^{\frac{-B\left(x,Q^2\right)\Delta^2}{2}}$, we get:

$$F_{2g}\left(x,r|Q^2\right)=\frac{1}{2\pi B\left(x,Q^2\right)}e^{-\frac{r^2}{2B\left(x,Q^2\right)}}\qquad\rho\left(x,r|Q^2\right)=f\left(x,Q^2\right)F_{2g}\left(x,r|Q^2\right). \tag{2.47}$$

Note that F_{2g}, both the spatial and momentum forms,depends on x and Q^2 only via B. Analysis of the HERA data gives us a parametrization for B [21] of the form:

$$B\left(x\right)=B_0+2\alpha'\ln\left(x_0/x\right). \tag{2.48}$$

Where for $Q^2\sim 3\text{GeV}^2$ fitting to the HERA data, the parameters take the values: $B_0=4\pm 0.4\text{GeV}^{-2}$, $\alpha'=0.14\pm 0.08\text{GeV}^{-2}$ and $x_0=0.0012$. For fixed x we can use DGLAP evolution, eq. (2.27), to see that $B\left(x,Q^2\right)$ vary very slowly with Q^2. Because of this we can take B to be a constant and write F_{2g} as a function of Δ or r only, neglecting its x and Q^2 dependence.

2.2.5 Mean Field Approximation

In the mean field approximation we can concider the partons as independent particles. Then the light cone wave function factorises to:

$$\psi\left(\left\{x_l,\vec{k}_l\right\}_{l=1}^{p}\right)=\prod_{l=1}^{p}\psi\left(x_l,\vec{k}_l\right). \tag{2.49}$$

Assuming this we can express the ${}_N$GPD functions as:

$$D_h\left(\left\{x_i,Q_i^2,\vec{\Delta}_i\right\}_{i=1}^N\right)\simeq\prod_{i=1}^N G_1\left(x_i,Q_i^2,\Delta_i\right)\simeq\prod_{i=1}^N f\left(x_i,Q_i^2\right)\cdot F_{2g}\left(\Delta_i\right). \tag{2.50}$$

Here $G_1\left(x_i,Q_i^2,\Delta_i\right)$ is the generalized single-parton distribution as defined in eq. (2.41), $f\left(x_i,Q_i^2\right)$ is the standard PDF, and $F_{2g}\left(\Delta_i\right)$ is the two-gluons form factor.

This approximation is not perfect, first this approximation loses the property of the GPD: $D_h\left(\sum_{i=1}^N x_i>1\right)=0$, meaning we can't work in region where x_i are too big. On the other hand, if x_i are too small we start to look at the region where the $1\otimes 2$ process is non-pertubative. In [10] it is stated that this approximation should hold for $10^{-1}>x_i>10^{-3}$.

For DPS we can write ${}_2$GPD and σ_{eff}:

$$\begin{aligned} D_h\left(x_1,x_2,Q_1^2,Q_2^2,\vec{\Delta}\right) &= G_1\left(x_1,Q_1^2,\vec{\Delta}\right)G_1\left(x_2,Q_2^2,\vec{\Delta}\right)\simeq f\left(x_1,Q_1^2\right)f\left(x_2,Q_2^2\right)F_{2g}^2\left(\Delta\right) \\ \Rightarrow\sigma_{eff} &= \left(\int\frac{d^2\Delta}{\left(2\pi\right)^2}F_{2g}^4\left(\Delta\right)\right)^{-1}=8\pi B. \end{aligned} \tag{2.51}$$

And for general N we get:

$$K_N\simeq\left(\int\left(\prod_{j=1}^N\frac{d^2\Delta_j}{\left(2\pi\right)^2}F_{2g}^2\left(\Delta_j\right)\right)\delta^{(2)}\left(\sum_{j=1}^N\vec{\Delta}_j\right)\right)^{-1}=N\left(4\pi B\right)^{N-1}. \tag{2.52}$$

2.2.6 Soft Gluon Emission

In addition to the hard out-going particles (jets) the partons in the hard process can also emit soft gluons. Since those gluons will be important to us we should note that for a collision with N partonic interactions the cross section to emit m gluons with transverse momenta $\{\mathbf{k}_i\}_{i=1}^m$ using the approximations above is given by:

$$\frac{d^m\sigma_N\left(\{\boldsymbol{k}_j\},\{\boldsymbol{\Delta}_i\}\right)}{d^2k_1\cdots d^2k_m}\sim\left|\mathcal{M}\left(\{\boldsymbol{k}_j\},\{\boldsymbol{\Delta}_i\}\right)\right|^2\left(\prod_{i=1}^N F_{2g}^2\left(\Delta_i\right)\sigma_i\right)\delta^{(2)}\left(\sum_{i=1}^N\vec{\Delta}_i\right). \tag{2.53}$$

Here $\mathcal{M}\left(\{\boldsymbol{k}_j\},\{\boldsymbol{\Delta}_i\}\right)$ is amplitude for the production of m gluons by N partons in the hadron wave function and σ_i is the cross section for the i'th partonic interaction. The corresponding m-particle spectrum is obtained by normalizing this expression with the cross section:

$$\sigma_N=\int\left(\prod_{i=1}^N d^2\Delta_i F_{2g}^2\left(\Delta_i\right)\sigma_i\right)\delta^{(2)}\left(\sum_{i=1}^N\vec{\Delta}_i\right). \tag{2.54}$$

The m-particle spectrum can now be written in coordinate space representation as:

$$\frac{d^m\sigma_N\left(\{\boldsymbol{k}_j\}\right)}{\sigma_N d^2k_1\cdots d^2k_m}=\frac{\int\left(\prod_{i=1}^N d^2r_i\right)d^2b\left|\mathcal{M}\left(\{\boldsymbol{k}_j\},\{\boldsymbol{r}_i\}\right)\right|^2\rho\left(\{\boldsymbol{r}_i\},\boldsymbol{b}\right)}{\int\left(\prod_{i=1}^N d^2r_i\right)d^2b\rho\left(\{\boldsymbol{r}_i\},\boldsymbol{b}\right)}. \tag{2.55}$$

Here $\rho\left(\{\boldsymbol{r}_i\},\boldsymbol{b}\right)$ is a quasi-probability distribution of the impact parameter $\boldsymbol{b}$ and the hard partons transverse positions $\{\boldsymbol{r}_i\}$, as seen in Fig. 2.9, and is given by:

$$\rho\left(\{\boldsymbol{r}_i\},\boldsymbol{b}\right)=\prod_{i=1}^{N}\int\left(\frac{d^2\Delta_i d^2r'_i}{\left(2\pi\right)^2}F_{2g}^2\left(\Delta_i\right)e^{i\vec{\Delta}_i\cdot\left(\boldsymbol{r}_i+\boldsymbol{r}'_i\right)}\delta^{(2)}\left(\boldsymbol{b}-\boldsymbol{r}_i+\boldsymbol{r}'_i\right)\right). \tag{2.56}$$

For the exponential parameterization we have chosen for $F_{2g}\left(\Delta_i\right)$ we get:

$$\rho\left(\{\boldsymbol{r}_i\},\boldsymbol{b}\right)=\frac{1}{\left(4\pi B\right)^N}\prod_{i=1}^{N}e^{-\frac{r_i^2}{4B}}e^{-\frac{\left(\boldsymbol{r}_i-\boldsymbol{b}\right)^2}{4B}}. \tag{2.57}$$

2.2.7 The Effective Cross Section

Using the mean field approach the clear connection between σ_{eff} and B in eq. (2.51) allows us to use experimental data to find what values of B we should consider.

For pp collisions in the LHC [24, 25, 26], σ_{eff} was found to be about $15\pm5mb$ meaning we should look at $B=1.5\pm0.5\text{GeV}^{-2}$, so in our thesis we will use the two values $B=1,\ 2\text{GeV}^{-2}$.

2.3 Quantum Interference model

In this section we will review the basic ideas of the quantum interference model [10, 11], and explain how to find the azimuthal cumulant in the corresponding frame work.

First we define the normalisation we will work with:

$$\left\langle e^{i\left(\sum_{j=1}^{s} n_j\phi_j\right)}\right\rangle\left(\{k_j,y_j\}_{j=1}^{s}\right)=M_s\frac{\int_\rho\int\left(\prod_{j=1}^{s}d\phi_j\right)e^{i\left(\sum_{j=1}^{s} n_j\phi_j\right)}f\left(\{\boldsymbol{k}_j\}_{j=1}^{s}\right)}{(2\pi)^s\prod_{j=1}^{s}\int_\rho f\left(\boldsymbol{k}_j\right)}. \tag{2.58}$$

Here $M_s=m^s/\binom{m}{s}$ is a normalization factor, the integral $\int_\rho$ means $\int_\rho\equiv\int\left(\prod_{i=1}^{N}d^2r_i\right)\rho\left(\{\boldsymbol{r}_i\}\right)$, $f\left(\boldsymbol{k}_j\right)$ is the 1-particle momentum distribution function defined in eq. (2.3) and $f\left(\{\boldsymbol{k}_j\}_{j=1}^{s}\right)$ is the s-particles momentum distribution function defined as $f\left(\{\boldsymbol{k}_j\}_{j=1}^{s}\right)\equiv\frac{d^sN}{d^3k_1\cdots d^3k_s}$, and n_j is the flow harmonic index of the j'th particle where we only look at the case where $\sum_{j=1}^{s}n_j=0$. With that all we need to to find the 1 and 3 particles differential multiplicity. This is a generalized form of the normalization in [11], where they only look at even values of s.

2.3.1 Defining The Model

We model multi-particle production in pp collisions as events of N partonics interctions in transverse positions $\{\mathbf{r}_i\}_{i=1}^{N}$. Each partonic process is represented by a line source with initial $SU\left(N_c\right)$ adjoint representation index $\{b_i\}_{i=1}^{N}$ at the rapidity of one of the colliding hadrons, emitting gluons with $SU\left(N_c\right)$ adjoint representation index $\{a_j\}_{j=1}^{m}$ and transverse momentum of $\{\mathbf{k}_j\}_{j=1}^{m}$ in the intermediate rapidity window and ending at the rapidity of the other hadron with final $SU\left(N_c\right)$ adjoint representation index $\{c_i\}_{i=1}^{N}$. Each multi-particle production amplitude is therefore of the type given in Fig. 2.12, where we need to account for any choices for sources emits any of the gluons.

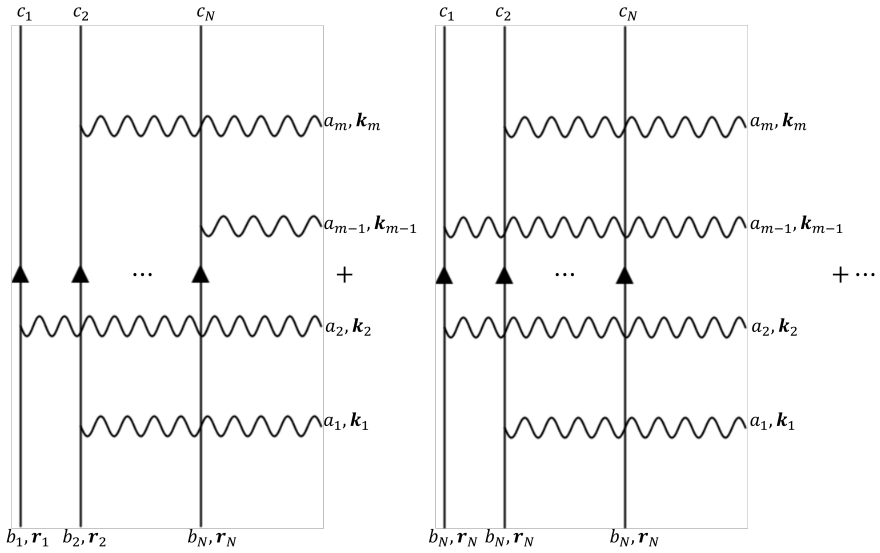

Figure 2.12: Example diagrams for N sources emitting m gluons. The vertical lines are the N sources with initial conditions of $\{\mathbf{r}_i, b_i\}_{i=1}^{N}$, and finale color index of c_i. The horizontal waves are the m emitted gluons with color index and transverse momenta of $\{a_j, \mathbf{k}_j\}_{j=1}^{m}$. Each diagram in the sum represent different choice of which gluons are emitted from which source, and to find the total amplitude we need to sum over all of those choices.

The emission vertix for a soft gluon is given by an eikonal vertex. If the source is positioned in $\mathbf{r}_i$ with a color index of b'_i before the emission and becomes $b"_i$ after the emission, and the emitted gluon has transverse momentum of $\mathbf{k}_j$ and color index a_j the eikonal vertex is given by:

$$T^{a_j}_{b'_i, b"_i} \vec{f}(\mathbf{k}_j)\, e^{i\mathbf{r}_i \cdot \mathbf{k}_j}, \tag{2.59}$$

here T^a is the adjoint representation of the $SU(N_c)$ generator, and $\vec{f}(\mathbf{k})$ is the vertex form function. $\vec{f}(\mathbf{k})$ is a two-dimensional vector in the transverse plane, that in the cross sections will appear dotted into another vertex function of the same momentum. We will not assume a specific functional shape of the vertex function, since it will not impact the results in a meaningful way, but we will assume two of it's properties, first, we normalize it to be: $\int d^2k \left|\vec{f}(\boldsymbol{k})\right|^2 = 1$, and second we assume that $\left|\vec{f}(\boldsymbol{k})\right|^2$ is independent of the momentum azimuthal angle. An example of a function that can fit what we need is coulombic radiation: $\vec{f}(\boldsymbol{k}) \propto \frac{1}{k^2}\boldsymbol{k}$.

When calculating cross sections of event samples we will use the quasi-probability distribution of the impact parameter $\mathbf{b}$ and the hard partons transverse positions $\{\boldsymbol{r}_i\}_{i=1}^{N}$ given in eq. (2.57). Denoting coordinates in the complex conjugate amplitude with primes, this means that initial and final data $\{\mathbf{r}_i, b_i, c_i\}_{i=1}^{N}$ and $\{\mathbf{r'}_i, b'_i, c'_i\}_{i=1}^{N}$

are averaged with the weight:

$$\rho\left(\{\boldsymbol{r}_i\},\boldsymbol{b}\right)\delta^{(2)}\left(\boldsymbol{r}_i-\boldsymbol{r'}_i\right)\delta_{b_ib'_i}\delta_{c_ic'_i}. \tag{2.60}$$

To find the spectrum of the emissions of m soft gluons of a collision with N partonic interactions for general N and m we will use few simplifications:

- Neglecting longitudinal phase factors.

  We only account for transverse momenta and transverse coordinates. We could supplement the model with longitudinal phase factors in the definition of the vertex function in eq. (2.59) by replacing: $\vec{f}\left(\mathbf{k}\right)e^{i\mathbf{r}\cdot\mathbf{k}}\rightarrow\vec{f}\left(\mathbf{k}\right)e^{i\mathbf{r}\cdot\mathbf{k}}e^{-i\left(k^+r^-+k^-r^+\right)}$ where the indices $\pm$ denote components of light-cone coordinates and momenta. For high collision energy, when both the emitting sources and the emitted gluons propagate close to the light-cone we get $k^-\approx 0$. Identifying the particle emitting source with an energetic parton of light cone momentum fraction p^+, it follows from the uncertainty relation that $r^-\ 1/p^+$, in the soft gluon limit $k^+\ll p^+$ we get that the total longitudinal phase is negligible: $k^+r^-+k^-r^+\approx k^+/p^+\approx 0$.

- Emitted gluons do not cross.

  We will assume that multi-gluons radiation is dominated by a ladder-type diagrams, in which the emitted gluons do not cross each other, and that the emitted gluons are ordered the same way in rapidity. the model is made to retains relevant features of QCD but that is simple enough to allow for the explicit calculation of soft multi-gluon interference for large m and N.

- Symmetrization in the m emitted particles

  We shall find that interference contributions to multi-particle emission cross sections are not always symmetric under interchange between final state momenta $\mathbf{k}_j$. This arise from different color constraints on the gluons we will identify with low or index ($j\ll m, or j\approx m$) and those near the center. As these differences are small and unimportant for our discussion, but since they lead to much longer expressions for higher order cumulants, we shall often randomize final results by averaging over all permutations of the m outgoing momenta.

- No modelling of hadronization.

  This model only allows us to calculate partonic spectra and momentum correlations.We assume that hadronization satisfies local parton-hadron duality

(LPHD), and use it to compare our results to measured hadron spectra and correlations. However, the simple LPHD prescription may not be phenomenologically viable for multi-particle correlations at soft transverse momentum, and that maybe a source of error not accounted for.

Using those assumptions we will be able to find the spectrum as shown in eq. (2.55), the connection between this spectrum and the s particle differential multiplicity is given by:

$$\frac{d^s N}{d\Gamma_1 \cdots d\Gamma_s} = \frac{d^s \sigma_N \left(\{\boldsymbol{k}_j\}_{j=1}^s\right)}{\sigma_N d\Gamma_1 \cdots d\Gamma_s}. \tag{2.61}$$

Here $d\Gamma_j = d^2 k_j = k_j dk_j d\phi_j$ is the transverse phase space of the j'th particle, note that we get that differential multiplicity is independent of rapidity under the first simplification we made where we neglect the longitudinal phase factor.

2.3.2 The Dipole Interference Term

In this section we want to look at the example of a pp collision with $N = 2$ sources and $m = 2$ emitted gluons and find the 2-particle spectrum. We will use this example to define terminology that will help us understand the the more general cases.

There are 16 diagrams that contributes to the $N = m = 2$ cross section, as seen in Fig. 2.13. In each diagram we say that the gluons are emitted from the sources on the left side of the diagram and are absorbed by the sources on the right side.

We define two types of gluons, the first is *diagonal* gluons, those are absorbed by the same source that emitted them, and *off-diagonal* gluons are absorbed by a different source than the one that emitted them. We divide the diagrams shown in Fig. 2.13 into 3 groups depending on how many *off-diagonal* gluons are in them. The 4 diagrams on the top line have no off-diagonal, the 4 diagrams on the second line from the top have 2 off-diagonal gluons, and the two bottom lines have 1 diagonal and 1 off-diagonal gluons, each of them have a different contribution to the cross section.

Each diagram give a contribution to the cross section proportional to the trace of the product of the $SU(N_c)$ adjoint representation of the gluons color indices connected to each source, this factor is called the color factor, i.e. in the top-left most diagram the color factor is given by:

$$Tr\left[T^b T^a T^a T^b\right] Tr\left[I\right] = N_c^2 \left(N_c^2 - 1\right)^2. \tag{2.62}$$

Here I is the $(N_c^2 - 1) \times (N_c^2 - 1)$ identity matrix the sum over repeating indices is implied and we used the identities $T^a T^a = N_c I$ and $Tr\left[I\right] = N_c^2 - 1$. The color

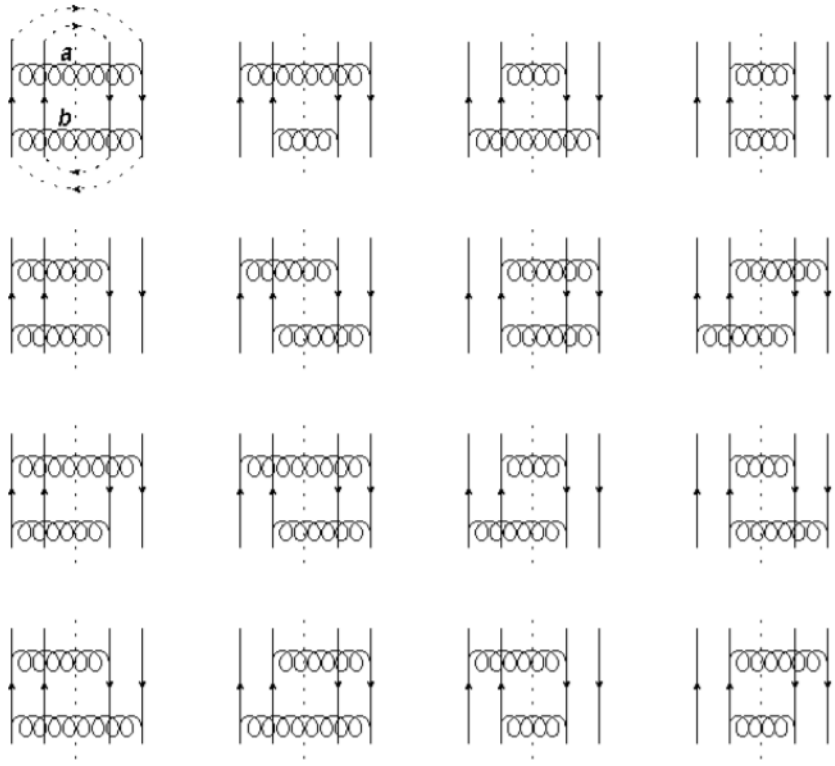

Figure 2.13: The 16 diagrams for the cross section of $N = m = 2$. The horizontal arrows are the 2 sources, the two pointing down are the conjugation of the two pointing up, where the other most ones are the same source and the inner ones are the other sources, as indicated by the dashed arrows on the most left top diagram. The two gluons that connect the sources with the conjugated sources are the emitted gluons, the one on top has color index a and the lower one has color index b, we say that they are emitted from the sources on the left side of the diagram and are absorbed by the sources on the right side. This diagram is taken from [10].

factors for all the diagrams in the top row are the same, this can be shown using this identity. Using the identity $Tr\left[T^aT^b\right] = N_c\delta^{ab}$ we can also show the color factor for the diagrams on the row second from the top is given by:

$$Tr\left[T^bT^a\right]Tr\left[T^aT^b\right] = N_c^2\left(N_c^2-1\right). \tag{2.63}$$

Meaning that a couple of off-diagonal gluons give us a factor of $\left(N_c^2-1\right)^{-1}$. The color factor for the bottom two rows is proportional to the trace of a single generator, $\propto Tr\left[T^a\right] = 0$, meaning the diagrams with only 1 off-diagonal gluons do not contribute to the cross section.

The other factor that changes between diagrams is the phases that come from the vertices, $e^{\mp i\mathbf{k}_j\cdot\mathbf{r}_i}$, where the positive (negative) phase come from the amplitude (complex conjugate amplitude). It is easy to see that for a diagonal gluon those phases cancel, leaving us with phases only for off-diagonal gluons.

To find the spectrum for the case of $N = m = 2$ we need the amplitude-squared, $\left|\mathcal{M}\left(\{\boldsymbol{k}_j\},\{\boldsymbol{r}_i\}\right)\right|^2$, and the quasi-probability distribution of the impact parameter and the sources positions, the latter is given in eq. (2.57). The amplitude-squared is the sum over all 16 diagrams in we have discussed, all together we can write:

$$\begin{aligned}\left|\mathcal{M}\left(\{\boldsymbol{k}_j\},\{\boldsymbol{r}_i\}\right)\right|^2 \;&\propto\; \left|\vec{f}\left(\boldsymbol{k}_1\right)\right|^2\left|\vec{f}\left(\boldsymbol{k}_2\right)\right|^2 N_c^2\left(N_c^2-1\right)^2 \\ &\times\; \left\{4+\frac{1}{N_c^2-1}\left(e^{i(\boldsymbol{k}_1+\boldsymbol{k}_2)\cdot(\boldsymbol{r}_1-\boldsymbol{r}_2)}+e^{i(\boldsymbol{k}_1-\boldsymbol{k}_2)\cdot(\boldsymbol{r}_1-\boldsymbol{r}_2)}+c.c.\right)\right\}.\end{aligned} \tag{2.64}$$

Here the 4 are the phase factors of the 2 diagonal gluons diagrams, the phases shown are from the 2 left most diagrams of the second row from the top, and *c.c.* stands for complex conjugate, it is easy to see that the two right-most diagrams on the second row from the top are the complex conjugate of the left most diagrams.

To simplify the quasi-probability distribution in eq. (2.57) we can take the impact parameter to be $\vec{b} = 0$, and normalize it to integrate 1, by replacing:

$$\int d^2b\rho\left(\{\boldsymbol{r}_i\},\boldsymbol{b}\right) \to \rho\left(\{\boldsymbol{r}_i\}\right) = \int d^2b 2^N\rho\left(\{\boldsymbol{r}_i\},\boldsymbol{b}\right)\delta^{(2)}\left(\boldsymbol{b}\right), \tag{2.65}$$

with that we can also write $\rho\left(\{\boldsymbol{r}_i\}\right) = \prod_{i=1}^N \rho\left(\boldsymbol{r}_i\right) = \prod_{i=1}^N \frac{1}{2\pi B}e^{\frac{-r_i^2}{2B}}$, separating the dependence the sources.

The spectrum can now be found using eq. (2.55). We get that the spectrum in first order in powers of $\left(N_c^2-1\right)^{-1}$ is therefore:

$$\frac{d^2\sigma_2\left(\boldsymbol{k}_1,\boldsymbol{k}_2\right)}{\sigma_2 d\Gamma_1 d\Gamma_2} \approx \left|\vec{f}\left(\boldsymbol{k}_1\right)\right|^2\left|\vec{f}\left(\boldsymbol{k}_2\right)\right|^2\left(1+\frac{e^{-B(\boldsymbol{k}_1+\boldsymbol{k}_2)^2}+e^{-B(\boldsymbol{k}_1-\boldsymbol{k}_2)^2}}{2\left(N_c^2-1\right)}\right) \tag{2.66}$$

This spectrum characterise the QCD dipole radiation, the interference effects decrease as for larger B, or larger distance between the sources.

We remember that we assumed that $\left|\vec{f}(\boldsymbol{k})\right|^2$ is independent of the momentum azimuthal angle, that leaves the first term, of the diagrams with only diagonal gluons, completely isotropic, that means it will not contribute to the azimuthal correlation. Meaning the correlations arise from interference between different amplitudes, where the gluons are emitted from different sources, but it's important to remember that does not mean an interference between the gluons.

Another important think to note is that this spectrum is symmetric to replacing any of the momenta by $\mathbf{k} \to -\mathbf{k}$, meaning the when looking at correlations of the form $\left\langle e^{in(\phi_1-\phi_2)} \right\rangle$ for odd n vanish identically.

2.3.3 Diagonal Gluons Corrections to the Dipole

In this section we will see what happens when we look at processes with more sources, $N > 2$, and more emitted gluons, $m > 2$, we will discuss the effects that diagonal gluons have on the spectrum and the two point cumulant.

In leading order in powers of $\left(N_c^2-1\right)^{-1}$ we only see two types of diagrams, the diagrams with m diagonal gluons, and the diagrams with $m-2$ diagonal.

The diagrams with only diagonal gluons don't see a drastic change, each of their contributions to the spectrum is proportional to a color factor of $\left(N_c^2-1\right)^N N_c^m$ and the product of the squares of the vertex functions for all the emitted gluons, $\prod_{j=1}^m \left|\vec{f}(\boldsymbol{k}_j)\right|^2$. Since by definition diagonal gluons connect each source to it's conjugate each gluon can be emitted by any of the sources but that also determines what source absorbs it, so in total we have N^m choices for only diagonal diagrams. In total we get that the contribution to the spectrum of only diagonal diagrams is given by:

$$\frac{d^m\sigma_N^{(diagonal)}}{d\Gamma_1\cdots d\Gamma_m} \propto N^m\left(N_c^2-1\right)^N N_c^m \prod_{j=1}^m \left|\vec{f}(\boldsymbol{k}_j)\right|^2. \tag{2.67}$$

The diagrams with 2 off diagonal gluons don't vanish only if the two are shared between a pair of sources, like in Fig. 2.14. In this diagram we see three types of relations between the diagonal and off diagonal gluons, we now want to use this as an example for how each type of relation effects the color factor of this diagram.

The total color factor of the diagram, assuming no other sources or gluons is given by:

$$Tr\left[T^eT^e\right] Tr\left[T^{c_j}T^bT^{c_j}T^a\right] Tr\left[T^{c_1}T^aT^dT^dT^{c_1}T^b\right] \left(Tr\left[I\right]\right)^2. \tag{2.68}$$

We can see that we can sum over d and e easly using the identity we used before:

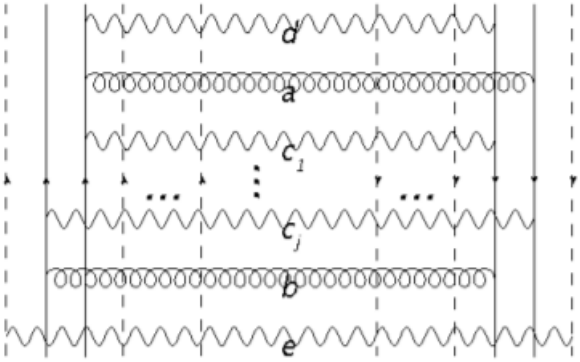

Figure 2.14: An example diagram for the single dipole term in the general N and m case. The curly lines, a and b, are the two off diagonal gluons that create the dipole, and the wavy lines, $c_1, ..., c_j, d$ and e, are diagonal gluons with different relations to the dipoles. When we look at the color factor for this diagram we will see that gluon e does not share a source with the off-diagonal gluons, the gluons c_1 and c_j are sandwiched between the off-diagonal gluons in the trace, and gluon d will just give us a trivial factor of $T^d T^d = N_c I$. This diagram is taken from [10].

$T^a T^a = N_c I$, e doesn't share a source with the dipole pair, and d appear right next to it self so they are both trivial. The gluons c_1 and c_j are different, but we can use the identity $T^b T^a T^b = \frac{N_c}{2} T^a$ to solve this trace, but each of them then give us a factor of $1/2$ that we didn't see before. We say that a diagonal gluon that shares it's source with off-diagonals gluon and is between them on the diagram are sandwiched by the off-diagonal gluons, those kind of gluons will give the diagram a factor of $1/2$ to the color factor.

It will be useful to us to sum over all diagrams with a single pair of off-diagonal gluons, since they all have the same source positions and gluons momenta dependence, summing over all of those diagrams we find we can define a factor that accounts those factors of $1/2$ for us, this factor is marked as $F^{(2)}_{corr}(N, m)$. The total contribution to the spectrum of the diagrams with a single pairs of off-diagonal gluons will be proportional to this correction factor.

To find $F^{(2)}_{corr}(N, m)$ we use the method done in [10]. For an ordered list of m gluons with one off-diagonal pair there are $(m - 1 - j)$ way to have $j = 1, 2, \ldots, m - 2$ diagonal gluons that are between the two off-diagonal gluons. For each configuration with j diagonal gluons between the two off-diagonal gluons there are $\binom{j}{l} 2^l (N - 2)^{j-l}$ of having l of them share a source with the off-diagonal gluons, making them sandwiched, each such contribution is then suppressed by a correction factor of $1/2^l$.

If we were to ignore the factor of $1/2^l$ it would be like assuming that all $m - 2$

diagonal gluons are incoherently superimposed to the interference pattern of the two off-diagonal gluons. The number of such incoherent superpositions is:

$$N_{incoh} = \sum_{j=0}^{m-2} N^{m-2-j} (m-1-j) \sum_{l=0}^{j} \binom{j}{l} 2^l (N-2)^{j-l} = \frac{m(m-1)}{2} N^{m-2}. \quad (2.69)$$

When we account for the factor of $1/2^l$ we get the real color factor, but we want to average it over all the diagrams we are counting, meaning we get that the color correction factor is given by:

$$\begin{aligned} F^{(2)}_{corr}(N,m) &= \frac{1}{N_{incoh}} \sum_{j=0}^{m-2} N^{m-2-j} (m-1-j) \sum_{l=0}^{j} \binom{j}{l} 2^l (N-2)^{j-l} \frac{1}{2^l} \\ &= \frac{2}{m(m-1)} N^{1-m} \left(N(N-1)^m + mN^m - N^{1+m} \right). \end{aligned} \quad (2.70)$$

We now want to note few properties of $F^{(2)}_{corr}(N,m)$ that can be useful for us. First, $F^{(2)}_{corr}(N,m) \leq 1$ where full equality is only for $m = 2$. There are three interesting limits that we can look at:

- The limit of $m = const$ and $N \to \infty$.

  Increasing the number of sources at fixed multiplicity m favors incoherent particle production and hence we find:

  $$\lim_{N\to\infty} F^{(2)}_{corr}(N,m)\Big|_{m=const} = 1 \quad (2.71)$$

- The limit of $m \to \infty$ for fixed average multiplicity per source $\bar{m} = m/N$.

  This limit is consistent with analyses of LHC pp data which indicate that the multiplicity of hard processes is proportional to the soft multiplicity [27]. We find that for any finite value of $\bar{m} = m/N$ the limit is also finite, specifically:

  $$\lim_{m\to\infty} F^{(2)}_{corr}(m/\overline{m}, m)\Big|_{\overline{m}=const} = \frac{2\overline{m} + 2e^{-\overline{m}} - 2}{\overline{m}^2}. \quad (2.72)$$

- The limit of $N = const$ and $m \to \infty$.

  For fixed number of sources, the color correction factor behaves asymptotically like:

  $$\lim_{m\to\infty} F^{(2)}_{corr}(N,m)\Big|_{N=const} \approx \frac{2N}{m} + O\left(\frac{N^2}{m^2}\right). \quad (2.73)$$

  Therefore, increasing multiplicity for a fixed number of sources leads to a lost in correlation.

We can not write the total contribution to the spectrum of the diagrams with a single pairs of off-diagonal gluons:

$$\begin{aligned}\frac{d^m\sigma_N^{(dipole)}}{d\Gamma_1\cdots d\Gamma_m} &\propto N^m\left(N_c^2-1\right)^N N_c^m\left(\prod_{j=1}^m\left|\vec{f}\left(\boldsymbol{k}_j\right)\right|^2\right)\\ &\times \frac{F_{corr}^{(2)}(N,m)}{N^2\left(N_c^2-1\right)}\sum_{(ab)}\sum_{(ij)}2^2\cos\left(\boldsymbol{k}_a\left(\boldsymbol{r}_i-\boldsymbol{r}_j\right)\right)\cos\left(\boldsymbol{k}_b\left(\boldsymbol{r}_i-\boldsymbol{r}_j\right)\right).\end{aligned} \tag{2.74}$$

Here the factor of N^-2 comes from having two less diagonal gluons, The factor of $\left(N_c^2-1\right)^{-1}$ comes from the difference between an all diagonal and 2 off-diagonal diagrams color factors, the sum over (ab) sums over all possible ordered pair choices of which of the m gluons are the two off diagonal ones, and the sum over (ij) is the sum over unordered pairs of sources, the $2^2\cos\left(\boldsymbol{k}_a\left(\boldsymbol{r}_i-\boldsymbol{r}_j\right)\right)\cos\left(\boldsymbol{k}_b\left(\boldsymbol{r}_i-\boldsymbol{r}_j\right)\right)$ is the same sum over phaces we had for the $N=m=2$ case.

Since we end up randomizing the gluons, and the sources are interchangable, we can usee this symmetries to take those sums to give us a factor that only depends on N and m, the sum over the gluons give us a factor of $\sum_{(ab)}\to 2!\binom{m}{2}$, and the sum over the sources gives us a factor of the form $\sum_{(ij)}\to\binom{N}{2}$. We now can rewrite the two particle spectrum:

$$\begin{aligned}\frac{d^m\sigma_N}{\sigma_N d\Gamma_1\cdots d\Gamma_m} &= \left(\prod_{j=1}^m\left|\vec{f}\left(\boldsymbol{k}_j\right)\right|^2\right)\\ &\times\left(1+\frac{2^2F_{corr}^{(2)}(N,m)}{N^2\left(N_c^2-1\right)}\binom{m}{2}2!\binom{N}{2}\cos\left(\boldsymbol{k}_1\cdot\boldsymbol{r}_{12}\right)\cos\left(\boldsymbol{k}_2\cdot\boldsymbol{r}_{12}\right)\right).\end{aligned} \tag{2.75}$$

Here $\boldsymbol{r}_{12}\equiv\boldsymbol{r}_1-\boldsymbol{r}_2$ is the displacement between the two sources.

The leading order in powers of $\left(N_c^2-1\right)^{-1}$ of the single particle differential multiplicity comes from the diagonal term of the cross section:

$$\frac{dN}{d\Gamma_j}=m\left|\vec{f}\left(\boldsymbol{k}_j\right)\right|^2. \tag{2.76}$$

To find the azimuthal correlations we integrate over a phase, meaning we can ignore the the diagonal contribution to the 2 particles differential multiplicity and write it as:

$$\begin{aligned}\frac{d^2N}{d\Gamma_1 d\Gamma_2} &= \left(\prod_{j=1}^2\left|\vec{f}\left(\boldsymbol{k}_j\right)\right|^2\right)\\ &\times\frac{2^3F_{corr}^{(2)}(N,m)}{N^2\left(N_c^2-1\right)}\binom{m}{2}\binom{N}{2}\cos\left(\boldsymbol{k}_1\cdot\boldsymbol{r}_{12}\right)\cos\left(\boldsymbol{k}_2\cdot\boldsymbol{r}_{12}\right).\end{aligned} \tag{2.77}$$

Here, again, this is only the unisotropic part to leading order in powers of $(N_c^2-1)^{-1}$. We now can use eq. (2.58) to find the two particles azimuthal correlations, remembering that for two particles the two particles azimuthal correlation is the same as the two particle symmetric cumulant, eq. (2.15), we can write:

$$sc_n\{2\} = \frac{2F_{corr}^{(2)}(N,m)\binom{N}{2}}{N^2(N_c^2-1)}(-1)^n\left(1+(-1)^n\right)^2\int_\rho J_n(k_1r_{12})J_n(k_2r_{12}). \tag{2.78}$$

Here $J_n(z)$ are the Bessel functions of the first kind that we get from the integral over the phases using the relation:

$$\int_0^{2\pi} d\phi e^{in\phi}\cos(z\cos(\phi-\alpha)) = \pi i^n e^{in\alpha}\left(1+(-1)^n\right)J_n(z). \tag{2.79}$$

Here α here is a general phase shift, but for us it is the azimuthal angle of the vector $\Delta\boldsymbol{r}_{12}$, where the finale phase cancels, we get $e^{in\alpha}e^{i(-n)\alpha}=1$.

We get few interesting results from eq. (2.78), first we get that for any odd n the cumulant vanishes duo to the factor of $\left(1+(-1)^n\right)^2$, this agrees with our observation on eq. (2.66) that the dipole symmetry to $\mathbf{k}\to-\mathbf{k}$ means that all odd harmonics vanish.

Another observation is that the 2-partlce cumulant is not separable for general momenta, for small momenta, $k\ll B^{-1/2}$, also called the hydrodinamic approximation, we can write $J_n(k_j\Delta r_{12})\approx\frac{(k_j\Delta r_{12})^n}{2^n n!}$ resulting in an integral that can be solved analytically, for even n we find:

$$sc_n\{2\}\approx\frac{2^3F_{corr}^{(2)}(N,m)\binom{N}{2}}{N^2(N_c^2-1)n!}\left(\sqrt{B}k_1\right)^n\left(\sqrt{B}k_2\right)^n. \tag{2.80}$$

We Find that the cumulant dependence on N and m is fully expressed in the factor $\frac{F_{corr}^{(2)}(N,m)\binom{N}{2}}{N^2}$, meaning it will behave very similarly to what we saw in the three limits we discussed for $F_{corr}^{(2)}(N,m)$.

2.3.4 General Cross Section

In this section we will want to find the cross section for any number of N sources and m emitted gluons.

Before we can find the general cross section we need to discuss diagrams with more then 2 off-diagonal gluons. For a diagram with off-diagonal gluons to have a non-vanishing color factor we find that for each source cannot have only one off-diagonal gluon emitted from it, this means that the off-diagonal gluons have to come in sets of two or more that create close loops of sources, the case of a dipole is the 2-loop, $1\to2\to1$, but more off-diagonal gluons can create loops of as many sources

as the number of off-diagonal gluons, but not necessarily as equal. A dipole is a 2 source loop, a tripole is a 3 source loop, $1 \to 2 \to 3 \to 1$, and a loop of a sources is called a-pole. A diagram of a tripole is seen in Fig. 2.15 on the left, going from top to bottom, the sources pairs of each gluon is $(12) \to (23) \to (31)$, where 1 stands for the inner most source and 3 the outer most source.

There are two reasons why there can be smaller loops then the number of off-diagonal gluons. The fist is that if there are 4 or more off-diagonal gluons they can group up in smaller chains, i.e. 4 off-diagonal gluons can form a 4-pole or 2 dipoles, but not a tripole and a single off-diagonal gluon on it's own. The second is that any part in the loop and be connected by any number of off-diagonal gluons, i.e. 3 off-diagonal gluons can create a dipole with an extra off-diagonal gluon. A diagram of a 3 gluon dipole with 3 sources is shown in Fig. 2.15 on the right, going from top to bottom, the sources pairs of each gluon is $(12) \to (21) \to (12)$, where 1 stands for the inner most source and 3 the outer most source, we see this is a dipole, only two sources are connected, with an additional gluon.

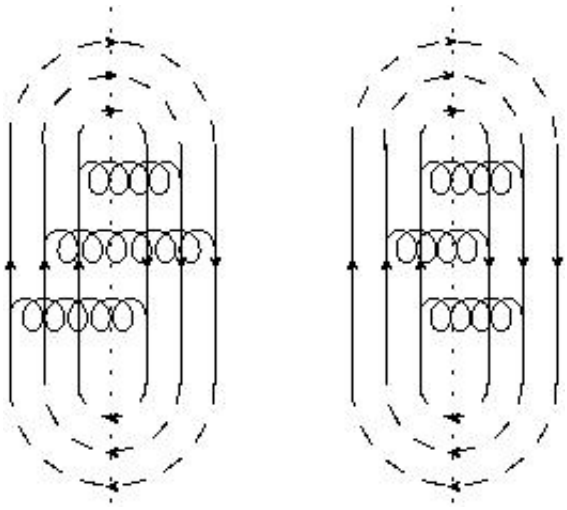

Figure 2.15: Two of the diagrams that contributes to the 3 point asymmetric cumulant for the case of $N = m = 3$. On the left we see a diagram of a tripole, each one of the 3 gluons is connected to a different pair sources. On the right we see a 3 gluon dipole, only two of the sources are connected by 3 off-diagonal gluons.

Each type of diagram, with different arrangements of off-diagonal gluons will have different color factors and different correction factors, but in the limit of $m \to \infty$ for fixed average multiplicity per source $\bar{m} = m/N$ we can find the different contributions and sum them up. Each off-diagonal gluon gives us a factor of N^{-1}, meaning off-diagonal loops with more gluons than sources will be suppressed compered to

loops with the sources but no extra gluons. In addition each off-diagonal gluon with momentum $\mathbf{k}$ that connects the sources 1 and 2 gives as a factor of $2\cos(\mathbf{k}\cdot\mathbf{r}_{12})$, where $\mathbf{r}_{12}\equiv\mathbf{r}_1-\mathbf{r}_2$.

Each a-pole comes with a color factor of $N_c^m\left(N_c^2-1\right)^{N-(a-1)}$ regardless of the numbers of gluons in it, note that this is true ingeneral only in the limit of $m\to\infty$ for fixed average multiplicity per source $\bar{m}=m/N$, so higher poles will be suppressed as well in powers of (N_c^2-1).

There are now two factors to consider when we want to compute the cross section, N and (N_c^2-1), in addition, each diagram type with different number of loops of different lengths and different numbers of gluons in them will have a different correction factor.

The first few terms of the total cross section is given by:

$$\begin{aligned}\frac{d^m\sigma_N}{d\Gamma_1\cdots d\Gamma_m} &\propto N^m\left(N_c^2-1\right)^N N_c^m\left(\prod_{j=1}^{m}\left|\vec{f}\left(\boldsymbol{k}_j\right)\right|^2\right)\\ &\times\left\{1+\frac{F_{corr}^{(2)}(N,m)}{N^2\left(N_c^2-1\right)}\sum_{(ab)}\sum_{(lm)}2^2\cos\left(\boldsymbol{k}_a\cdot\boldsymbol{r}_{lm}\right)\cos\left(\boldsymbol{k}_b\cdot\boldsymbol{r}_{lm}\right)\right.\\ &+\frac{F_{corr}^{(3,2)}(N,m)}{4N^3\left(N_c^2-1\right)}\sum_{(abc)}\sum_{(lm)}2^3\cos\left(\boldsymbol{k}_a\cdot\boldsymbol{r}_{lm}\right)\cos\left(\boldsymbol{k}_b\cdot\boldsymbol{r}_{lm}\right)\cos\left(\boldsymbol{k}_c\cdot\boldsymbol{r}_{lm}\right)\\ &+\frac{F_{corr}^{(3)}(N,m)}{N^3\left(N_c^2-1\right)^2}\sum_{(abc)}\sum_{(lm)(mn)(ln)}2^3\cos\left(\boldsymbol{k}_a\cdot\boldsymbol{r}_{lm}\right)\cos\left(\boldsymbol{k}_b\cdot\boldsymbol{r}_{mn}\right)\cos\left(\boldsymbol{k}_c\cdot\boldsymbol{r}_{ln}\right)\\ &+\left.O\left(\frac{1}{N^4\left(N_c^2-1\right)^2}\right)\right\}. \end{aligned}\tag{2.81}$$

The sums over the gluons, $\sum_{(ab)}$ and $\sum_{(abc)}$ in the shown terms, go over ordered sets of gluons, in diagrams with m_off off-diagonal gluons there are $\binom{m}{m_{off}}m_{off}!$ terms in that sum. The sums over the sources, $\sum_{(lm)}$ and $\sum_{(lm)(mn)(ln)}$ in the shown terms, go over non-ordered sets of sources, for an a-pole there are $\binom{N}{a}$ terms in the sum, for diagrams with l loop we mark the loop lengths as $\{a_i\}_{i=1}^{l}$ we find $\binom{N}{a_1}\binom{N-a_1}{a_2}\cdots\binom{N-\sum_{i=1}^{l-1}a_i}{a_l}=\frac{N!}{\prod_{i=1}^{l}(a_i!)\left(N-\sum_{i=1}^{l}a_i\right)!}$ terms in the sum.

The first line in eq. (2.81) are the factors of the full diagonal diagrams, the to terms in the second line is the fully diagonal gluon diagrams and diagrams with a single 2-gluon dipole, the third line is the term for the diagrams with only a 3-gluon dipole, The fourth line is the term for the 3-gluon tripole diagrams, and the last line shows we are neglecting terms of higher orders in powers of N^{-1} and $\left(N_c^2-1\right)^{-1}$, like a double dipole diagrams, the 4-gluon tripole, and more.

The factor of 4^{-1} in the the 3-gluon comes from the color factor. The correction factors $F_{corr}^{(3,2)}(N,m)$ and $F_{corr}^{(3)}(N,m)$ can be found the same way we got $F_{corr}^{(2)}(N,m)$. The detail of the calculation can be found in appendix B, we find: $F_{corr}^{(3,2)}(N,m) = F_{corr}^{(3)}(N,m)$, specifically:

$$F_{corr}^{(3)}(N,m) = \frac{(m-3)!}{m!}\left(6\,(m-2N)\,N^2 + 6\,(N-1)^{m-1}\,N^{3-m}\,(m+2N-2)\right). \tag{2.82}$$

This correction factor behaves very similarly to $F_{corr}^{(2)}(N,m)$ in the three limits we have discussed, specifically for the limit of $m \to \infty$ for fixed average multiplicity per source $\bar{m} = m/N$ we get:

$$\lim_{m\to\infty} F_{corr}^{(2)}(m/\overline{m},m)\Big|_{\overline{m}=const} = 6\frac{e^{-\overline{m}}\,(\overline{m}+2)}{\overline{m}^3} + 6\frac{\overline{m}-2}{\overline{m}^3}. \tag{2.83}$$

2.3.5 The Real Expansion Parameter

The way we expressed the cross section in eq. (2.81) is somewhat misleading. Note that the diagrams with more off-diagonal loop with more gluons then sources are suppressed by a factor of N^{-1} for each additional gluon. It was found in [11] for each a-pole we need to add a factor $\frac{m^a}{(N_c^2-1)^{a-1}}$. This implies that the expansion is only valid for small m. Because m is finite this this parameter series can summed explicitly giving us a genuine $\frac{1}{N_c}$ and $\frac{1}{N}$.

Chapter 3

3-Point Asymmetric Cumulant

3.1 Introduction

Sizeable n'th harmonic coefficients v_n for azimuthal momentum asymmetries have been observed at the LHC in nucleus-nucleus (AA), proton-nucleus (pA) and proton-proton (pp) collisions [8, 9, 28, 5, 29, 30]. These asymmetries indicate a collective mechanism that relates all particles produced in a given collision. The dynamical origin of these collectivity phenomena continues to be sought in competing and potentially contradicting pictures.

There are two basic approaches towards the explanation of this collective behaviour. The first approach is based on the final state interactions, like viscious fluid dynamics simulations [31] or kinetic transport models [32, 33, 34, 35, 36] of heavy ion collisions. In the AA collisions the jet quenching phenomena provides an alternative confirmation for such a approach. However the jet quenching is missing in smaller pp and pA collision systems. Moreover, in marked contrast to any final state explanation of flow anisotropies v_n in pp collisions, the phenomenologically successful modelling of soft multi-particle production in modern multi-purpose pp event generators [37] are based on free-streaming partonic final state distributions supplemented by independent fragmentation into hadrons. Efforts to go beyond this picture are relatively recent, see e.g. [38, 39]. Therefore two contradictory pictures to describe the multiparticle dynamics in small systems currently exist– the one based on the final state interactions, and the second that does not involve the final state interactions. One approach in the second direction corresponds to the recent works in the framework of Colour Glass Condensate (CGC) [40, 41, 42], see [43] for a recent review, based on the parton saturation hypothesis, that recently made significant progress towards phenomenological description of correlations in small systems.

Recently a QCD based simple model, based on the theory of multiparton interactions (MPI) in pp collisions [44, 45, 46, 47, 48, 49, 50, 51, 52, 53] , and not involving the saturation effects, was proposed in [10, 11] to study the effects of quantum interference and colour flow in high multiplicity pp events. The strong simplification of the model consists in neglecting a dynamically explicit formulation of the scattering process: all gluons in the incoming wave function are assumed to be freed in the scattering process with the same (possibly small) probability. The model pictures the incoming hadronic wave function as a collection of N colour sources in adjoint representation distributed in transverse space according to a classical density $\rho(\vec{r}_i)$. On the amplitude level, emission of a gluon is taken into account in soft gluon/eikonal approximation.

In Ref. [11] the flow coefficients $v_n\{2s\}$, determined by $2s$ point symmetric cumulants

$$sc_n\{2s\} \equiv \left\langle\left\langle e^{in(\sum_{i=1}^{i=s}\phi_i - \sum_{i=s+1}^{i=2s}\phi_i)}\right\rangle\right\rangle. \tag{3.1}$$

were calculated. Here $\langle\langle\cdots\rangle\rangle$ means averaging over the multiparticle final states and taking the cumulant. The phases ϕ_i are the azimuthal angles of measured soft hadrons.

The model [10, 11] predicts both the collectivity phenomena and the qualitatively correct scale of correlations as well as their behaviour as the functions of the transverse momenta.

Consequently, it makes sense to study the other recently measured flow phenomena in high multiplicity pp collisions in this framework of this model.

One group of potentially interesting cumulants are the three point asymmetric cumulants, The corresponding cumulants are often denoted as $ac_n\{3\}$:

$$ac_n\{3\} \equiv \left\langle\left\langle e^{in(\phi_1-\phi_3)}e^{in(\phi_2-\phi_3)}\right\rangle\right\rangle = \left\langle\left\langle e^{in(\phi_1+\phi_2-2\phi_3)}\right\rangle\right\rangle. \tag{3.2}$$

These cumulants were recently studied experimentally [12]. Since we consider in this paper only $ac_n\{3\}$ cumulants, we shall denote them as simply ac_n below.

The purpose of the paper is to calculate the three point correlations (eq. (3.2)) and to compare these correlators to the available experimental data [12]. We shall see that our results are in qualitative agreement with the experimental data although there is not enough experimental data for detailed comparison.

We shall give the detailed predictions for transverse momenta dependence and for the scale (characteristic magnitude) of the three point cumulant . We shall also discuss the dependence of this cumulant on multiplicity.

Recall that the model [10, 11] was based on large N_c and N expansion and then the results were extrapolated to $N_c = 3$.

3.2 Basic formalism.

3.2.1 The Model [10, 11]

Each pp collision is considered as an event consisting of N emitting sources characterized by two-dimentional transverse positions $\boldsymbol{r}_j$ and the initial colours in the adjoint representation b_j. Physically these sources correspond to multiparton interactions (MPI). In other words each source is a collision of two partons-one from each of the colliding nucleons.

The emission amplitude of the gluon with colour a and transverse momentum $\vec{k}$ from a source in transverse position $\vec{r}_j$ is given by an eikonal vertex:

$$T^a_{b_j c_j} \overrightarrow{f}(\boldsymbol{k})\, e^{i\boldsymbol{k}\cdot\boldsymbol{r}_j}, \tag{3.3}$$

where $T^a_{b_j c_j}$ are the adjoint generators of $SU(N_c)$, and $\overrightarrow{f}(\boldsymbol{k})$ is a vertex function. The concrete form of $\vec{f}$ will not influence our results (see below). For example, for the case of coulombic radiation we have $\vec{f} = \vec{k}/k^2$. However since the relevant momenta are small the function f must be taken to be a nonperturbative one. In the cross section the emitted gluon can be absorbed by the same source in the complex conjugated amplitude ("diagonal gluons") or by different source ("off-diagonal gluons"), leading to multiparticle correlations.The simplest diagrams contributing to multiparticle cross section and to correlations are presented in Fig. 3.1. In the left there is a diagram with 2 sources and 2 diagonal gluons, in the right there are still 2 sources but gluons are off-diagonal:they are emitted by one source and absorbed by another leading to azimuthal correlations.

After calculating cross sections for given source positions we average over the source positions with a classical probability distribution $\rho(\{\boldsymbol{r}_j\})$, corresponding to the distribution of multiparton interactions in the pp collision [45]:

$$\frac{d\hat{\sigma}}{d^2\vec{k}_1 .... d^2\vec{k}_m} = \prod_{i=1}^{N} \int d^2\boldsymbol{r}_i \rho(\boldsymbol{r}_i) \hat{\sigma}(\vec{k}_i, \boldsymbol{r}_i), \tag{3.4}$$

where $\sigma(k_i, \boldsymbol{r}_i)$ is the cross section of production of m gluons for sources in fixed transverse positions $\boldsymbol{r}_i$. In this paper we shall neglect so called $1 \to 2$ mechanism for MPI [45, 48, 50]., and carry all calculations in the mean field approximation. In this case the source/MPI distribution in pp system has a Gaussian form:

$$\rho(\{\boldsymbol{r}_j\}) = \prod_{i=1}^{i=N} \frac{1}{2\pi B} e^{\frac{-r_i^2}{2B}}, \tag{3.5}$$

where the parameter B is determined from the analysis of the one particle GPD data at HERA [54]. As it was noted in [10], the mean field approach to MPI

corresponds to $B = 4$ GeV^{-2}, the actual experimental data reparametrized in the mean field form, i.e. assuming factorization of MPI cross-sections corresponds to $B = 2$ GeV^{-2}, and the best fit for experimental data for symmetric correlators sc_n considered in [10, 11] corresponds to $B = 1$ GeV^{-2}, this was justified (though not proved) in [10] by arguments due to possible contribution of very small dipoles due to so called $1 \to 2$ mechanism in MPI [45, 48, 50]. In this paper we shall see that the value of B influences only transverse momentum dependence, and the value $B = 1$ GeV^{-2} seems to be in the best agreement with the experimental data.

We shall work in the limit of a large number of sources N, m finite, $N \to \infty$ [10, 11], and $N_c \to \infty$ and classify all diagrams in powers of $1/N_c, 1/N$.

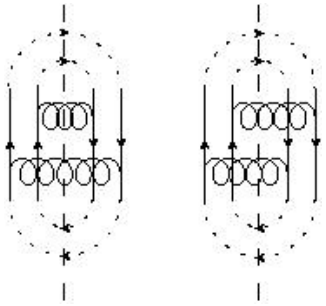

Figure 3.1: The simplest diagrams contributing to total cross section and to correlations: left-2 diagonal gluons, right-interference corresponding to two off-diagonal gluons forming dipole.

The Correlation Functions.

The correlation functions we are interested in have the general form

$$K^{(n)}(k_1, .., k_s) = M_s \frac{\int_\rho d\phi_1 ... d\phi_s \exp\left[i(\sum_{i=1}^{i=s} n_i \phi_i)\right] \frac{d^s N}{d\Gamma_1 ... d\Gamma_s}}{(2\pi)^s \prod_{i=1}^{i=s} \int_\rho \frac{dN}{d\Gamma_i}}, \tag{3.6}$$

where $\sum_i n_i = 0$, and $\int_\rho = \int \prod_i d^2 y_i \rho(\vec{y}_i)$ is the averaging over position of the sources. The standard s-particle spectrum has the form

$$\frac{d^s N}{d\Gamma_1 ... \Gamma_s} = \binom{m}{s} \frac{d^s \hat{\sigma}}{\hat{\sigma} d\Gamma_1 ... d\Gamma_s}. \tag{3.7}$$

Here $\hat{\sigma}$ is the cross section for the production of s gluons, and the normalisation factor M is fixed as

$$M_s = m^s / \binom{m}{s}. \tag{3.8}$$

Here m is the total multiplicity, and s is the number of measured gluons. We assume local parton-hadron duality (LPHD)[54], so radiated gluon correlations and multiplicities coincide with correlations and multiplicities in the soft hadronic spectrum,

The number of radiated gluons is in one to one correspondence with a number of radiated soft hadrons.

In this paper we shall be interested in the case $s = 3, n_1 = n, n_2 = n, n_3 = -2n$,i.e. in

$$K^{(n)}(k_1, k_2, k_3) = M_3 \frac{\int_\rho d\phi_1 ... d\phi_3 \exp\left[in(\phi_1 + \phi_2 - 2\phi_3)\right] \frac{d^3N}{d\Gamma_1 ... \Gamma_3}}{(2\pi)^s \prod_{i=1}^{i=3} \int_\rho \frac{dN}{d\Gamma_i}}. \tag{3.9}$$

3.2.2 The differential cross section.

The relevant differential cross section was calculated in [10]: We can now write $\hat{\sigma}$ explicitly in the limit $N \to \infty$, i.e. omitting terms that are zero as $N \to \infty$

$$\begin{aligned}
\hat{\sigma} \quad &\propto \quad N_c^m (N_c^2 - 1)^N N^m \prod_{i=1}^{m} |\overrightarrow{f}\,(\boldsymbol{k}_i)|^2 \\
&\times \quad (1 + \frac{F_{corr}^{(2)}(N,m)}{N^2(N_c^2-1)} \sum_{ab} \sum_{lm} 2^2 cos\left(\mathbf{k}_a \cdot \Delta\mathbf{r}_{lm}\right) cos\left(\mathbf{k}_b \cdot \Delta\mathbf{r}_{ml}\right) \\
&+ \quad \frac{F_{corr}^{(3)}(N,m)}{4N^3(N_c^2-1)} \sum_{(abc)} \sum_{(lm)} 2^3 \cos\left(\mathbf{k}_a \cdot \Delta\mathbf{r}_{lm}\right) \cos\left(\mathbf{k}_b \cdot \Delta\mathbf{r}_{lm}\right) \cos\left(\mathbf{k}_c \cdot \Delta\mathbf{r}_{lm}\right) \\
&+ \quad \frac{F_{corr}^{(3)}(N,m)}{N^3(N_c^2-1)^2} \sum_{(abc)} \sum_{(lm)(mn)} 2^3 \cos\left(\mathbf{k}_a \cdot \Delta\mathbf{r}_{lm}\right) \cos\left(\mathbf{k}_b \cdot \Delta\mathbf{r}_{mn}\right) \cos\left(\mathbf{k}_c \cdot \Delta\mathbf{r}_{nl}\right) \\
&+ \quad O\left(N^{-4}\right)).
\end{aligned} \tag{3.10}$$

Here the sums go over all ordered combinations of off-diagonal gluons and non ordered combinations of sources. Using eq. (3.10) we can find any correlation function for any number of particles.

The first term in eq. (3.10) corresponds to diagonal gluons, the second is a dipole term, which is a leading contribution to symmetric cumulants [11]. The leading contribution to asymmetric correlator (eq. (3.2)) comes from the third and fourth terms in the expansion (eq. (3.10)) corresponding to 3-gluon dipole (which is actually 1/N suppressed relative to a second term) and a tripole diagram, depicted in the diagram of Fig. 3.2. Note that the tripole diagram has a finite value in the $N \to \infty$ limit.

The factors $F_{corr}^{(2)}(N,m), F_{corr}^{(3)}(N,m)$ correspond to the contribution of diagonal gluons to the interference diagrams. As it was shown in [10] the diagonal gluons lead to the multiplicative renormalisation of the correlators, given by the corresponding coefficients F_{corr}.

3.2.3 The $1/N_c$ Expansion.

Recall the structure of the expansion discussed in [10, 11] for even harmonics for symmetric cumulants. The expansion was in two parameters: $1/(N_c^2-1)$ and in $1/N$. The leading contribution came from the dipole diagram which was of order $1/(N_c^2-1)$, and the leading approximation in $1/(N_c^2-1), 1/N$ was considered , so that we could discard all $1/N$ suppressed diagrams. (Note however that odd harmonics appeared only due to 1/N suppressed terms in the differential cross section expansion). It was shown in [10], that the real parameters of the expansion for given multiplicity were $m^2/((N_c^2-1)N)$ where N is the number of sources, and m is the multiplicity. The leading terms in this expansion however can be resummed, as it was done in [11]. The corresponding diagrams are built from up to $[N/2]$ sources and correspond to nonintersecting dipoles ([] means the integer part).

For the case of the 3 point cumulant the situation is more complicated. For the symmetric cumulants we were able to show that the $1/N$ suppressed diagrams can be neglected. On the other hand for the three point cumulant the leading diagram in the $N \to \infty$ limit is a tripole (see Fig. 3.3 (above)). However this diagram is suppressed by $1/(N_c^2-1)^2$ in the large N_c limit. On the other hand the diagram corresponding to the dipole with three off-diagonal gluons (Fig. 3.3 (below)) has zero limit for large N, i.e. it is suppressed as $1/N$, while it is only $1/(N_c^2-1)$ in the large N_c limit. Thus we shall expect that 1/N corrections will play a significant role for three point correlator if we extrapolate to finite $1/N_c$. In fact we shall see below that the dipole with 3 gluons will dominate numerically up to rather large number of sources. Thus we shall take into account both the tripole and the dipole with three off-diagonal gluons. We shall also take into account the leading terms in the expansion in $m^2/(N_c^2-1)$ for both leading and subleading (1/N, i.e. dipole with 3 off-diagonal gluons) terms in the expansion. It is easy to show in analogy to the symmetric case [11] that such expansion corresponds to the inclusion of up to $[N/2]$ nonintersecting integrated out dipoles with 2 off-diagonal gluons. (By "integrated out" we mean that we integrate over momenta of the corresponding nonobservable off-diagonal gluons). It is easy to see that all other diagrams are subleading, i.e. suppressed by higher powers of $1/(N_c^2-1)$, or $1/N$, i.e as $1/(N_c^2-1)^a 1/N^b, a+b \geq 3$.

For numerical calculations we extrapolate our results to finite $N_c = 3$ and to finite N, actually fixing $\bar{m} = m/N$, in the limit $m, N \to \infty$ as the parameter of the model. We use the same values of $\bar{m}$ as it was done for symmetric cumulants in [11].

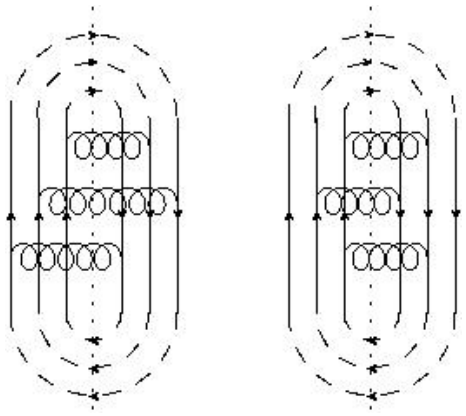

Figure 3.2: Left: The tripole diagram for $N = m = 3$. Right: 3-gluon dipole diagrams for $N = m = 3$.

3.3 The Tripole and 3-Gluon Dipole.

In this section we shall consider the simplest case of N=m=3. There are two contributions in this case: first from the tripole diagram, second from dipole with 3 gluons. Note that each of these two diagrams will be the building block for the case of arbitrary m, N.

We shall start from analysing the single tripole term, that corresponds to the case $N = m = 3$. The corresponding diagram is depicted in Fig. 3.2 (left). Note that in this case there are 3!=6 ordered combinations of gluons, in addition there are 3 ways to put the phases on 3 available gluons, so we get, using eq. (3.10) the multiplier 144:

$$\begin{aligned} ac_n^{(3,3)} &\equiv \frac{T_n}{(N_c^2-1)^2} \\ &= \frac{144}{(N_c^2-1)^2 3^3}\int_\rho\int d\phi_1 d\phi_2 d\phi_3 e^{in(\phi_1+\phi_2-2\phi_3)}\cos\left(\mathbf{k}_1\cdot\Delta\mathbf{r}_{12}\right)\cos\left(\mathbf{k}_2\cdot\Delta\mathbf{r}_{23}\right)\cos\left(\mathbf{k}_3\cdot\Delta\mathbf{r}_{31}\right), \end{aligned} \tag{3.11}$$

where $ac^{3,3}$ is the contribution of the tripole diagram into the total ac.

Consider now the contribution of 3-gluon dipole to the asymmetric three point cumulant. The corresponding diagram is depicted in Fig. 3.2 (right). We note that for the 3-gluon dipole only two of the 3 sources are involved and so the multiplier gets a factor of $\begin{pmatrix} 3 \\ 2 \end{pmatrix}$ and a factor of 4^{-1} from the colour trace, and the multiplier becomes 108:

$$ac_n^{(3,2)} \equiv \frac{\tilde{T}_n}{N_c^2-1}$$

$$
\begin{aligned}
&= \frac{144\binom{3}{2}/4}{(N_c^2-1)3^3}\int_\rho\int d\phi_1 d\phi_2 d\phi_3 e^{in(\phi_1+\phi_2-2\phi_3)}\cos\left(\mathbf{k}_1\cdot\Delta\mathbf{r}_{12}\right)\cos\left(\mathbf{k}_2\cdot\Delta\mathbf{r}_{12}\right)cos\left(\mathbf{k}_3\cdot\Delta\mathbf{r}_{12}\right)\\
&= \frac{108}{(N_c^2-1)3^3}\int_\rho\int d\phi_1 d\phi_2 d\phi_3 e^{in(\phi_1+\phi_2-2\phi_3)}\cos\left(\mathbf{k}_1\cdot\Delta\mathbf{r}_{12}\right)\cos\left(\mathbf{k}_2\cdot\Delta\mathbf{r}_{12}\right)\cos\left(\mathbf{k}_3\cdot\Delta\mathbf{r}_{12}\right),
\end{aligned}
\tag{3.12}
$$

where $ac^{3,2}$ is the dipole contribution into the cumulant. Below we shall denote the asymmetric cumulant for tripole as T_n and the asymmetric cumulant for 3-gluon dipole as $\tilde{T}_n$, while reserving the notation ac_n for total asymmetric three point cumulant for the case of general N, m. The total value of the three point cumulant

$$
ac_n = ac_n^{3,2} + ac_n^{3,3}. \tag{3.13}
$$

3.3.1 The Tripole Momentum Dependence

We start by defining α_{ij} to be the azimuthal phase of $\overrightarrow{r}_{ij} \equiv \overrightarrow{r}_i - \overrightarrow{r}_j$.

We can now take the integral over the 3 azimuthal angles of vectors $\vec{k}_1, \vec{k}_2, \vec{k}_3$ using:

$$
\int_0^{2\pi} d\phi_1 e^{in\phi_1}\cos\left(k_1\Delta r_{12}\cos\left(\phi_1-\alpha_{12}\right)\right) = \pi i^n e^{in\alpha_{12}}\left(1+(-1)^n\right)J_n\left(k_1\Delta r_{12}\right) \tag{3.14}
$$

Here $J_n(z)$ is the n-th Bessel function of the first kind. Using eq. (3.14) we obtain

$$
T_n(k_1,k_2,k_3) = \frac{2^4\pi^3 2\left(1+(-1)^n\right)^2}{3\left(2\pi\right)^3}\int_\rho e^{in(\alpha_{12}+\alpha_{23}-2\alpha_{31})}J_n\left(k_1\left|\mathbf{r}_{12}\right|\right)J_n\left(k_2\left|\mathbf{r}_{23}\right|\right)J_{2n}\left(k_3\left|\mathbf{r}_{31}\right|\right). \tag{3.15}
$$

Note that due to antisymmetry $\vec{k}\to-\vec{k}$ all correlation functions with odd n's vanish.

Consider now the integral over the sources:

$$
\left(\begin{array}{ccc}\overrightarrow{r}_1 & \overrightarrow{r}_2 & \overrightarrow{r}_3\end{array}\right)\to\left(\begin{array}{ccc}\overrightarrow{r}_{12} & \overrightarrow{r}_{23} & \overrightarrow{r}_3\end{array}\right) = \left(\begin{array}{ccc}\overrightarrow{r}_1-\overrightarrow{r}_2 & \overrightarrow{r}_2-\overrightarrow{r}_3 & \overrightarrow{r}_3\end{array}\right). \tag{3.16}
$$

We can simplify the latter expression since the integral over d^2r_3 is a simple gaussian integral:

$$
\int d^2r_3\frac{e^{-\frac{r_1^2+r_2^2+r_3^2}{2B}}}{\left(2\pi B\right)^3} = \int d^2r_3\frac{e^{-\frac{\left(\overrightarrow{r}_{12}+\overrightarrow{r}_{23}+\overrightarrow{r}_3\right)^2+\left(\overrightarrow{r}_{23}+\overrightarrow{r}_3\right)^2+r_3^2}{2B}}}{\left(2\pi B\right)^3} = \frac{e^{-\frac{r_{12}^2+\overrightarrow{r}_{12}\cdot\overrightarrow{r}_{23}+r_{23}^2}{3B}}}{3\left(2\pi B\right)^2}. \tag{3.17}
$$

Using eq. (3.17) we obtain the final expression for T_n:

$$
T_n \equiv \frac{2^4}{3^2\left(2\pi B\right)^2}\int dr_{12}dr_{23}d\alpha_{12}d\alpha_{23}r_{12}r_{23}e^{-\frac{r_{12}^2+r_{12}r_{23}\cos(\alpha_{12}-\alpha_{23})+r_{23}^2}{3B}+in(\alpha_{12}+\alpha_{23})}
$$

$$\times \quad \left(\frac{r_{12}\cos(\alpha_{12})+r_{23}\cos(\alpha_{23})-i\left(r_{12}\sin(\alpha_{12})+r_{23}\sin(\alpha_{23})\right)}{\sqrt{r_{12}^2+2r_{12}r_{23}\cos(\alpha_{12}-\alpha_{23})+r_{23}^2}}\right)^{2n}$$

$$\times \quad J_n(k_1r_{12})\,J_n(k_2r_{23})\,J_{2n}\left(k_3\sqrt{r_{12}^2+2r_{12}r_{23}\cos(\alpha_{12}-\alpha_{23})+r_{23}^2}\right). \tag{3.18}$$

Where we use $e^{in\alpha}=\left(\frac{x+iy}{|\vec{r}|}\right)^n$ to find α_{31} in terms of α_{12},α_{23} (Here $\vec{r}=(x,y)$, hence $x+iy=r\exp(i\alpha)$).

For very small momenta (i.e. all $k_i << 1/B^{1/2}$). we obtain

$$T_n \simeq \frac{2^{4-2n}\left(B^2 Sym(k_1k_2k_3^2)\right)^n}{3\,(n!)^2}. \tag{3.19}$$

where Sym means symmetrization over 3 gluons (and division by 1/3). The details of calculation are given in Appendix A.

3.3.2 The 3-Gluons Dipole Momentum Dependence

In the same way as we did to T_n we can get a simplified form of $\tilde{T}_n$, taking the integral over the phases gives us:

$$\begin{aligned}\tilde{T}_n(k_1,k_2,k_3) &= \frac{2^2\cdot 2\left(1+(-1)^n\right)^2}{(2\pi)^3}\int_\rho e^{in(\alpha_{12}+\alpha_{12}-2\alpha_{12})}J_n(k_1r_{12})\,J_n(k_2r_{12})\,J_{2n}(k_3r_{12})\\ &= \frac{2^4\cdot 2\left(1+(-1)^n\right)^2}{(2\pi)^3}\int_\rho J_n(k_1r_{12})\,J_n(k_2r_{12})\,J_{2n}(k_3r_{12})\,.\end{aligned} \tag{3.20}$$

We note that here too due to antisymmetry $\vec{k}\to-\vec{k}$ all correlation functions with odd n's vanish. The integral over the position of the sources is now a gaussian with two vector variables. Using the transformation:

$$\left(\begin{array}{cc}\vec{r}_1 & \vec{r}_2\end{array}\right)\to\left(\begin{array}{cc}\vec{r}_{12} & \vec{r}_2\end{array}\right)=\left(\begin{array}{cc}\vec{r}_1-\vec{r}_2 & \vec{r}_2\end{array}\right), \tag{3.21}$$

we can take the integral over d^2r_2 and over the azimuthal part of $\vec{r}_{12}$:

$$\int d^2r_2d\alpha_{12}\frac{e^{-\frac{r_1^2+r_2^2}{2B}}}{(2\pi B)^2}=\int d^2r_2d\alpha_{12}\frac{e^{-\frac{\left(\vec{r}_{12}+\vec{r}_2\right)^2+r_2^2}{2B}}}{(2\pi B)^2}=\frac{e^{-\frac{r_{12}^2}{4B}}}{2B}. \tag{3.22}$$

Using eq. (3.22) we obtain the final expression for $\tilde{T}_n$:

$$\tilde{T}_n\equiv\frac{2}{B}\int dr_{12}r_{12}e^{-\frac{r_{12}^2}{4B}}J_n(k_1r_{12})\,J_n(k_2r_{12})\,J_{2n}(k_3r_{12})\,. \tag{3.23}$$

For very small momenta (i.e. all $k_i << 1/B^{1/2}$). we obtain

$$\tilde{T}_n \simeq \frac{2^2 \left(B^2 Sym\left(k_1 k_2 k_3^2\right)\right)^n}{\left(n!\right)^2}. \tag{3.24}$$

where Sym means symmetrization over 3 gluons (and division by 1/3). The details of calculation are given in Appendix A.

3.3.3 Numerical Results.

The value of three point cumulant is

$$ac_n = T_n/(N_c^2-1)^2 + \tilde{T}_n/(N_c^2-1) \tag{3.25}$$

where n is the harmonics number (we depict n=2,4 cases).

We cannot calculate the integrals T_n and $\tilde{T}_n$ analytically, so we will depict several types of different behaviour of $T_2, T_4, \tilde{T}_2$ and $\tilde{T}_4$ as functions of momenta. On the other hand the correlators have nontrivial structure as functions of k_1, k_2, k_3. Namely they depend in the polar coordinates:

$$k_3 = k_r \cos(\theta)\ k_1 = k_r \sin(\theta)\cos(\phi)\ k_2 = k_r \sin(\theta)\sin(\phi)\ k_r = \sqrt{k_1^2+k_2^2+k_3^2} \tag{3.26}$$

in a nontrivial way: the value of the cumulant depends not ony on k_r but also on θ, ϕ. Indeed, already for very small $k_1, k_2, k_3 \to 0$

$$ac_2^3 \sim k_1^2 k_2^2 k_3^2 (k_1^2+k_2^2+k_3^2) \sim k_r^8 \sin(2\theta)^2 \sin(2\phi)^2 \sin(\theta)^2 \tag{3.27}$$

In order to better understand the structure of the cumulant we shall consider 3 cases:

- **Case I**: All the momenta are equal to each other, $k_1 = k_2 = k_3 = k$.
- **Case II**: $\theta, \phi = const$, and we consider the cumulant and its parts as functions of k_r
- **Case III**: We consider the cumulant as function of θ, ϕ for several values of k_r.

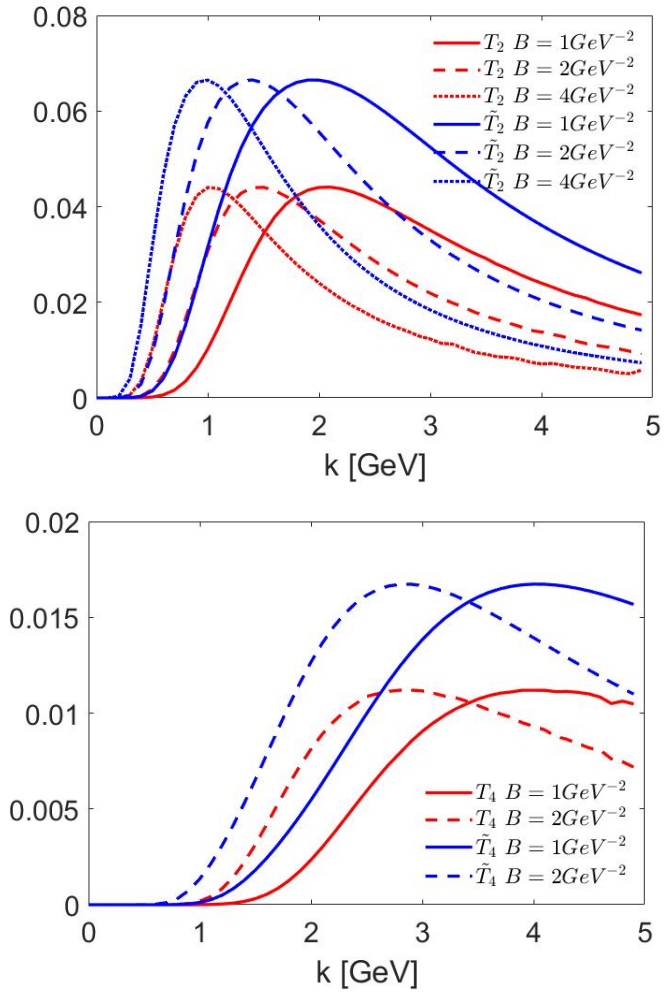

Figure 3.3: Above: The integrals T_2 and $\tilde{T}_2$ when all momenta are equal, $k_1 = k_2 = k_3 = k$ for different values of the parameter $B = 1(2, 4)GeV^{-2}$ in full (dashed,dotted) line. Below: The integrals T_4 and $\tilde{T}_4$ when all momenta are equal, $k_1 = k_2 = k_3 = k$ for different values of the parameter $B = 1(2)GeV^{-2}$ in full (dashed) line.

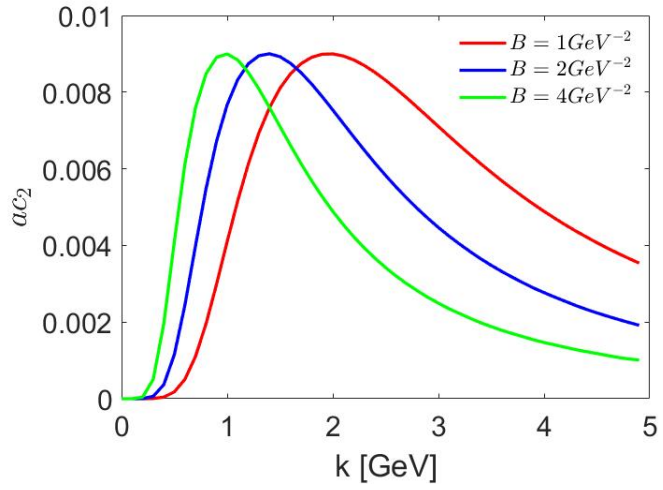

Figure 3.4: The cumulant ac_2 for $N = m = 3, N_c = 3$, $k_1 = k_2 = k_3$

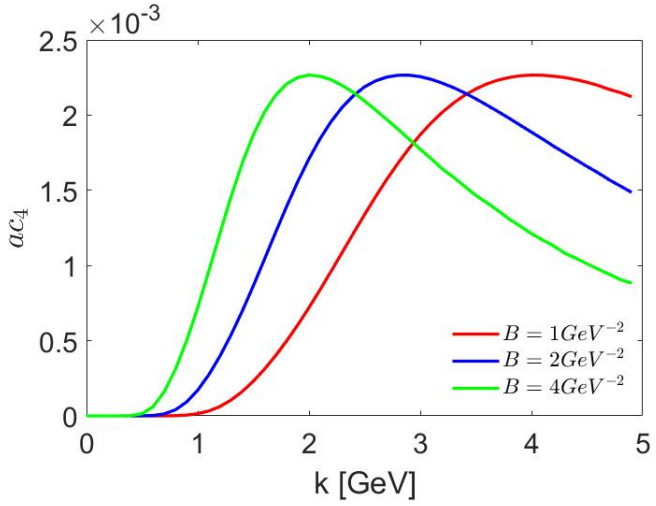

Figure 3.5: The cumulant ac_4 for $N = m = 3, N_c = 3$ for $k_1 = k_2 = k_3$

In Fig. 3.3 above we depict the dependence of T_2 and $\tilde{T}_2$ on k. We see that for equal k, the integrals increases up to k of order $1/\sqrt{B}$, and then slowly decreases, with value at maximum of order $T_2 \approx 0.04, \tilde{T}_2 \approx 0.07$ that depend on B very weakly. Note also that the maximum is located approximately at the same place where the maximum for the similar graph for symmetric cumulant (second harmonic) is located, and their k dependence look very similar.

We see that both integrals vanish at $k = 0$, and as $k \to \infty$ we get slowly $T_2 \to 0$ and $\tilde{T}_2 \to 0$. Both T_2 and $\tilde{T}_2$ have maximum in the same point, and their k-dependence is very similar.

We observe very similar behaviour as a function of k for T_4 and $\tilde{T}_4$ in Fig. 3.3 below, except the fourth harmonics is 4-5 times smaller and the maximum is shifted to larger k-s.

In Fig. 3.4 we depict the corresponding full three point cumulant ac_2, i.e. the second harmonic dependence on k, for the model case N=m=3. In this case even for $N_c = 3$ the diagram with 3 gluons in a dipole is a dominant one, giving 90 percent of the value of the cumulant. Similarly we depict ac_4 in Fig. 3.5.

An interesting feature of the momentum dependence of the cumulant is that the direction in (ϕ, θ) along which the cumulant is maximal is the one corresponding to $k_1 = k_2 = k_3$. We illustrate this by considering the dependence of ac_2, as well as tripole and dipole diagrams on the direction in k-space in Fig. 3.6 and Fig. 3.7.

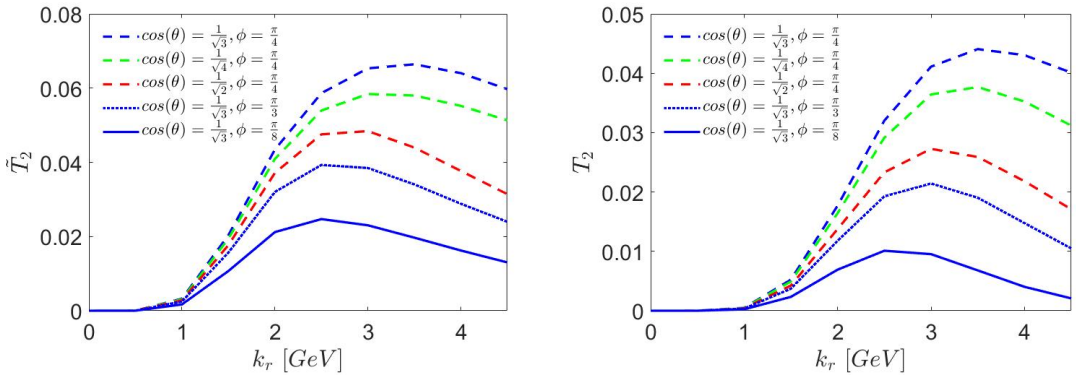

Figure 3.6: The integrals T_2 and $\tilde{T}_2$ for different directions, $\theta, \phi = const$, k_r is changing

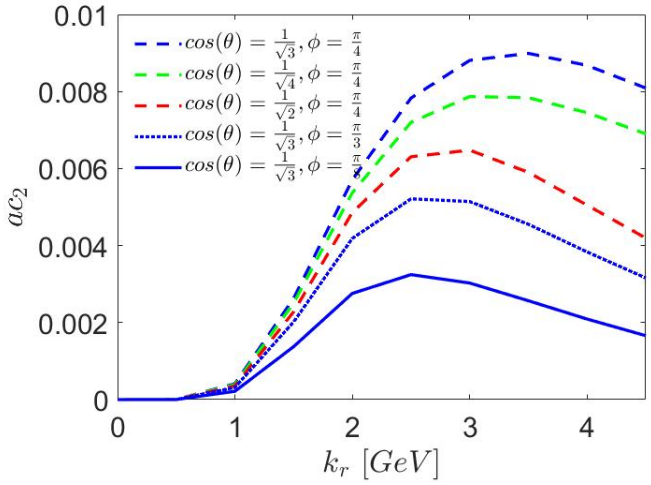

Figure 3.7: The full cumulant ac_2 for different directions, $\theta, \phi = const$, k_r is changing. B=1 GeV^{-2}

We see from Fig. 3.6 and Fig. 3.7 that indeed the direction $k_1 = k_2 = k_3$ (i.e. $\cos(\theta) = 1/\sqrt{3}, \phi = \pi/4$) corresponds to an absolute maximum. On the other hand we see common structure in each direction, with increase up to some maximum value and then slow decrease depending on the direction. The Fig. 3.6 and Fig. 3.7 are done for $B = 1\text{GeV}^{-2}$, for other values of B the behaviour is qualitatively similar.

In order to understand better the two dimensional structure we also consider the behaviour of the cumulant as a function of θ, ϕ for $k_r = 2, 4, 6$ GeV. This is depicted in Fig. 3.8 and Fig. 3.9.

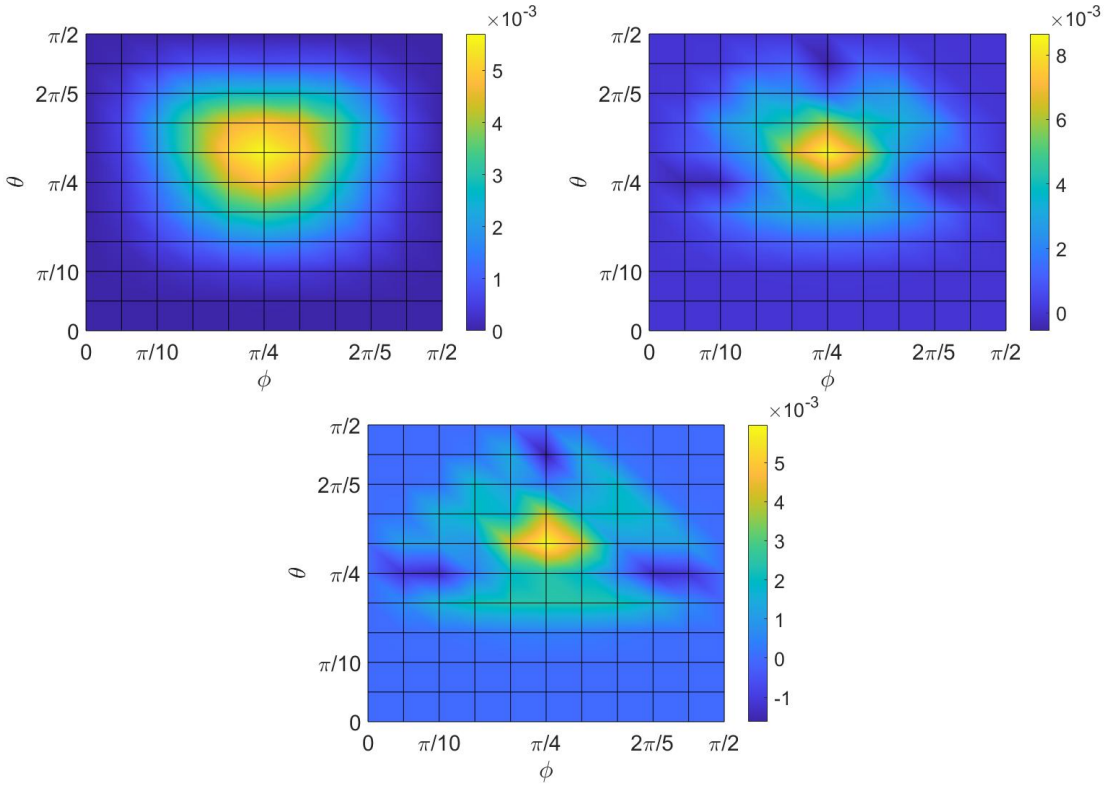

Figure 3.8: The cumulant ac_2 for N=m=3 $N_c = 3$ when $k_r = 2, 4, 6$GeV (from top left, top right, bottom) and B=1 GeV^{-2}

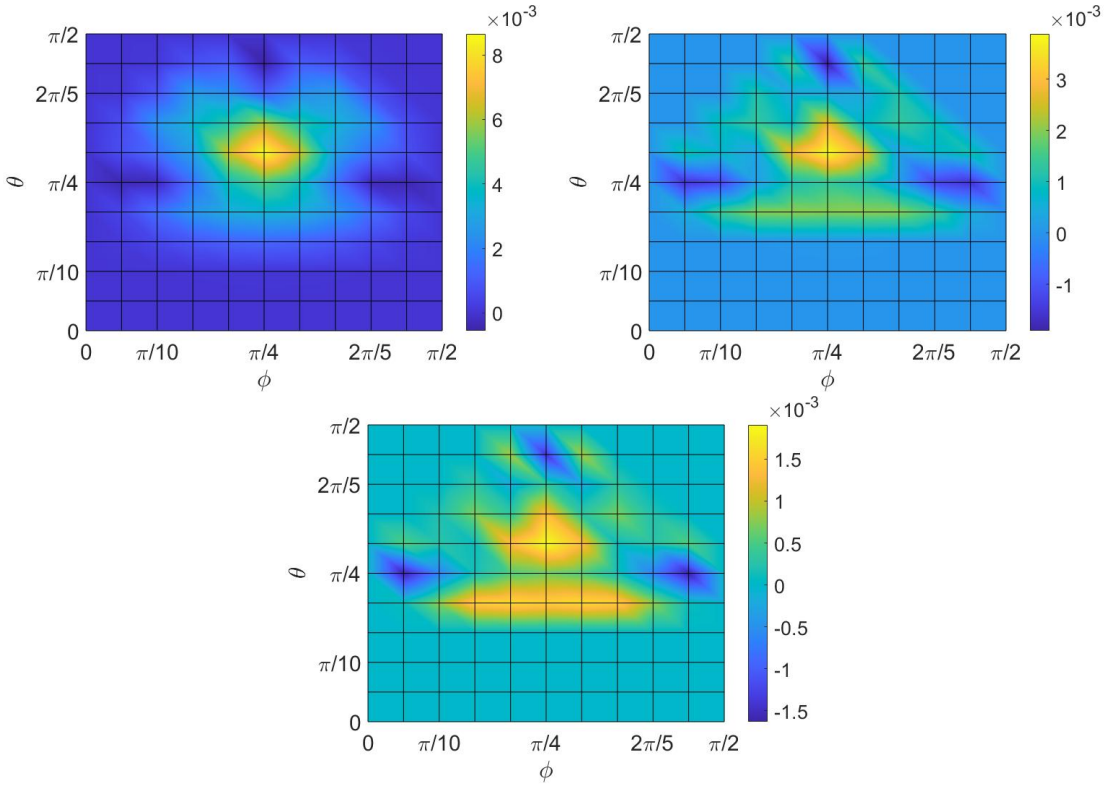

Figure 3.9: The cumulant ac_2 for N=m=3 $N_c = 3$ when $k_r = 2, 4, 6$GeV (from top left, top right, bottom) and B=4 GeV^{-2}

Recall, that the case $B = 1$ GeV $^{-2}$corresponds to the best fit for even symmetric cumulants in [10], while B=4 GeV^{-2} corresponds to the mean field approach with the effective cross section for MPI two times bigger than the experimental one. We limit ourselves by depicting the second harmonic. Note that the structure of the cumulant for $B = 2, 3$ GeV^{-2} is very similar to the one for B=1 GeV^{-2}, so we do not depict it here. and starts to change only for larger B that correspond to the effective DPS cross sections bigger than the experimental one.

Let us note that due to very similar form of the $k-$dependence of T_n and $\tilde{T}_n$, except their scale, the similar dependence on k-s will continue for the case of arbitrary m, N (with different overall coefficient depending on N,m).

We also compared the numerical results for small momenta with the the analytic expression (Eq. (3.19)) and expression (eq. (3.24)) and found that they coincide.

3.4 High Multiplicity.

3.4.1 Higher Order Diagrams.

We now consider the general case of $N, m > 3$. It was already noted above that the leading behaviour in powers of $1/(N_c^2 - 1)$ (and a resummation of series in terms of $m^2/(N_c^2 - 1)$) corresponds to diagrams with one tripole and arbitrary number of nonintersecting dipoles. However in this case there is also the term contributing to the cumulant that is suppressed by 1/N but of the first order in $1/(N_c^2 - 1)$. The corresponding resummation, analogous to the resummation for tripole, will lead to inclusion of the series corresponding to the diagrams with one dipole with 3 off-diagonal gluons and up to $[N/2 - 1]$ nonintersecting dipoles, such that each of the sources has only 2 (or zero) gluons coming out. Numerically for $N_c = 3$ the term with 3 gluon dipole is a dominant one up to very large multiplicities of order 100.

Consequently there are three types of diagrams we have to consider:

- **Type a**: The diagrams with arbitrary (up to N/2) number of dipoles with 2 off-diagonal gluons. These diagrams were considered in detail in [11]. Such diagrams, contribute to the total cross section $\hat{\sigma}$.

- **Type b**: There is one tripole and $d < N/2$ nonintersecting dipoles with 2 off-diagonal gluons.

- **Type c**: There is one dipole with 3 off-diagonal gluons and d nonintersecting dipoles with 2 off-diagonal gluons each.

Let us recall the calculation of the combinatorial coefficients for the case a).We first pick 2 gluons and 2 sources for each 2-gluon dipole. From the picked gluons we get a factor of $\binom{1}{2}$:

$$\binom{m}{2}\binom{m-2}{2}...\binom{m-2d+2}{2}\frac{1}{d!}=\frac{(m)!}{2^d d!\,(m-2d)!}. \tag{3.28}$$

The sources give us a similar factor of:

$$\binom{N}{2}\binom{N-2}{2}...\binom{N-2d+2}{2}=\frac{(N)!}{2^d\,(N-2d)!}. \tag{3.29}$$

For type b diagrams we have an additional multiplier coming from the number of choices of the 3-gluon dipole given by:

$$3\binom{m}{3}3!\binom{N}{2} \tag{3.30}$$

For type c the number of choices for the tripole give us a factor:

$$3\binom{m}{3}3!\binom{N}{3} \tag{3.31}$$

Only diagrams of type b and c contribute to harmonics of $n>0$ so we can write:

$$\begin{aligned}
\frac{d^3\hat{\sigma}}{\prod_{i=1}^{i=3}d\Gamma_i} \;&\propto\; N_c^m(N_c^2-1)^N N^m\prod_{i=1}^{i=3}|\overrightarrow{f}(\boldsymbol{k}_i)|^2\\
&\times\;\{\sum_{d=0}^{\lfloor(N-2)/2\rfloor}\left(\frac{\hat{D}_0F_{corr}^{(2)}(N,m)}{N^2(N_c^2-1)}\right)^d\frac{2^33!F_{corr}^{(3)}(N,m)}{N^34(N_c^2-1)}\frac{m!N!}{d!3!2!(m-2d-3)!(N-2d-2)!}\\
&\times\;\int_\rho\cos\left(\mathbf{k}_1\cdot\mathbf{r}_{12}\right)\cos\left(\mathbf{k}_2\cdot\mathbf{r}_{12}\right)\cos\left(\mathbf{k}_3\cdot\mathbf{r}_{12}\right)\\
&+\;\sum_{d=0}^{\lfloor(N-3)/2\rfloor}\left(\frac{\hat{D}_0F_{corr}^{(2)}(N,m)}{N^2(N_c^2-1)}\right)^d\frac{2^33!F_{corr}^{(3)}(N,m)}{N^3(N_c^2-1)^2}\frac{m!N!}{d!(3!)^2(m-2d-3)!(N-2d-3)!}\\
&\times\;\int_\rho\cos\left(\mathbf{k}_1\cdot\mathbf{r}_{12}\right)\cos\left(\mathbf{k}_2\cdot\mathbf{r}_{23}\right)\cos\left(\mathbf{k}_3\cdot\mathbf{r}_{31}\right)\;\}\,.
\end{aligned} \tag{3.32}$$

Here we defined the integral $\hat{D}_0$ corresponding to the off-diagonal dipole component of the wave function of the nucleon fully integrated out i.e. integrated both over the source positions and the momenta of the gluons:

$$\hat{D}_0\equiv\int(r_{12}dr_{12})\left(\prod_{j=1,2}k_jdk_j\left(\left|\overrightarrow{f}(\mathbf{k}_j)\right)\right|^2\right)\frac{e^{-\frac{r_{12}^2}{4B}}}{2B}J_0\left(k_1r_{12}\right)J_0\left(k_2r_{12}\right). \tag{3.33}$$

This integral is determined by a normalized radiation amplitude $\vec{f}$ and like in [11] can be considered as a free parameter (coinciding with the one in [11]). This integral is expected to be between 0 and 1 [11].

As was already noted above, it was shown in [10] that the diagonal gluons contribute to the interference diagrams by renormalizing them, i.e. multiplying by factors $F(m,N)$ that can be easily calculated. For renormalisation factors $F^{(2)}$ and $F^{(3)}$ connected with diagonal gluons for dipole and tripole diagrams relevant for our discussion we have the explicit expressions:

$$F^{(3)}(N,m)=\frac{(m-3)!}{m!}(6(m-2N)N^2+6(N-1)^{m-1}N^{3-m}(-2+m+2N)). \quad (3.34)$$

In the limit $N\to\infty, m\to\infty, m/N=\bar{m}=const$, we have

$$F^{(3)}(N,m)\to F^{(3)}(\bar{m})=6\frac{e^{-\bar{m}}(2+\bar{m})}{\bar{m}^3}+6\frac{\bar{m}-2}{\bar{m}^3}. \quad (3.35)$$

In the same way it was obtained in [10]

$$F^{(2)}(N,m)=\frac{2N^{1-m}(N(N-1)^m+mN^m-N^{1+m})}{m(m-1)}, \quad (3.36)$$

and in the limit $N\to\infty, m\to\infty, m/N=\bar{m}=const$, we have

$$F^{(2)}(N,m)\to F^{(2)}(\bar{m})=\frac{2\bar{m}+2e^{-\bar{m}}-2}{\bar{m}^2}. \quad (3.37)$$

For the the 3-gluon dipole we get a correction factor that is the same as $F^{(3)}(N,m)$, as calculated in appendix B. For nonintersecting dipoles/tripoles it is possible to prove that the corresponding renormalisation factors factorize.

To find the differential multiplicity we also need to find the total cross section $\hat{\sigma}$ in the same approximation. This cross section is equal to

$$\begin{aligned}
\hat{\sigma} \;\propto\; & N_c^m(N_c^2-1)^N N^m \\
\times\; & \{\sum_{d=0}^{\lfloor N/2\rfloor}\left(\frac{\hat{D}_0 F^{(2)}_{corr}(N,m)}{N^2(N_c^2-1)}\right)^d \frac{m!N!}{d!\,(m-2d)!\,(N-2d)!} \\
+\; & \frac{3^3 F^{(3)}_{corr}(N,m)\,\hat{\tilde{T}}_0}{N^3(N_c^2-1)}\sum_{d=0}^{\lfloor (N-2)/2\rfloor}\left(\frac{\hat{D}_0 F^{(2)}_{corr}(N,m)}{N^2(N_c^2-1)}\right)^d \frac{m!N!}{d!2!3!\,(m-2d-3)!\,(N-2d-2)!} \\
+\; & \frac{3^3 F^{(3)}_{corr}(N,m)\,\hat{T}_0}{N^3(N_c^2-1)^2}\sum_{d=0}^{\lfloor (N-3)/2\rfloor}\left(\frac{\hat{D}_0 F^{(2)}_{corr}(N,m)}{N^2(N_c^2-1)}\right)^d \frac{m!N!}{d!(3!)^2\,(m-2d-3)!\,(N-2d-3)!}\},
\end{aligned} \quad (3.38)$$

where we define the integrals:

$$\hat{\tilde{T}}_0 \equiv \frac{2}{3^3}\int (r_{12}dr_{12})\prod_{j=1}^{3} k_j dk_j \left|\overrightarrow{f}(\mathbf{k}_j)\right|^2 \frac{e^{-\frac{r_{12}^2}{4B}}}{B} J_0(k_1 r_{12})\, J_0(k_2 r_{12})\, J_0(k_3 r_{12}), \tag{3.39}$$

$$\begin{aligned}\hat{T}_0 &\equiv \frac{2^2}{3^5}\int \left(d^2r_{12}d^2r_{23}\right)\prod_{j=1}^{j=3} k_j dk_j \left|\overrightarrow{f}(\mathbf{k}_j)\right|^2 \frac{e^{-\frac{r_{12}^2+\overrightarrow{r}_{12}\cdot\overrightarrow{r}_{23}+r_{23}^2}{3B}}}{(2\pi B)^2} \\ &\times J_0(k_1 r_{12})\, J_0(k_2 r_{23})\, J_0(k_3|\overrightarrow{r}_{12}+\overrightarrow{r}_{23}|),\end{aligned} \tag{3.40}$$

corresponding to the integrated out tripole and integrated out dipole with 3 off-diagonal gluons. Note that the radiation amplitude $\vec{f}$ defines the $\hat{T}_0$ and $\hat{\tilde{T}}_0$ values, i.e. they are not free parameter of the model anymore, i.e. if we know $\hat{D}_0$ the values of $\hat{T}_0$ and $\hat{\tilde{T}}_0$ are correlated with the value of $\hat{D}_0$.

For the differential multiplicity we obtain:

$$\begin{aligned}\frac{d^3N}{d\Gamma_1 d\Gamma_2 d\Gamma_3} &= \frac{d^3\sigma}{\sigma d\Gamma_1 d\Gamma_2 d\Gamma_3} \\ &\approx \left(\prod_{i=1}^{i=3}\left|\overrightarrow{f}(\boldsymbol{k}_i)\right|^2\right)\hat{\sigma}^{-1} \\ &\times \left[\frac{2F_{corr}^{(3)}(N,m)}{N^3\left(N_c^2-1\right)}\sum_{d=0}^{\lfloor (N-2)/2\rfloor}\left(\frac{\hat{D}_0 F_{corr}^{(2)}(N,m)}{N^2\left(N_c^2-1\right)}\right)^d \frac{m!N!}{d!2!3!\,(m-2d-3)!\,(N-2d-2)!}\right. \\ &\times \int_\rho \cos(\mathbf{k}_1\cdot\mathbf{r}_{12})\cos(\mathbf{k}_2\cdot\mathbf{r}_{12})\cos(\mathbf{k}_3\cdot\mathbf{r}_{12}) \\ &+ \frac{2^3F_{corr}^{(3)}(N,m)}{N^3\left(N_c^2-1\right)^2}\sum_{d=0}^{\lfloor (N-3)/2\rfloor}\left(\frac{\hat{D}_0 F_{corr}^{(2)}(N,m)}{N^2\left(N_c^2-1\right)}\right)^d \frac{m!N!}{d!(3!)^2\,(m-2d-3)!\,(N-2d-3)!} \\ &\times \left.\int_\rho \cos(\mathbf{k}_1\cdot\mathbf{r}_{12})\cos(\mathbf{k}_2\cdot\mathbf{r}_{23})\cos(\mathbf{k}_3\cdot\mathbf{r}_{31})\right],\end{aligned} \tag{3.41}$$

where

$$\hat{\sigma} \equiv \sum_{d=0}^{\lfloor N/2\rfloor}\left(\frac{\hat{D}_0 F_{corr}^{(2)}(N,m)}{N^2\left(N_c^2-1\right)}\right)^d \frac{m!N!}{d!\,(m-2d)!\,(N-2d)!}. \tag{3.42}$$

is the total cross section. We have shown by direct numerical calculation that the contribution to the total cross section of the integrated out 3-gluon dipole and of the integrated out tripole are negligible compered to the 2-gluon dipole terms, so we can ignore the dependence on $\hat{T}_0$ and $\hat{\tilde{T}}_0$

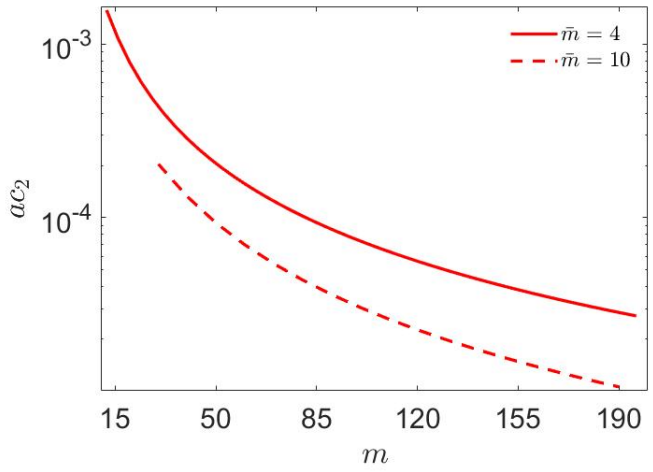

Figure 3.10: The dependence of the maximum value of ac_2 (as a function of momenta) on multiplicity m for different values of $\bar{m}$ where $\hat{D}_0 = 0.1$ and $N_c = 3$.

For differential one gluon distribution we have in this approximation:

$$\frac{dN}{d\Gamma} = m \left| \overrightarrow{f}\,(\boldsymbol{k}) \right|^2 . \tag{3.43}$$

We will can now write for the parts corresponding to the 3-gluon dipole and a the tripole contribution

$$\begin{aligned}
ac_n^{3,2}\{3\} &= \frac{3^3 F_{corr}^{(3)}(N,m)}{\binom{m}{3}\hat{\sigma}N^3(N_c^2-1)}\tilde{T}_n/3 \\
&\times \sum_{d=0}^{\lfloor (N-2)/2 \rfloor} \left(\frac{\hat{D}_0 F_{corr}^{(2)}(N,m)}{N^2\left(N_c^2-1\right)} \right)^d \frac{m!N!}{d!2!3!(m-2d-3)!(N-2d-2)!} \\
ac_n^{3,3}\{3\} &= \frac{3^3 F_{corr}^{(3)}(N,m)}{\binom{m}{3}\hat{\sigma}N^3(N_c^2-1)^2}T_n \\
&\times \sum_{d=0}^{\lfloor (N-3)/2 \rfloor} \left(\frac{\hat{D}_0 F_{corr}^{(2)}(N,m)}{N^2\left(N_c^2-1\right)} \right)^d \frac{m!N!}{d!(3!)^2(m-2d-3)!(N-2d-3)!} \\
ac_n &= ac_n^{3,2}\{3\} + ac_n^{3,3}\{3\} .
\end{aligned} \tag{3.44}$$

Note that taking $\hat{D}_0 = 0$ or equivalently, only $d = 0$ term in the expansion for $\hat{\Sigma}$ we return to the result (eq. (3.11)) for for N=m=3 of the previous section.

3.4.2 Numerical Results.

We now look at ac as a function of the multiplicity for different values of $\bar{m} \equiv m/N$.

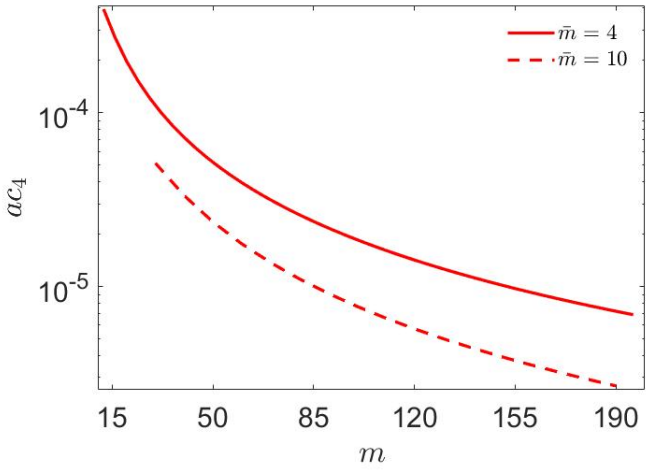

Figure 3.11: The dependence of the maximum value of ac_4 (as a function of momenta) on multiplicity m for different values of $\bar{m}$ where $\hat{D}_0 = 0.1$ and $N_c = 3$.

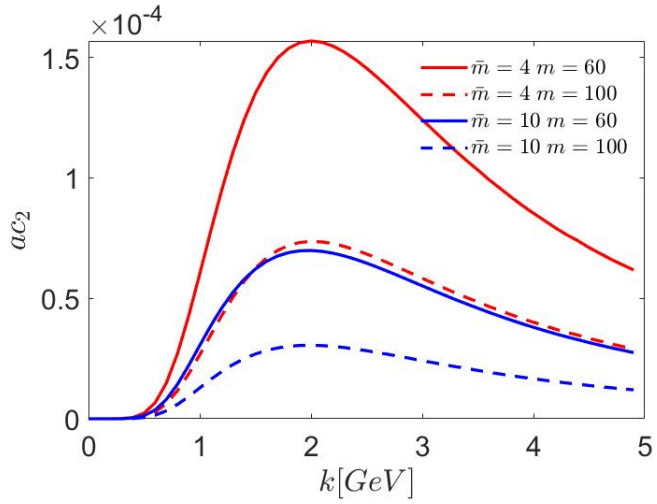

Figure 3.12: The form of the ac_2 for $k_1 = k_2 = k_3$ and for different values of multiplicity m, with $\hat{D}_0 = 0.1$, $B = 1$ GeV^{-2},$N_c = 3$.

We first look at ac_2 as a function of m for fixed values of $\bar{m} = 4, 10$. In Fig. 3.10 we depict the dependence on m of the maximum value of ac_2 as function of transverse momenta. We see that the value of ac_2 decreases slowly with multiplicity, and the characteristic scale of ac_2 for moderate $m \sim 50$ is of order 2×10^{-4}.

It is interesting to note that the scale of two point correlator $v_2^2 \equiv sc_2\{2\}$, calculated in [11] was $\sim 4 - 5 \times 10^{-3}$, i.e. we observe a decrease of order $2(N_c^2 - 1)$ going from v_2^2 to ac_2, and the ratio between the two very weakly depends on multiplicity.

In Fig. 3.11 we depict the analogous dependence of ac_4. We depict the k-dependence of ac_2 for various multiplicities in Fig. 3.12. We see that the k-dependence is practically independent on multiplicity (up to an overall scaling factor), and is the same as in N=m=3 case.

3.4.3 Comparison with the Experimental Results.

It will be interesting to compare our results with the recent experimental data [12]. In that paper the average of the second harmonic over experimental data was taken with momenta varying in two different kinematic regions $k \in [0.3, 3]\, GeV$ and $k \in [0.5, 5]\, GeV$.

Recall that we can completely separate the dependence of the momenta and n, in the form of $\tilde{T}_n$ and T_n, and the dependence on all other parameters like multiplicity, number of sources, N_c and the model constant $\hat{D}_0$, It is convenient to define:

$$\begin{aligned} R^{3,2}\left(N, m, N_c, \hat{D}_0\right) &\equiv \frac{ac_n^{3,2}\{3\}}{\tilde{T}_n} \\ R^{3,3}\left(N, m, N_c, \hat{D}_0\right) &\equiv \frac{ac_n^{3,3}\{3\}}{T_n}. \end{aligned} \tag{3.45}$$

Since all of the dependence on the momenta in our model is contained in k-dependent functions $T_n(k_1, k_2, k_3)$ and $\tilde{T}_n(k_1, k_2, k_3)$ we can calculate the averages:

	$B = 1$ GeV^{-2}	$B = 2$ GeV^{-2}	$B = 4$ GeV^{-2}
$\langle T_2\rangle_{0.3-3GeV} = \frac{\int_{0.3}^{3} dk_1 dk_2 dk_3 T_2}{(3-0.3)^3}$	9.4×10^{-3}	6.5×10^{-3}	2.7×10^{-3}
$\left\langle \tilde{T}_2\right\rangle_{0.3-3GeV} = \frac{\int_{0.3}^{3} dk_1 dk_2 dk_3 T_2}{(3-0.3)^3}$	2.1×10^{-2}	1.6×10^{-2}	1.1×10^{-2}
$\langle T_2\rangle_{0.5-5GeV} = \frac{\int_{0.5}^{5} dk_1 dk_2 dk_3 T_2}{(5-0.5)^3}$	4.1×10^{-3}	1.4×10^{-3}	1.5×10^{-3}
$\left\langle \tilde{T}_2\right\rangle_{0.5-5GeV} = \frac{\int_{0.5}^{5} dk_1 dk_2 dk_3 T_2}{(5-0.5)^3}$	1.4×10^{-2}	8.7×10^{-3}	5.0×10^{-3}

Table 3.1: Avreges of the integrals for different ranges of k_1, k_2, k_3 and values of B

The value of the cumulant is obtained by calculating:

$$\langle ac_2\{3\}\rangle = R^{3,2}\left\langle \tilde{T}_2 \right\rangle + R^{3,3}\langle T_2\rangle . \tag{3.46}$$

The results are depicted in Fig. 3.1313:

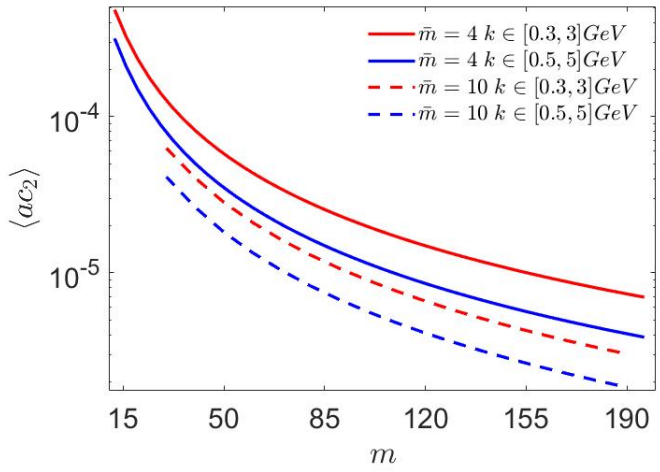

Figure 3.13: The 3 point cumulant ac^3 averaged over region $0.5 < k_i < 3$ and $0.5 < k_i < 5$ (i=1,2,3)

We depict in Fig. 3.14 the theoretical value of the second harmonic (integrated over the region $0.5 \leq k \leq 3$ together with experimental data, namely the ATLAS result after additional analysis, done in [56] to eliminate nonflow effects. Note that the values of m, that are obtained here using LPHD concept, correspond to a total number of soft hadrons which is approximately $m \sim 1.5 N_{\text{charged}}$, where N_{charged} is a number of charged particles measured in the ATLAS experiment. (The high multiplicity sample used by ATLAS is dominated by π mesons [57], the factor 3/2 then comes from isotopic invariance, since π mesons form a triplet in the isotopic space). The two different types of data, with or without gap are depicted, meaning the gap of 0.5 units between subevents to limit nonflow is taken or not are depicted. We refer the reader to [12, 56] for the details of the experimental analysis.

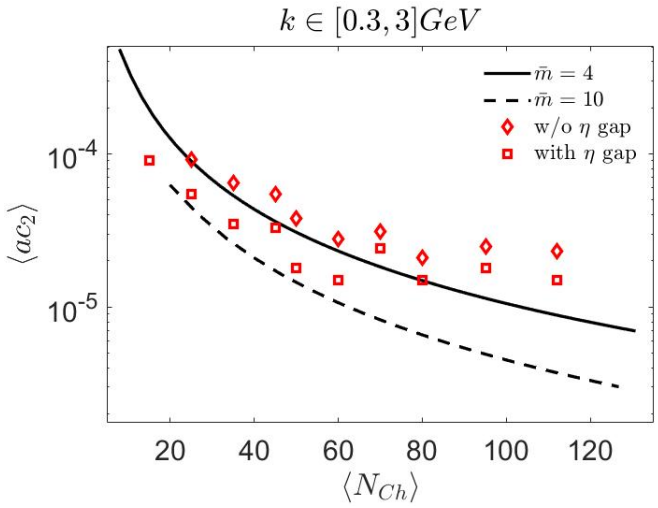

Figure 3.14: The 3 point cumulant ac_2 averaged over region $0.5 < k_i < 3$ and $0.5 < k_i < 3$ (i=1,2,3), compared with experimental data. The experimental data is depicted after additional analysis [56] of the ATLAS results, made to minimize nonflow effects, where the two types of experimental points correspond to analysis with or without the gap of 0.5 units between subevents.

We see rather good agreement with experimental data for $m \leq 120 (N_{charged} \leq 80)$ and if we average over region $0.5 \leq k \leq 3$ GeV.

However for higher multiplicities the theoretical result decreases with total multiplicity m rather rapidly, contrary to the experimental data, which shows the independence of ac on multiplicity for large m. In addition the ATLAS data for average ac_2 over the region $0.5 \leq k \leq 5$ GeV tend to increase relative to average over $0.5 \leq k \leq 3$ GeV, while Fig. 3.13 shows the opposite trend. Note however that these averages are very sensitive to explicit k-dependence and even small inaccuracy in k-dependence leads to rather large inaccuracy in the average. Moreover, our results may be less accurate for large transverse momenta, where soft gluon approximation is less accurate.

Chapter 4

Conclusions.

We have studied the influence of the effects of colour interference and colour flow on the three point asymmetric cumulants using the model [10, 11].

We get qualitative agreement of our results for asymmetric correlator with the scale of available experimental data [12], at least for moderate multiplicities $m \sim 100$. Note that only integrated experimental data is available, decreasing the possibility of detailed comparison with the experimental results. This data seems however to be very sensitive on precise transverse momenta dependence. Thus the detailed comparison between theoretical and experimental results demands further measurements, in particular the detailed study of transverse momenta dependence, as it was done already for symmetric correlators.

From our side we carried the detailed study of the transverse momenta dependence and characteristic scale of the correlator.

The discrepancy with the experimental data is seen in the decrease of the ac cumulant with multiplicity m at high multiplicities, the analogous behaviour was also noted for symmetric cumulants in [11]. The experimental data indicates that cumulants are virtually independent of multiplicity. On the other hand let us note that there may be significant uncertainties in the experimental data, related to separation of the flow and nonflow effects [56]. We expect that further study of the model, in particular inclusion of higher suppressed diagrams (like quadrupole like ones) will improve the dependence on multiplicity both for symmetric and asymmetric correlators [58].

Appendix A

Small momenta limit

Consider the case of the very small transverse momenta for a tripole. Looking at very small momenta, $k_j \ll B^{-1/2}$ for all 3 momenta we can take the Taylor expansion of the Bessel functions

$$J_n(z) \simeq \frac{z^n}{n! 2^n} \tag{A.1}$$

to find:

$$\begin{aligned} T_n &\simeq \frac{2^{4(1-n)} \left(k_1 k_2 k_3^2\right)^n}{3^2 (n!)^2 (2n)! (2\pi B)^2} \int dr_{12} dr_{23} d\alpha_{12} d\alpha_{23} r_{12}^{1+n} r_{23}^{1+n} e^{-\frac{r_{12}^2 + \overrightarrow{r}_{12} \cdot \overrightarrow{r}_{23} + r_{23}^2}{3B}} \\ &\times \left(\cos(\alpha_{12}) + \sin(\alpha_{12})\right)^n \left(\cos(\alpha_{23}) + \sin(\alpha_{23})\right)^n \\ &\times \left(r_{12}\cos(\alpha_{12}) + r_{23}\cos(\alpha_{23}) - i\left(r_{12}\sin(\alpha_{12}) + r_{23}\sin(\alpha_{23})\right)\right)^{2n}. \end{aligned} \tag{A.2}$$

Note that from dimensional analysis for small momenta

$$a c_n \propto \left(B^2 k_1 k_2 k_3^2\right)^n \tag{A.3}$$

Simplifying the integral (eq. (A.2)) we obtain in the limit of small k_i:

$$\begin{aligned} T_n &\simeq \frac{(3B)^2 2^{4(1-n)} \left(3^2 B^2 k_1 k_2 k_3^2\right)^n}{3^2 (n!)^2 (2n)! (2\pi B)^2} \int_{R^4} dx_1 dx_2 dy_1 dy_2 \\ &\times \frac{\partial^n}{\partial \alpha^n} \frac{\partial^n}{\partial \beta^n} \frac{\partial^{2n}}{\partial \gamma^{2n}} e^{-\left(x_1^2 + x_1 x_2 + x_2^2 + y_1^2 + y_1 y_2 + y_2^2\right) + \alpha(x_1 + i y_1) + \beta(x_2 + i y_2) + \gamma(x_1 + x_2 - i(y_1 + y_2))} \Big|_{\alpha=\beta=\gamma=0} \\ &= \frac{2^{4(1-n)} \left(3^2 B^2 k_1 k_2 k_3^2\right)^n}{(n!)^2 (2n)! (2\pi)^2} \frac{\partial^n}{\partial \alpha^n} \frac{\partial^n}{\partial \beta^n} \frac{\partial^{2n}}{\partial \gamma^{2n}} \frac{4\pi^2}{3} e^{\frac{2}{3}\gamma(\alpha+\beta)} \Big|_{\alpha=\beta=\gamma=0} \\ &= \frac{2^{4(1-n)} \left(3^2 B^2 k_1 k_2 k_3^2\right)^n}{3 (n!)^2 (2n)!} (2n)! \left(\frac{2}{3}\right)^{2n} = \frac{2^{4+2n} \left(B^2 k_1 k_2 k_3^2\right)^n}{3 (n!)^2}. \end{aligned} \tag{A.4}$$

Note that all expressions above are understood to be symmetrized over gluons 1,2,3, i.e. equal to sum $\frac{1}{3}\sum_{1,2,3}$.

We can also use the same approximation to find:

$$\tilde{T}_n \simeq \frac{2^{1-4n}\left(Sym\left(k_1 k_2 k_3^2\right)\right)^n}{B\left(n!\right)^2(2n)!}\int dr_{12} r_{12}^{1+4n} e^{-\frac{r_{12}^2}{4B}}. \tag{A.5}$$

This lives us with an integral that is easly solved by taking $u = \frac{r_{12}^2}{4B}$ and we get the result:

$$\tilde{T}_n \simeq \frac{2^2\left(B^2 k_1 k_2 k_3^2\right)^n}{\left(n!\right)^2}. \tag{A.6}$$

Appendix B

3-gluons dipole correction

In the same way they found the correction in Ref. [10], we can find the correction factor for the case for the 3-gluon dipole. We note that if we are are looking at an ordered list of emitted gluons with only three off -diagonal gluons that make the 3-gluon dipole we can divide the diagonal gluons into 4 kinds. If the off-diagonal gluons are $(1, 2, 3)$ the diagonal gluons can be before 1, between 1 and 2, between 2 and 3 and after 3. The ones between 1 and 2 and between 2 and 3 will give us a factor of $1/2$ if they are on the same sources as the off-diagonal gluons, and will give us a factor of 1 otherwise. We first need the number of incoherent diagrams, which will be:

$$\begin{aligned} N_{incoh} &= \sum_{j_{12}=0}^{m-3} \sum_{j_{23}=0}^{m-3-j_{12}} N^{m-3-j_{12}-j_{23}}(m-2-j_{12}-j_{23}) \\ &\times \sum_{l_{12}=0}^{j_{12}} \left(\begin{array}{c} j_{12} \\ l_{12} \end{array} \right) 2^{l_{12}}(N-2)^{j_{12}-l_{12}} \\ &\times \sum_{l_{23}=0}^{j_{23}} \left(\begin{array}{c} j_{23} \\ l_{23} \end{array} \right) 2^{l_{23}}(N-2)^{j_{23}-l_{23}} \\ &= \frac{m!}{3!(m-3)!} N^{m-3} \end{aligned} \tag{B.1}$$

where j_{ab} counts the number of diagonal gluons between a and b and l_{ab} counts how many of them are on the same gluons as the 3-gluons dipole.

The correction coefficient is then calculated by taking into account the factor of $1/2^l$, coming from identity $T^a T^b T^a = T^b/2$:

$$F^{(3,2)}(N, m) = \frac{1}{N_{incoh}} \sum_{j_{12}=0}^{m-3} \sum_{j_{23}=0}^{m-3-j_{12}} N^{m-3-j_{12}-j_{23}}(m-2-j_{12}-j_{23})$$

$$\times \sum_{l_{12}=0}^{j_{12}} \begin{pmatrix} j_{12} \\ l_{12} \end{pmatrix} 2^{l_{12}} (N-2)^{j_{12}-l_{12}} 2^{-l_{12}}$$

$$\times \sum_{l_{23}=0}^{j_{23}} \begin{pmatrix} j_{23} \\ l_{23} \end{pmatrix} 2^{l_{23}} (N-2)^{j_{23}-l_{23}} 2^{-l_{23}}$$

$$= \frac{(m-3)!}{m!}(6(m-2N)N^2 + 6(N-1)^{m-1}N^{3-m}(-2+m+2N)). \tag{B.2}$$

We note that this is exactly $F^{(3)}(N,m)$, as we can see from [10].

Bibliography

[1] V. Khachatryan *et al.* [CMS Collaboration] JHEP **1009** (2010) 091 doi:10.1007/JHEP09(2010)091 [arXiv:1009.4122 [hep-ex]].

[2] V. Khachatryan *et al.* [CMS Collaboration], Phys. Lett. B **765** (2017) 193 doi:10.1016/j.physletb.2016.12.009 [arXiv:1606.06198 [nucl-ex]].

[3] M. Aaboud *et al.* [ATLAS Collaboration] JHEP **03** (2017) 157 doi:10.1007/JHEP03(2017)157

[4] J. Kim *et al.* [ALICE Collaboration], PoS EPS-HEP2019 (2020) 293 doi:10.22323/1.364.0293

[5] M.Aaboudetal *et al.*. [ATLAS Collaboration], Eur. Phys. J. **C77** (2017) no.6,428 [arXiv:1705.04176[hep-ex]].

[6] M. Aaboud *et al.* [ATLAS Collaboration] Eur. Phys. J. C **78** (2018) 997 [arXiv:1808.03951 [nucl-ex]].

[7] G. Aad *et al.* [ATLAS Collaboration] Phys. Rev. C **101** (2020) 024906 [arXiv:1911.04812v2 [nucl-ex]].

[8] K.Aamodtetal *et al.*, [ALICE Collaboration], Phys. Rev. Lett. **107** (2011) 032301 [arXiv:1105.3865[nucl-ex]].

[9] B.B.Abelevetal *et al.*, [ALICE Collaboration], Phys. Rev. **C90** (2014) no.5,054901 [arXiv:1406.2474[nucl-ex]].

[10] B. Blok, C. D. Jakel, M. Strikman, U. A. Wiedemann, J. High Energy Phys. **1712** (2017) 074 [arXiv:1708.08241 [hep-ph]].

[11] B. Blok, U. A. Wiedemann, Phys. Lett. B **795** (2019) 259-265 [arXiv:1812.04113[hep-ph]].

[12] M. Aaboud *et al.* [ATLAS Collaboration], Phys. Lett. B **789** (2019) 444-471 [arXiv:1807.02012v2 [nucl-ex]].

[13] U. Heinz, M. Jacob [arXiv:0002042 [nucl-th]].

[14] A. Bilandzic, R. Snellings, S. Voloshin, Phys. Rev. C **83** (2011) 044913 doi:10.1103/PhysRevC.83.044913 [arXiv:1010.0233 [nucl-ex]].

[15] S. S. Padula PoS ICHEP2016 **358** (2016) doi:10.22323/1.282.0358

[16] S. Acharya *et al.* [ALICE Collaboration], JHEP **09** (2018) 006 [arXiv:1805.04390 [nucl-ex]].

[17] N. Borghini, P. M. Dinh and J. Y. Ollitrault, Phys.Rev. C **63** (2001) 054906 [arXiv:nucl-th/0007063].

[18] N. Borghini, P. M. Dinh and J. Y. Ollitrault, Phys. Rev. C **64** (2001) 054901 doi:10.1103/PhysRevC.64.054901 [nucl-th/0105040].

[19] C. Zhang, J. Jia, J. Xu, Phys. Lett. B **792**, 138–141 (2019). [arXiv:1812.03536v3 [nucl-th]].

[20] S. Alekhin, J. Blümlein, S. Moch, R. Placakyte Phys. Rev. D **96**, 014011 (2017) doi:10.1103/PhysRevD.96.014011 [arXiv:1701.05838 [hep-ph]]

[21] B. Blok, M. Strikman, Adv. Ser. Direct. High Energy Phys. **29** (2019) 63–99, [arXiv:1709.00334 [hep-ph]].

[22] L. Frankfurt, M. Strikman, C. Weiss Ann.Rev.Nucl.Part.Sci. **55**:403-465 (2005) [arXiv:hep-ph/0507286]

[23] L. Frankfurt, C. E. Hyde, M. Strikman and C. Weiss, Phys. Rev. D 75 (2007) 054009 doi:10.1103/PhysRevD.75.054009 [hep-ph/0608271].

[24] J. Kuechler [ALICE and ATLAS and CMS Collaborations], PoS LHCP **2016** (2016) 133.

[25] M. Aaboud *et al.* [ATLAS Collaboration], JHEP **1611** (2016) 110 doi:10.1007/JHEP11(2016)110 [arXiv:1608.01857 [hep-ex]].

[26] P. Gunnellini [CMS Collaboration], "Study of high pT particle production from double parton scatterings at the CMS experiment," 23-27 Nov 2015, Trieste, Italy. (http://indico.ictp.it/event/a14280/)

[27] M. Y. Azarkin, I. M. Dremin and M. Strikman, Phys. Lett. B **735** (2014) 244 doi:10.1016/j.physletb.2014.06.040 [arXiv:1401.1973 [hep-ph]].

[28] V.Khachatryan *et al.*, [CMS Collaboration], Phys. Rev. Lett. **115** (2015) no.1,012301 [arXiv:1502.05382[nucl-ex]].

[29] A.Adareetal *et al.* [PHENIX Collaboration], Phys. Rev. Lett. **114** (2015) no.19,192301 [arXiv:1404.7461[nucl-ex]].

[30] L.Adamczyketal *et al.*. [STAR Collaboration], Phys. Lett. **B747** (2015) 265 [arXiv:1502.07652[nucl-ex]].

[31] P. Romatschke and U. Romatschke, doi:10.1017/9781108651998 [arXiv:1712.05815 [nucl-th]].

[32] N. Borghini and C. Gombeaud, Eur. Phys. J. C **71** (2011), 1612 doi:10.1140/epjc/s10052-011-1612-7 [arXiv:1012.0899 [nucl-th]].

[33] J. Xu and C. M. Ko, Phys. Rev. C **83** (2011), 034904 doi:10.1103/PhysRevC.83.034904 [arXiv:1101.2231 [nucl-th]].

[34] J. Uphoff, F. Senzel, O. Fochler, C. Wesp, Z. Xu and C. Greiner, Phys. Rev. Lett. **114** (2015) no.11, 112301 doi:10.1103/PhysRevLett.114.112301 [arXiv:1401.1364 [hep-ph]].

[35] A. Kurkela, U. A. Wiedemann and B. Wu, Eur. Phys. J. C **79** (2019) no.9, 759 doi:10.1140/epjc/s10052-019-7262-x [arXiv:1805.04081 [hep-ph]].

[36] A. Kurkela, A. Mazeliauskas and R. Törnkvist, [arXiv:2104.08179 [hep-ph]].

[37] A. Buckley, J. Butterworth, S. Gieseke, D. Grellscheid, S. Hoche, H. Hoeth, F. Krauss, L. Lonnblad, E. Nurse and P. Richardson, *et al.* Phys. Rept. **504** (2011), 145-233 [arXiv:1101.2599 [hep-ph]].

[38] N. Fischer and T. Sjöstrand, JHEP **01** (2017), 140 doi:10.1007/JHEP01(2017)140 [arXiv:1610.09818 [hep-ph]].

[39] C. Bierlich, G. Gustafson and L. Lönnblad, Phys. Lett. B **779** (2018), 58-63 doi:10.1016/j.physletb.2018.01.069 [arXiv:1710.09725 [hep-ph]].

[40] M. Mace, V. V. Skokov, P. Tribedy and R. Venugopalan, Phys. Rev. Lett. **121** (2018) no.5, 052301 [erratum: Phys. Rev. Lett. **123** (2019) no.3, 039901] [arXiv:1805.09342 [hep-ph]].

[41] A. Bzdak, B. Schenke, P. Tribedy and R. Venugopalan, Phys. Rev. C **87** (2013) no.6, 064906 doi:10.1103/PhysRevC.87.064906 [arXiv:1304.3403 [nucl-th]].

[42] T. Altinoluk, N. Armesto, G. Beuf, A. Kovner and M. Lublinsky, Phys. Lett. B **751** (2015), 448-452 doi:10.1016/j.physletb.2015.10.072 [arXiv:1503.07126 [hep-ph]].

[43] T. Altinoluk and N. Armesto, Eur. Phys. J. A **56** (2020) no.8, 215 doi:10.1140/epja/s10050-020-00225-6 [arXiv:2004.08185 [hep-ph]].

[44] J.R. Gaunt and W.J. Stirling, JHEP **1003**, 005 (2010)

[45] B. Blok, Yu. Dokshitzer, L. Frankfurt and M. Strikman, Phys. Rev. D **83**, 071501 (2011)

[46] M. Diehl, PoS D **IS2010** (2010) 223

[47] J.R. Gaunt and W.J. Stirling, JHEP **1106**, 048 (2011)

[48] B. Blok, Yu. Dokshitser, L. Frankfurt and M. Strikman, Eur. Phys. J. C **72**, 1963 (2012)

[49] M. Diehl, D. Ostermeier and A. Schafer, JHEP **1203** (2012) 089

[50] B. Blok, Y. Dokshitzer, L. Frankfurt and M. Strikman, Eur. Phys. J. C **74** (2014) 2926

[51] M. Diehl, J. R. Gaunt and K. Schönwald, JHEP **1706** (2017) 083

[52] A. V. Manohar and W. J. Waalewijn, Phys. Rev. D **85** (2012) 114009

[53] P. Bartalini and J. R. Gaunt, editors, "Multiple Parton Interactions at the LHC," Adv. Ser. Direct. High Energy Phys. **29** (2018), pp.1-450 doi:10.1142/10646

[54] Y. L. Dokshitzer, V. A. Khoze, A. H. Mueller and S. I. Troian, "Basics of perturbative QCD," Gif-sur-Yvette, France: Ed. Frontieres (1991) 274 p..

[55] Bateman, H., Erdelyi,A. Higher Transcendental Functions, Vol.I-III. McGraw-Hill Book Company, New York 1953 .

[56] C. Zhang, J. Jia and J. Xu, Phys. Lett. B **792** (2019), 138-141 doi:10.1016/j.physletb.2019.03.035 [arXiv:1812.03536 [nucl-th]].

[57] J. Jia, private communication.

[58] B. Blok and R. Segev, in preparation.

המרכזי המתאים. המונמט המרכזי של מספר זוגי של חלקיקים נקרה המומנט הסמטרי, עבור מספר אי-זוגי של חלקיקים המומנט המרכזי נקרה אסימטרי מכיוון שהוא מחייב שנסתכל על הרמוניות שונות עבור החלקיקים השונים.

התזה הזו מסודרת בצורה הבאה:

במבוא אנחנו מסבירים את המטרות של המחקר שלנו.

בפרק השני אנחנו נותנים סיקור של הרעניונות הבסיסיים של הדרך חשיבה החדשה עבור אירועים בעלי מספר תוצרים גבוהה בהתנגשויות פרוטון-פרוטון בהתבסס על התאבכות קוונטית ואינטרקציה מרובת פרטונים. ספציפית אנחנו מסבירים את הגאומטריה של התנגשות מרובת תוצרים ואת הכלים מניסיניים והמתמטיים שנשתמש בהם כדי לתאר את התלות האופקית בין החלקיקים, אז אנחנו מסכמים את הרעיונות הבסיסיים של אינטרקציה מרובת פרטונים, ואז מפרטים את הפרטים של המודל בו נשתמש כדי לחשב את המומנט האסימטרי של שלושה חלקיקים.

בפרק שלוש אנחנו מבצעים את החישוב של המומנט האסימטרי המתקבל עבור שלושה חלקיקיסת וחוקרים את התלות של מומנט זה בתנע של החלקיקים ומספר החלקיקים הנפלטים, ולבסוף משווים את החישוב לתוצאות אשר נמדדו ב-LHC. ספציפית אנחנו מתחילים מלבסס מחדש את הבעיה המרכזית ולהזיג אותה בתור הכלים של המודל שאנחנו עובדים איתו, ואז אנחנו מסכמים את הכלים של המודל שאנחנו צריכים בשביל לחשב את המונמט האסימטרי של שלושה חלקיקים, לאחר מכן אנחנו מחשבים את המומנט האסימטרי של שלושה חלקיקים כתלות בתנע של החלקיקים עבור המקרה הפשוט של שלוש אינטרקציות פרטוניות ושלושה חלקיקים שנפלטו, ולבסוף אנחנו מוצאים את התלות של המומנט האסימטרי עבור שלושה חלקיקים במספר החלקיקים שנפלטו ומשווים את התוצאות למדידות הקיימות.

פרק ארבע מציג את מסקנות המחקר.

תקציר

התצפיות האחרונות מראות תלות אופקית לא טריוויאלית בהתנגשויות פרוטון-פרוטון (החלקיקים הנפלטים מההתנגשות מראים קשר בכיוונים שלהם במישור המאונך לציר ההתנגשות) בעלות מספר תוצרים גבוהה במאיץ ההדרונים הגדול (LHC), תלות זו מכונה גם תופעת **רכס**. תצפיות אלו העלו התעניינות משמעותית. התעניינות זו עלתה מכיוון שתלות דומה נצפה לפני כן בהתנגשויות של יונים כבדים ב-LHC ובמאיץ היונים הכבדים היחסותיים (RHIC), כאשר עבור יונים כבדים תופעת הרכס נחשבה לסימן חשוב ליצירה של פלזמת קווארק-גלואונים (QGP). תופעת הרכס נראת טבעית במסגרת של QGP, בגלל האינטרציה החזקה בין החלקיקים הנוצרים במצב הסופי שלהם, אבל בהתנגשויות פרוטון-פרוטון שטח החתך הקטן יותר והצפיפיות הנמוכה מהווים קושי עבור הסבר על ידי QGP, בנוסף התנגשויות פרוטון-פרוטון מתאימות לתוצאות של יוצרי מונטה-קרלו שמניחים כי החלקיקים הנפלטים לא תלויים אחד בשני. זה הוביל למחקרים של מודלים חדשים שיסבירו את תופעת הרכס, ספציפית פותח מודל חדש שמבוסס על התאבכות קוונטית ואינטרקציה מרובת פרטונים (MPI). עד כו הפורמליזם הזה שומש בהצלחה לחישוב התלות הסימטרית.

בחיבור זה אנחנו חוקרים את ההשפעה של התאבכות קוונטית וזרימת צבע על התלות בין שלושה חלקיקים שמתוארת על ידי המומנט האסימטרי באירועים בעלי מספר תוצרים גבוהה בהתנגשויות פרוטון-פרוטון. אנחנו משתמשים במודל שפותח לאחרונה לחקירת ההתנהגות הקולקטיבית במומנטים הסימטריים. אנחנו מראים שהמומנט האסימטרי המתקבל עבור שלושה חלקיקים מתאים איכותית לתוצאות שנמדדו כאשר מתשמשים באותם פרמטרים בהם השתמשו כדי לחשב את המומנטים הסימטריים. התוצאות שלנו מראות שהתלות במצב ההתחלתי של החלקיקים הסופיים חייבת להיות משמעותית, ואולי אפילו שולטת בהסבר של התלות עבור אירועים בעלי מספר תוצרים גבוהה בהתנגשויות פרוטון-פרוטון.

על מנת לחקור את התלות האופקית בין החלקיקים ביותר פרטים, נהוג לפתח צפיפות החלקיקים במרחב התנע כסדרת פורייה עבור הזווית האופקית, כאשר המקדמים של הסדרה הזו נקראים הרמוניות זרימה, טכניקה זו נקרת אנליזת זרימה. הקשר בין ההרמוניות זרימה והתלות האופקית נהיה מדוייק יותר כאשר מסתכלים על תלות בין כמה שיותר חלקיקים, אבל כאשר מסתכלים על מספר חלקיקים גבוהה צריך להפחית את התלות של תתי הקבוצות, הגודל שנותן לנו את הרמוניית הזרימה הוא המומנט

הדרכה

המחקר נעשה בהנחיית פרופסור בלוק בוריס בפקולטה לפיזיקה.

אני מודה לטכניון על התמיכה הכספית הנדיבה בהשתלמותי.

חישוב מומנט אסימטרי עבור שלושה חלקיקים בהתנגשויות פרוטון-פרוטון מרובות תוצרים ב-LHC

חיבור על מחקר

לשם מילוי חלקי של הדרישות לקבלת התואר מגיסטר למדעים בפיזיקה

רן שגב

הוגש לסנט הטכניון - מכון טכנולוגי לישראל
אדר א' ה'תשפ"ב, חיפה, פברואר 2022

חישוב מומנט אסימטרי עבור שלושה חלקיקים בהתנגשויות פרוטון-פרוטון מרובות תוצרים ב-LHC

רן שגב